

UNIVERSITY OF CALIFORNIA, SAN DIEGO

Hyperbolic polyhedra: volume and scissors congruence

A dissertation submitted in partial satisfaction of the
requirements for the degree
Doctor of Philosophy

in

Mathematics

by

Yana Zilberberg Mohanty

Committee in charge:

Professor Justin Roberts, Chair
Professor Peter Doyle, Cochair
Professor Zheng-Xu He
Professor Kenneth Intriligator
Professor Robert Skelton

2002

Copyright
Yana Zilberberg Mohanty, 2002
All rights reserved.

The dissertation of Yana Zilberberg Mohanty is approved, and it is acceptable in quality and form for publication on microfilm:

Co-Chair

Chair

University of California, San Diego

2002

“Beauty will save the world.”

–Dostoevsky

TABLE OF CONTENTS

	Signature Page	iii
	Dedication	iv
	Table of Contents	v
	List of Figures	vii
	List of Tables	x
	Acknowledgements	xii
	Vita	xiii
	Abstract of the Dissertation	xiv
1	Introduction	1
	1.1 Scissors congruence	1
	1.2 Volume of ideal hyperbolic tetrahedra	2
	1.3 Volumes of non-ideal hyperbolic tetrahedra	7
	1.4 The Kubert identities	13
2	A new formula for the volume of a hyperbolic tetrahedron	14
	2.1 Background	15
	2.2 Exterior Algebra in Minkowski Space	17
	2.3 Main Theorem	20
	2.4 Alternative Approach	24
	2.5 Special Cases	28
	2.6 A numerical example of the computation of the volume of a hyperbolic tetrahedron using the method outlined in Table 2.2 of §2.4	28
3	A scissors congruence proof of the Regge symmetry	32
	3.1 Murakami and Yano’s formula for the volume of a hyperbolic tetrahedron	33
	3.2 Warm-up for the development Leibon’s set of formulas for the volume of a hyperbolic tetrahedron	35
	3.3 Leibon’s formulas for the volume of a hyperbolic tetrahedron	38
	3.3.1 Computation of the volume formula using the root z_- of the equation (3.28)	48

3.3.2	Computation of the volume formula using the root z_+ of the equation (3.28)	51
3.4	A scissors congruence proof of the Regge symmetry	57
4	On the geometric proof that the Lobachevsky function satisfies the Kubert identities	72
4.1	Analytic proof of the Kubert identities	74
4.2	The Kubert identities viewed as identities on simplices; the Dehn invariant	75
4.3	Attempts and obstacles in the geometric proof of the Kubert identities	78
4.3.1	Two geometric proofs of the Kubert identity in the case $n = 3$	78
4.3.2	The geometric proof of the cyclotomic identities	80
4.3.3	Obstacles in extending the geometric proof of the cyclotomic identities to a geometric proof of the Kubert identities	81
4.4	A scissors congruence proof of the Kubert identities based on the algebraic proof of Dupont and Sah	88
4.4.1	Dupont and Sah's proof of the Kubert identities	88
4.4.2	The method used to apply Dupont and Sah's proof to a get a geometric proof of the Kubert identities	95
4.4.3	"Geometrization" of Dupont and Sah's proof of the Kubert identity $n=2$	95
4.4.4	"Geometrization" of Dupont and Sah's proof of the Kubert identity $n=3$	99
4.4.5	"Geometrization" of Dupont and Sah's proof of the Kubert identity $n=4$	108
5	Conclusion	120
	Bibliography	122

LIST OF FIGURES

1.1	Ideal hyperbolic tetrahedron with dihedral angles α , β , and γ at the vertex at infinity in the half-space model	4
1.2	An ideal hyperbolic tetrahedron and its reflection in a) the half-space model b) the Klein model	5
1.3	The projection of Figure 1.2a) onto the plane at infinity	6
1.4	a) $T(A, B, C)$ b) $T_3(A, B, C, A', B', C')$ c) $T_1(A, B, C, A', B', C')$ d) $T_0(A, B, C, A', B', C')$. The hollow circles denote ideal points	7
1.5	Derivation of the formula for the volume of a hyperbolic tetrahedron with one finite vertex	8
1.6	Hyperbolic tetrahedron with infinite vertex I	9
1.7	Thurston's proof that $\Delta abc = \Delta a'b'c' - \Delta aa'b' - \Delta bb'c' - \Delta cc'a'$	10
1.8	The decomposition of a tetrahedron into six orthoschemes	11
2.1	Finite hyperbolic tetrahedron $T_0(A, B, C, A', B', C')$	14
2.2	Hyperbolic tetrahedron T with one of its edges extended to infinity	15
2.3	Orthoscheme O_{jk} shown as part of the tetrahedron which it is used to decompose. The tetrahedron is drawn with a dotted line	19
2.4	Hyperbolic tetrahedron T with one of its edges extended to infinity	21
3.1	Tetrahedron $T(A, B, C, A', B', C')$ with its dihedral angles denoted by letters	32
3.2	Polyhedron D	35
3.3	An ideal hyperbolic prism	36
3.4	A triangulation of an ideal hyperbolic prism	37
3.5	Polyhedron C	39
3.6	Polyhedron U	40
3.7	Decomposition of polyhedron U via the 2220 method; the edges of U are shown with thin and dashed lines, while the cuts of the decomposition are shown with thicker and dotted lines.	41
3.8	Decomposition of polyhedron U , Part I: the tetrahedra	42
3.9	Decomposition of polyhedron U , Part II: the octahedron O	43
3.10	Octahedron O in the half-space model	44
3.11	Four tetrahedra that satisfy equations (3.24)	45
3.12	Non-linear condition for ensuring that four tetrahedra fit together to make an octahedron	46
3.13	A triangular prism divided into two parts	51
3.14	a) The original octahedron O with its dihedral angles labeled. b) The dual octahedron O'	54

3.15	Octahedron O in the half-space model, triangulated according to the construction in §1.2	59
3.16	Tetrahedra in the triangulation of the octahedron O that correspond to the first 8 terms in formula (3.50)	60
3.17	Tetrahedra in the triangulation of the octahedron O' that correspond to the last 8 terms in formula (3.50)	60
3.18	Polyhedron $U_{R_b(T)}$	62
3.19	Octahedron $O_{R_b(T)}$	63
3.20	Polyhedron of Figure 3.16 with two tetrahedra interchanged. These two tetrahedra have been shown as shaded	63
3.21	Mirror image of the polyhedron of Figure 3.20	64
3.22	Octahedron $P(O)$	65
3.23	Octahedron $P(O)$ in the Klein model	65
3.24	Mirror image of the polyhedron of Figure 3.17 where the interchanged tetrahedra have been shown as shaded	66
3.25	Octahedron $P(O')$	66
3.26	Octahedron $P(O')$ in the Klein model	67
3.27	Dividing the polyhedron of Figure 3.16 into two scissors congruent parts	68
3.28	One of the two congruent halves comprising the polyhedron of Figure 3.16	69
3.29	One of the two congruent halves comprising the polyhedron of Figure 3.17	69
3.30	One of the two congruent halves comprising the polyhedron of Figure 3.21	70
3.31	One of the two congruent halves comprising the polyhedron of Figure 3.24	71
4.1	Calculation of the Dehn invariant of an ideal hyperbolic tetrahedron	76
4.2	A geometric proof of the Kubert identity in the case $n = 3$ based on a construction by Thurston	79
4.3	A geometric proof of the Kubert identity in the case $n = 3$	79
4.4	A geometric proof of the identity $2 \sin 2\theta = (2 \sin \theta)(2 \sin(\theta + \pi/2))$	81
4.5	A geometric proof of the identity $2 \sin 3\theta = (2 \sin \theta)(2 \sin(\theta + 2\pi/3))(2 \sin(\theta + 4\pi/3))$	82
4.6	Calculating the dihedral angle between two planes in \mathbb{H}^3	83
4.7	A geometric proof of the identity $n = 4$ cyclotomic identity shown in solid lines. The dashed lines are needed in addition to the solid lines to prove the Kubert $n = 4$ identities	85

4.8	An illustration of the three ways to describe an ideal hyperbolic tetrahedron by its cross ratio. The triangles in a), b) and c) are all similar to each other.	89
4.9	The triangle of Figure 4.8 scaled by $1/z$	89
4.10	Geometric interpretation in the Klein model of the cocycle relation as stating that the union along faces of two hyperbolic tetrahedra can be divided into three tetrahedra	90
4.11	A geometric proof of the generalized Kubert identity $\{z^2\} = 2\{z\} + 2\{-z\}$	98
4.12	A geometric proof of the generalized Kubert identity $\{z^3\} = 3\{z\} + 3\{\omega z\} + 3\{\omega^2 z\}$, where $\omega = \exp(2\pi i/3)$	103
4.13	Partial sketch of the geometric proof of the generalized Kubert identity $\{z^4\} = \sum_{j=0}^4 4\{\omega^j z\}$, where $\omega = i$ and the coordinates of the vertices r, t, b_i , and g_i are given in (4.114)	111

LIST OF TABLES

2.1 Procedure for computing the volume V of an arbitrary hyperbolic tetrahedron with Gram matrix $G = [-\cos \alpha_{ij}]$ 23

2.2 Procedure for computing the volume V of an arbitrary hyperbolic tetrahedron with Gram matrix $G = [-\cos \alpha_{ij}]$. D denotes the matrix with diagonal entries -1,1,1,1 and 0 elsewhere, and W has the vectors outputted by the Gram-Schmidt routine as its rows. 25

4.1 Values of $f_1, f_2, f_1/f_2, (1 - f_2)/(1 - f_1), f_1(1 - f_2)/f_2/(1 - f_1)$ at 0 and ∞ 97

4.2 Values of $f_1, f_2, f_1/f_2, (1 - f_2)/(1 - f_1), f_1(1 - f_2)/f_2/(1 - f_1)$ at 0 and ∞ 101

4.3 Values of $f_1(f_1), f_2(f_1), f_1(f_1)/f_2(f_1), (1 - f_2(f_1))/(1 - f_1(f_1)), f_1(1 - f_2)/f_2/(1 - f_1)$ at 0 and ∞ 104

4.4 Data needed to prove that $\frac{f_1(x)}{f_2(x)} = -\frac{(x-\omega/z)(x-\omega^2/z)z^2}{(x-1)(1+x+xz)}$ obeys the relation (4.43) 107

4.5 Data needed to prove that $\frac{1-f_2(x)}{1-f_1(x)} = -\frac{(x+1/(z+1))(x-1/z)z(z+1)}{(x-\omega)(x-\omega^2)}$ obeys the relation (4.43) 107

4.6 Expanding $\{z^4\}$ by the cocycle relation; $a = 1/z, b = 1, d = 0$ 110

4.7 Expanding $\{z^3/(z^3 - 1)\}$ by the cocycle relation; $a = -1/z, b = 0, d = -1$ 111

4.8 Expanding $\{z^2/(z^2 - 1)\}$ by the cocycle relation; $a = \omega^3/z, b = 0, d = \omega^3$ 112

4.9 Expanding $\{z^3/(z^3 - 1)\}$ by the cocycle relation; $a = 0, b = -(1 + z + s)/2/(1 + z + z^2), d = \omega^3$. $b_1 = z(2 + \omega - \omega z^2 - \omega(z - 1)s)/2$. 112

4.10 The cocycle relation used to prove that the linear fractional transformation $f_1(\frac{1-f_2(f_1)}{1-f_1(f_1)}) = \frac{2\omega(x+1/z)z(1+z)}{(x-\omega^3)(1-2\omega+z+s)}$ obeys (4.43). $t = z(\omega + z - \omega z^2)$. 114

4.11 The cocycle relation used to prove that the linear fractional transformation $f_1(\frac{1-f_2(f_1)}{1-f_1(f_1)})/f_2(\frac{1-f_2(f_1)}{1-f_1(f_1)}) = (x+1/z)z(1+z)(1+z+s)/((1+z+z^2)(1-2\omega+z+s)(x+\frac{1+z+s}{2(1+z+z^2)}))$ obeys (4.43). $g_1 = \frac{z(1+z-\omega z^3)}{1-\omega+z}$. 114

4.12 Expanding $\{-z^3/(1+z+z^2)\}$ by the cocycle relation; $a = -1/z, b = 1, d = 0$ 114

4.13 Expanding $\{-z^2\}$ by the cocycle relation; $a = \omega^3/z, b = -1, d = 0$. $g_2 = \omega z^3/(z^2 + z\omega - 1)$ 115

4.14 Expanding $\{z/(1+z+z^2)\}$ by the cocycle relation; $a = -1, b = -(1+z+s)/2/(1+z+z^2), d = 0$. $b_2 = z(1+3z+z^2+z^3+(z^2-1)s)/2/(1+z+z^2)$ 116

- 4.15 Expanding $\{-z(1+z+z^2)\}$ by the cocycle relation; $a = 1/z$, $b = \omega$,
 $d = 0$. $r = z + \omega^3(z^2 - z)$ 116
- 4.16 Expanding $\{(1+z+z^2)/(1+\omega+z+z^2)\}$ by the cocycle relation;
 $a = (-1-z+s)/2/(1+z+z^2)$, $b = 0$, $d = -1$. $r = z + \omega^3(z^2 - z)$,
 $b_1 = z(2 + \omega - \omega z^2 - \omega(z - 1)s)/2$ 117
- 4.17 The cocycle relation used to prove that the linear fractional trans-
formation $f_1(f_1(\frac{1-f_2}{1-f_1}))$ obeys (4.43). $r = z + \omega^3(z^2 - z)$, $b_1 =$
 $z(2 + \omega - \omega z^2 - \omega(z - 1)s)/2$, $g_3 = \omega(1 - z^3) + z$ 117
- 4.18 The cocycle relation used to prove that the linear fractional trans-
formation $(1 - f_2(f_1(\frac{1-f_2}{1-f_1}))) / (1 - f_1(f_1(\frac{1-f_2}{1-f_1})))$ obeys (4.43). $r =$
 $z + \omega^3(z^2 - z)$, $b_1 = z(2 + \omega - \omega z^2 - \omega(z - 1)s)/2$ 118
- 4.19 Expanding $\{-\omega(1+z+z^2)/(1-\omega+z)\}$ by the cocycle relation;
 $a = -(1+z+s)/2/(1+z+z^2)$, $b = \omega$, $d = 0$. $r = z + \omega^3(z^2 - z)$,
 $b_3 = z(1-\omega+(2-\omega)z+z^2+2z^3+(1-\omega+z)s)/(2+z(1-\omega+z)(1+z+s))$ 118
- 4.20 Expanding $\{-\omega z(1-\omega+z)\}$ by the cocycle relation; $a = 1/(\omega -$
 $1 - z)$, $b = -1$, $d = 0$. $r = z + \omega^3(z^2 - z)$ 119

ACKNOWLEDGEMENTS

I have been fortunate to have had a thesis advisor with the amazing creativity and instincts of Peter Doyle. As a teacher, he was undaunted (or, at least, seemed that way) by the vast planes of my mathematical ignorance, and I will be forever grateful to him for having always been patient with me. Most importantly, he has inculcated in me a sense of mathematical aesthetics, and over the years that has helped me realize that beauty is as important a criterion in mathematics and it is in the arts.

Another piece of luck for me was when Justin Roberts joined the department. He introduced me to a whole world of ideas that was connected to my work, and this made me look forward to my mathematical life after graduation. His enthusiasm and support meant a lot to me.

Greg Leibon has the energy that transmits even over silent videos. I am grateful for his encouragement, and for the generosity with which he shared his time and ideas.

I appreciate the time my committee members, John He, Ken Intriligator, and Bob Skelton took to acquaint themselves with my dissertation. I am particularly thankful to John He for taking an interest in my work.

Who knows how much of this would have been possible without the support of my husband Bibhu, who has put up with a tremendous amount of *mishigas* over the past several years.

VITA

- 1989 B. S. E. E., *magna cum laude*, University of California
Los Angeles
- 1989–1990 Member of Technical Staff, Hughes Aircraft Company,
El Segundo, California
- 1994 M. S., University of Massachusetts, Amherst
- 1994–1995 Applications Engineer, Loral Test and Information
Systems, San Diego, California
- 1997–2002 Teaching assistant, Department Mathematics, Univer-
sity of California San Diego
- 1999 M. A., University of California San Diego
- 2002 Ph. D., University of California San Diego

ABSTRACT OF THE DISSERTATION

Hyperbolic polyhedra: volume and scissors congruence

by

Yana Zilberberg Mohanty

Doctor of Philosophy in Mathematics

University of California San Diego, 2002

Professor Justin Roberts, Chair

In this dissertation we solve several problems relating to volumes of hyperbolic polyhedra and scissors congruence. Regarding volumes, we derive a new formula for the volume of a general hyperbolic tetrahedron in three dimensions. This formula is a sum of the Lobachevsky function applied to functions of the dihedral angles of the tetrahedron, and it was developed by using the hyperboloid model of hyperbolic space and an exterior algebra on vectors in Minkowski space.

We then make use of Gregory Leibon's formula for the volume of a hyperbolic tetrahedron to solve a problem posed by Justin Roberts of whether the Regge symmetry is a scissors congruence in hyperbolic space by producing a constructive proof. This proof involves permuting certain components of Leibon's construction.

Finally, we show several geometric proofs of the Kubert identities in the cases $n = 2, 3, 4$. Some of these are extensions of the geometric proof of the cyclotomic identities. Others involve exposing the geometry underlying Dupont and Sah's proof of the generalized Kubert identities in [5].

Chapter 1

Introduction

1.1 Scissors congruence

Given two polyhedra of equal volume, when can we decompose one of them into a finite number of pieces by planar cuts so that these pieces can be rearranged into the other one? The present dissertation addresses this question in several examples in hyperbolic space.

The problem is known as *scissors congruence*, and its solution in 2-dimensional geometry of constant curvature was found centuries ago: if two polygons have the same area, they are scissors congruent to one another. Guaranteeing scissors congruence gets much more difficult once the dimension increases to three. It was only in 1901 that Max Dehn provided a counterexample as an answer to Hilbert's third problem, which asked whether two Euclidean polyhedra of equal volume are scissors congruent. The counterexample was the cube and regular tetrahedron of equal volume. Dehn showed that these two polyhedra are not equidecomposable by introducing a new quantity pertaining to a polyhedron now known as the *Dehn invariant*.

Definition 1 *The Dehn invariant of a polyhedron P is defined as*

$$D(P) = \sum_A l(A) \otimes (\theta(A)/\pi), \quad (1.1)$$

where A runs through the collection of the edges of P , $l(A)$ and $\theta(A)$ are the respective lengths and dihedral angles, and D takes values in the tensor product $\mathbb{R} \otimes_{\mathbb{Z}} (\mathbb{R}/(\pi\mathbb{Z}))$.

Dehn proved that in order for two polyhedra to be scissors congruent their Dehn invariants, as well as their volumes, must agree. An easy computation shows that the Dehn invariant of a cube is 0, while that of a regular tetrahedron is not. That the volume and Dehn invariant were indeed *sufficient* for proving scissors congruence in Euclidean space was first proved by Sydler as recently as 1965. The completeness of the Dehn invariant and volume in hyperbolic 3-space as well as Euclidean n -spaces with $n > 4$ is still unknown.

1.2 Volume of ideal hyperbolic tetrahedra

In hyperbolic three-space there is an intimate connection between finding the volumes of polyhedra and showing that they are scissors congruent. This connection is due to the method of determining volumes of hyperbolic tetrahedra that was first devised by Lobachevsky and later reworked by Milnor in [10].

Definition 2 *The Poincaré ball model of hyperbolic space, \mathbb{H}^3 , is given by the set $\mathbb{B}^3 = \{(x, y, z) | x^2 + y^2 + z^2 \leq 1\}$ together with the metric $ds^2 = 4(dx^2 + dy^2 + dz^2)/(1 - (x^2 + y^2 + z^2))^2$.*

The Poincaré model is conformal, meaning that it preserves circles and angles. Geodesics are subsets of circles orthogonal to the sphere $\mathbb{S}^2 = \{(x, y, z) | x^2 + y^2 + z^2 = 1\}$, while planes are subsets of spheres orthogonal to \mathbb{S}^2 .

Stereographically projecting the Poincaré model onto $\mathbb{S}^3 = \{x, y, z, w | x^2 + y^2 + z^2 + w^2 = 1\}$ and then projecting orthogonally down to \mathbb{B}^3 gives the Klein model of projective space. The Klein model is not conformal, but is convenient to use for representing polyhedra since geodesics in the Klein model are straight lines.

Inverting the Poincaré model in the sphere of radius 2 centered at a boundary point of \mathbb{B}^3 results in the *half-space* model of \mathbb{H}^3 , which is also conformal.

Definition 3 *The half-space model of \mathbb{H}^3 is given by the set $\mathbb{R}^{3+} = \{(x, y, z) | z \geq 0\}$ together with the metric $ds = \sqrt{dx^2 + dy^2 + dz^2}/z$. The plane at infinity in the half-space model is the plane $z = 0$, while the point at infinity is the image of the center of the sphere in which the Poincaré model was inverted.*

Geodesics in the half-space models are semicircles and lines orthogonal to the plane at infinity, and planes are hemispheres and planes orthogonal to the plane at infinity.

Definition 4 *An ideal hyperbolic tetrahedron is the convex hull in \mathbb{H}^3 of 4 points on the boundary of \mathbb{B}^3 (in the Poincaré ball model).*

Given any ideal hyperbolic tetrahedron, if we place one of its vertices the point at infinity in the half-space model then the three faces meeting at that vertex will form the walls of a triangular prism, as shown in Figure 1.1. The vertices at infinity in that drawing have been denoted by hollow dots. This convention will be followed throughout the dissertation. Since the half-space model is conformal, the dihedral angles at the edges which meet at the vertex at infinity are actually the same as the angles of the Euclidean triangle that forms the cross section of the prism. In particular, these dihedral angles add up to π . Applying this condition to each of the four vertices of the tetrahedron and solving the resulting system of equations results in the second and third parts of the following lemma.

Lemma 1 *The three dihedral angles meeting at a vertex of an ideal hyperbolic tetrahedron add up to π . It follows that the dihedral angles at each pair of opposite (non-adjacent) edges are equal. Moreover, the triplet of dihedral angles is the same at each of the four vertices.*

Continuing with this placement of the ideal tetrahedron in the half-space model, we calculate its volume by integrating the differential element of volume $dV = dx dy dz/z^3$ to obtain

$$V(T(\alpha, \beta, \gamma)) = \mathfrak{I}(\alpha) + \mathfrak{I}(\beta) + \mathfrak{I}(\gamma), \quad (1.2)$$

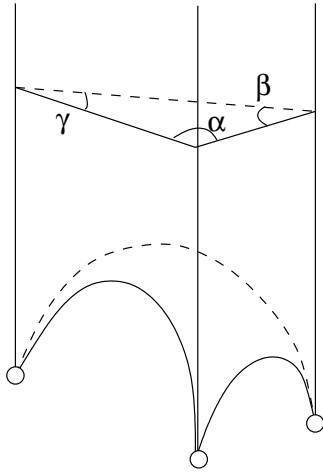


Figure 1.1: Ideal hyperbolic tetrahedron with dihedral angles α , β , and γ at the vertex at infinity in the half-space model

where $T(\alpha, \beta, \gamma)$ is an ideal tetrahedron whose dihedral angles at any given vertex are α , β , and γ and

$$\mathfrak{L}(\theta) := - \int_0^\theta \log 2|\sin u| du \quad (1.3)$$

is the *Lobachevsky function*. The details of the derivation of (1.2) can be found in [10].

Lemma 2 *The function \mathfrak{L} defined by (1.3) is odd and π -periodic.*

Proof. $\mathfrak{L}(-\theta) = - \int_0^{-\theta} \log 2|\sin u| du = \int_0^\theta \log 2|\sin u| du = -\mathfrak{L}(\theta)$, after a change in the variable of integration. To see that \mathfrak{L} is π -periodic, we first use the following simple argument to show that $\mathfrak{L}(\pi/2) = 0$ [6]. Note that the symmetry of the \sin function implies that

$$L(\pi/2) = - \int_0^{\pi/2} \log 2|\sin u| du = - \int_0^{\pi/2} \log 2|\cos u| du \quad (1.4)$$

and

$$L(\pi) = - \int_0^\pi \log 2|\sin u| du = -2 \int_0^{\pi/2} \log 2|\sin u| du = 2\mathfrak{L}(\pi/2). \quad (1.5)$$

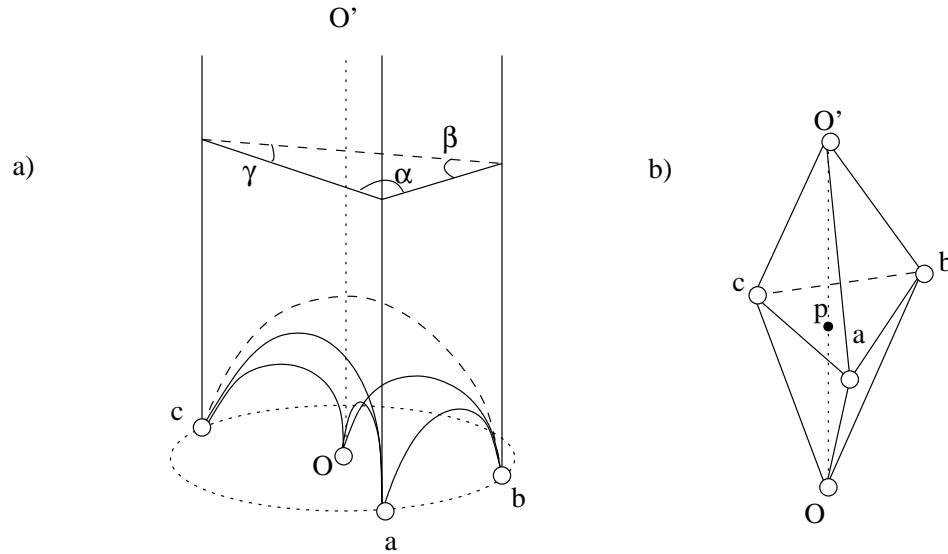


Figure 1.2: An ideal hyperbolic tetrahedron and its reflection in a) the half-space model b) the Klein model

By (1.4) and (1.5),

$$\begin{aligned}
 2\mathcal{I}(\pi/2) &= -\int_0^{\pi/2} \log 2|\sin u|du - \int_0^{\pi/2} \log 2|\cos u|du \\
 &= -\int_0^{\pi/2} \log 2|\sin 2u|du \\
 &= -\frac{1}{2} \int_0^{\pi} \log 2|\sin u|du \\
 &= \mathcal{I}(\pi/2)
 \end{aligned} \tag{1.6}$$

It follows that $\mathcal{I}(\pi/2) = 0$, and, therefore, by symmetry of \sin , $\mathcal{I}(\pi) = 0$. Then the π -periodicity of \sin implies that \mathcal{I} , too, is π -periodic. \square

It is instructive to illustrate the geometry behind formula (1.2). If we reflect the vertex at infinity in Figure 1.1 in the plane determined by the other three vertices, we will end up with two copies of the original tetrahedron. This is illustrated in Figure 1.2. Note that reflecting in a plane modeled by a hemisphere in the half-space model interchanges the center of the hemisphere which determines that plane with the point at infinity. Thus, in Figure 1.2a), the point O is the center of the circle that determines the plane of the face $\{a, b, c\}$.

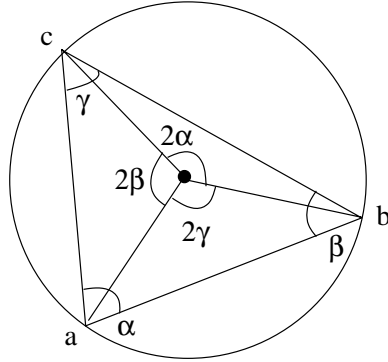


Figure 1.3: The projection of Figure 1.2a) onto the plane at infinity

The line through O and O' that is perpendicular to the plane at infinity divides the polyhedron $\{a, b, c, O, O'\}$ into the three tetrahedra $\{a, b, O, O'\}$, $\{b, c, O, O'\}$, and $\{c, a, O, O'\}$.

Definition 5 *An isosceles ideal tetrahedron is an ideal hyperbolic tetrahedron having two of the three dihedral angles at any of its vertices equal.*

Figure 1.3 shows that the projections of $\{a, b, O, O'\}$, $\{b, c, O, O'\}$, and $\{c, a, O, O'\}$ onto the plane at infinity are isosceles triangles, so all three of these tetrahedra are isosceles. The classical result that the angle subtended by an arc from the center of a circle is twice the angle subtended by the same arc from the circumference of that circle gives the angles labeled as 2α , 2β , and 2γ in Figure 1.3. Thus $\mathcal{J}(\theta)$ is the volume of half of an isosceles ideal tetrahedron with apex angle 2θ . In Figure 1.2b), for example, $\mathcal{J}(\gamma)$ is the volume of the tetrahedron $\{a, b, p, O'\}$. Its apex angle is 2γ , as seen in Figure 1.3.

As the above discussion shows, equation (1.2) is not only an elegant formulation of the volume of a tetrahedron, but is also a decomposition of an arbitrary ideal tetrahedron into the halves of three isosceles ideal tetrahedra. This fact is used extensively in this dissertation to prove scissors congruence results.

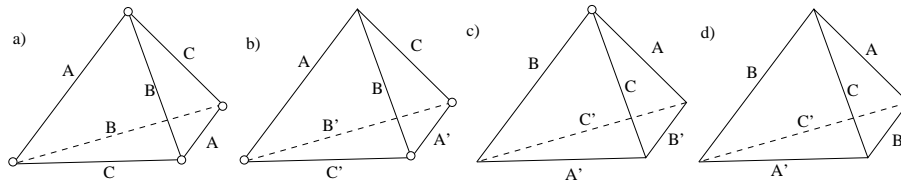


Figure 1.4: a) $T(A, B, C)$ b) $T_3(A, B, C, A', B', C')$ c) $T_1(A, B, C, A', B', C')$ d) $T_0(A, B, C, A', B', C')$. The hollow circles denote ideal points

1.3 Volumes of non-ideal hyperbolic tetrahedra

We begin by introducing some notation that will be used throughout this work. Since an ideal hyperbolic tetrahedron has the same set of angles, say A , B , and C at any of its vertices, we will refer to it as $T(A, B, C)$. $T_j(A, B, C, A', B', C')$ will be used to describe a hyperbolic tetrahedron with at least j ideal vertices and dihedral angles A, B, C, A', B', C' , where every letter and its prime denote angles at opposite edges. In the case of a tetrahedron with at least one (three) ideal vertices, the unprimed letters stand for the edges which meet at an ideal (finite) vertex. This notation is summarized in Figure 1.4.

In cases (b) and (c), the six dihedral angles of the tetrahedron are not linearly independent. In case (b), A', B', C' can be found by the linear system of three equations which result from the fact that the dihedral angles at each of the ideal vertices add up to π . Thus

$$\begin{aligned} A' &= \frac{\pi + A - B - C}{2} \\ B' &= \frac{\pi + B - A - C}{2} \\ C' &= \frac{\pi + C - A - B}{2}. \end{aligned} \tag{1.7}$$

It follows that $T_3(A, B, C, A', B', C') = T_3(A, B, C, (\pi + A - B - C)/2, (\pi + B - A - C)/2, (\pi + C - A - B)/2)$. Similarly, in case (c) the constraint $A' + B' + C' = \pi$ implies the identity $T_1(A, B, C, A', B', C') = T_1(A, B, \pi - A - B, A', B', C')$.

The formula for the volume of $T_3(A, B, C, A', B', C')$ can be derived from the construction in Figure 1.5. There we extend the edges ap , bp , and cp so that they

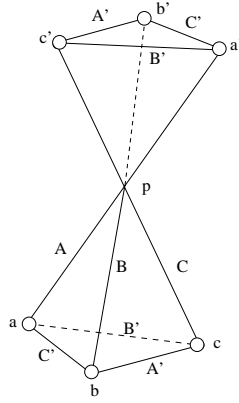


Figure 1.5: Derivation of the formula for the volume of a hyperbolic tetrahedron with one finite vertex

end at the infinite points a' , b' , and c' , respectively. It follows that

$$\{a, b, c, p\} + \{c', b', a', p\} = \{a, b, c, c'\} + \{a, a', b', c'\} - \{a, b, b', c'\}, \quad (1.8)$$

where $\{x_1, x_2, x_3, x_4\}$ denotes the oriented hyperbolic tetrahedron with vertices x_1 , x_2 , x_3 , and x_4 . The two tetrahedra on the left hand side of (1.8) can be viewed as a “twisted” or non-convex prism determined by the vertices $\{a, b, c, a', b', c'\}$. Then the right hand side of (1.8) is the standard decomposition of a triangular prism into three tetrahedra. In the case of the convex prism the tetrahedron $\{a, b, b', c'\}$ has negative volume due to its orientation. The orientation is reversed by the “twisting”. The relationship between the object in Figure 1.5 and that of a convex ideal prism will be discussed further in §3.2.

Since $\{a', b', c', p\}$ is congruent to $\{a, b, c, p\} = T(A, B, C)$, (1.8) leads to

$$2V(T_3(A, B, C, A', B', C')) = V(T(A', B', C)) + V(T(A, B', C')) - V(T((C - C'), (\pi - B), B')). \quad (1.9)$$

By (1.2) and (1.9) and the π -periodicity of \mathfrak{L} ,

$$V(T_3(A, B, C, A', B', C')) = \frac{1}{2}[\mathfrak{L}(A) + \mathfrak{L}(A') + \mathfrak{L}(B) + \mathfrak{L}(B') + \mathfrak{L}(C) + \mathfrak{L}(C') - \mathfrak{L}\left(\frac{\pi + A + B + C}{2}\right)]. \quad (1.10)$$

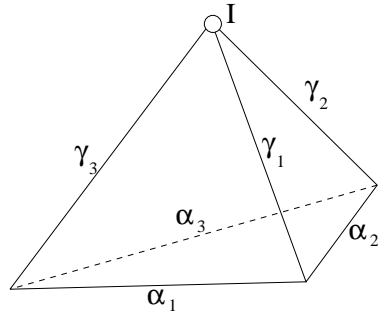


Figure 1.6: Hyperbolic tetrahedron with infinite vertex I

The ideas used to derive (1.10) can be extended to develop a formula for the volume of a hyperbolic tetrahedron with at most three finite vertices. This formula has been found by Vinberg in [16].

$$\begin{aligned}
 V(T_1(\gamma_1, \gamma_2, \gamma_3, \alpha_3, \alpha_1, \alpha_2)) &= \frac{1}{2} \sum_{i=1}^3 [\mathfrak{I}(\gamma_i) + \mathfrak{I}(\frac{1}{2}(\pi + \alpha_i - \alpha_{i+1} - \gamma_i)) \\
 &+ \mathfrak{I}(\frac{1}{2}(\pi - \alpha_i + \alpha_{i+1} - \gamma_i)) - \mathfrak{I}(\frac{1}{2}(\pi - \alpha_i - \alpha_{i+1} + \gamma_i)) - \mathfrak{I}(\frac{1}{2}(-\pi + \alpha_i + \alpha_{i+1} + \gamma_i))],
 \end{aligned}
 \tag{1.11}$$

where $\alpha_4 = \alpha_1$. $T_1(\gamma_1, \gamma_2, \gamma_3, \alpha_3, \alpha_1, \alpha_2)$ denotes the tetrahedron with at least one ideal vertex which has α_1, α_2 , and α_3 as the dihedral angles at the edges connecting its finite vertices and γ_1, γ_2 , and γ_3 as the dihedral angles at the edges which meet at one of its infinite vertices, as shown in Figure 1.6. Vinberg's formula also extends to the volume of a hyperbolic pyramid with an n -gonal base and an ideal apex. One simply replaces the 3 in the summation on the right hand side of (1.11) with n and extends the index on α_i and γ_i to n .

We now give a proof of (1.11) that is different from Vinberg's. Our proof takes inspiration from Figure 1.7 which Thurston uses to prove that a finite hyperbolic triangle can be expressed as the difference between an ideal triangle and three $\frac{2}{3}$ -ideal ones in [15].

Proof. Consider $T = T_1(A, B, C, A', B', C')$ in the Poincaré ball model of \mathbf{H}^3 . Let the face opposite to the infinite vertex of T be determined by the finite vertices

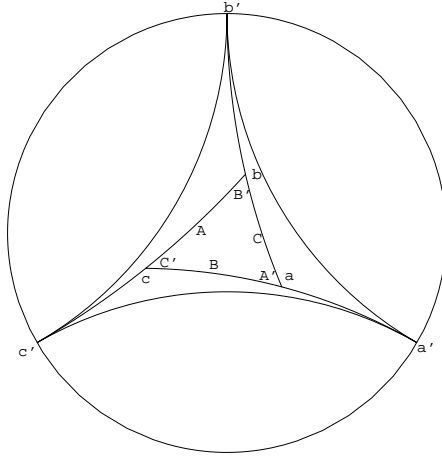


Figure 1.7: Thurston's proof that $\triangle abc = \triangle a'b'c' - \triangle aa'b' - \triangle bb'c' - \triangle cc'a'$

a , b , and c , and let this face coincide with the equatorial plane of the ball, as shown in Figure 1.7. Now extend each of the edges to infinity and connect the infinite points which are labeled by primed lower case letters in Figure 1.7. The primed capital letters in Figure 1.7 denote the dihedral angles at the edges connecting the corresponding vertex of T to its ideal vertex, while the unprimed capital letters denote the dihedral angles at the corresponding edges of T . Let I be the infinite vertex of T . Then

$$\{a, b, c, I\} = \{a', b', c', I\} - \{a, a', b', I\} - \{b, b', c', I\} - \{c, c', a', I\} \quad (1.12)$$

The dihedral angles of the tetrahedra on the right hand side of (1.12) can be easily deduced from the dihedral angles of $T_1(A, B, C, A', B', C')$ by using (1.7). For instance,

$$\begin{aligned} \{a, a', b', I\} = T_3(\pi - A', \pi - C, B, \\ (\pi - A' + C - B)/2, (\pi + A' - C - B)/2, (\pi + A' + C + B)/2). \end{aligned} \quad (1.13)$$

The dihedral angles of $\{b, b', c', I\}$ and $\{c, c', a', I\}$ can be computed by cyclically permuting the letters in (1.13).

Using these results along with (1.12) and the fact that $\{a', b', c', I\}$ inherits its dihedral angles from those of $\{a, a', b', I\}$, $\{b, b', c', I\}$ and $\{c, c', a', I\}$ we can

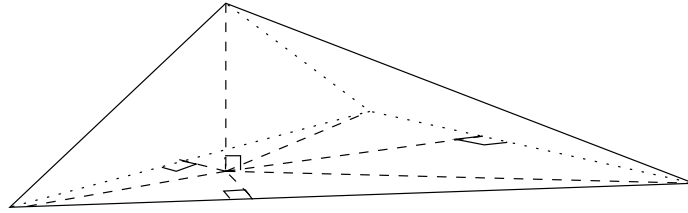


Figure 1.8: The decomposition of a tetrahedron into six orthoschemes

conclude that

$$\begin{aligned}
 T_1(A, B, C, A', B', C') = & \\
 & T((\pi + C - A' - B)/2, (\pi + A - B' - C)/2, (\pi + B - C' - A)/2) - \\
 & T_3(\pi - A', \pi - C, B, (\pi - A' + C - B)/2, (\pi + A' - C - B)/2, (\pi + A' + C + B)/2) - \\
 & T_3(\pi - C', \pi - B, A, (\pi - C' + B - A)/2, (\pi + C' - B - A)/2, (\pi + C' + B + A)/2) - \\
 & T_3(\pi - B', \pi - A, C, (\pi - B' + A - C)/2, (\pi + B' - A - C)/2, (\pi + B' + A + C)/2).
 \end{aligned} \tag{1.14}$$

Applying (1.10) to (1.14) yields formula (1.11). Starting with an n -gon instead of $\triangle abc$ gives the proof for an pyramid with an n -gonal base and an infinite vertex.

□

Finding the volume formula for a hyperbolic tetrahedron all of whose vertices are finite is considerably more difficult. The oldest method dates back to Lobachevsky, and involves decomposing the tetrahedron into six orthoschemes, as shown in Figure 1.8. One then uses the formula for the volume of an orthoscheme derived by Lobachevsky. Orthoschemes, also known as birectangular tetrahedra, are tetrahedra having the property that that the dihedral edges at the three non-coplanar edges are $\pi/2$. It will be shown in a later chapter how Lobachevsky's formula can be used to derive an explicit formula for the volume of an arbitrary hyperbolic tetrahedron in terms of its dihedral angles. One serious disadvantage of this formula is that it involves sums of \mathbb{J} applied to non-linear functions of

the angles of the orthoschemes. Since the dihedral angles of the orthoschemes used to decompose a tetrahedron are not, in general, linearly dependent on the dihedral angles of the tetrahedron, the resulting expression contains two levels of non-linearity in its dependence on the dihedral angles of the original tetrahedron. Thus, such a formula obscures the dihedral angle data of the original tetrahedron in addition to being rather long and complicated.

In 1999 Cho and Kim developed a volume formula for the general tetrahedron in terms of the \mathcal{J} without decomposing the tetrahedron into orthoschemes [2]. However, the arguments of \mathcal{J} in their formula are implicitly defined by a system of polynomial equations. In 2001 Murakami and Yano modified Cho and Kim's formula so as to make it an explicit function of the dihedral angles of a tetrahedron. Their formula possesses some remarkable symmetries and, but did not have an obvious geometric interpretation as they presented it. Inspired by the work of Murakami and Yano, Gregory Leibon came up with a new family of formulas similar to theirs which did have a very clear geometrical interpretation. In this dissertation we make use of his construction to solve a problem posed by Justin Roberts of whether the Regge symmetry is a scissors congruence in hyperbolic geometry by producing a constructive proof.

We also present an alternate formula for the volume of a tetrahedron which uses \mathcal{J} applied to function of its dihedral angles. We do this by a simple geometric construction which allows us to use (1.11).

The formula has been validated by numerical agreement with Hsiang's formula for the volume of a tetrahedron [8] as well as the formula derived by decomposing the tetrahedron into orthoschemes. Hsiang's approach did not use the Lobachevsky function and was thus completely different from that of Cho-Kim, Murakami-Yano, and the present thesis.

1.4 The Kubert identities

It can be easily shown that the function $\mathcal{J}(\theta) := -\int_0^\theta \log 2|\sin u|du$ satisfies what are known as the Kubert identities:

$$\mathcal{J}(n\theta) = n \sum_{k \pmod n} \mathcal{J}(\theta + k\pi/n) \quad (1.15)$$

for every integer n . Furthermore, (1.15) can be used to determine the Fourier series for \mathcal{J} up to a constant.

From the perspective of the earlier discussion about volumes and scissors congruences, the Kubert identities can be interpreted as identities relating volumes of certain ideal isosceles hyperbolic tetrahedra. This naturally leads to the question of whether the isosceles ideal tetrahedron $T(2n\theta, \pi/2 - n\theta, \pi/2 - n\theta)$ whose volume is given by twice the left hand side of (1.15) is scissors congruent to n n -tuples of isosceles ideal tetrahedra $T(2\theta + k\pi/n, \pi/2 - \theta - k\pi/2n, \pi/2 - \theta - k\pi/2n)$, where k varies from 0 to $n - 1$, whose volume is twice the right hand side of (1.15). The Dehn invariants of these two collections of tetrahedra can be easily computed to be equal, but this still does not guarantee their equidecomposability since the Dehn invariant and volume have not yet been proved to be sufficient for showing scissors congruence in \mathbb{H}^3 .

In 1982 Dupont and Sah proved that the tetrahedra whose volumes are represented by (1.15) are indeed scissors congruent [5]. However, their proof is purely algebraic; that is, it does not attempt to illustrate how these tetrahedra actually fit together. In this dissertation, we demonstrate the geometry underlying their proof and show how it connects to the cyclotomic identities

$$2 \sin(n\theta) = \prod_{k=0}^{n-1} 2 \sin(\theta + k\pi/n) \quad (1.16)$$

which are used to prove the Kubert identities analytically. This scissors congruence proof of the Kubert identities can be used to determine the Lobachevsky function up to a constant.

Chapter 2

A new formula for the volume of a hyperbolic tetrahedron

Let $T = T_0(A, B, C, A', B', C')$ denote a hyperbolic tetrahedron with finite vertices and dihedral angles A, B, C, A', B', C' , where every letter and its prime denote angles at opposite edges (see Figure 2.1). The basic strategy of our calculation of the volume of T is as follows. As shown in Figure 2.2, where the vertices of T are labeled as p_i , we extend the edge connecting p_1 to p_2 to the point at infinity which we call v_1^∞ . After calculating the dihedral angles of the tetrahedron T' determined by the points $\{v_1^\infty, p_2, p_3, p_4\}$ we find that

$$V(T) = V(\{v_1^\infty, p_2, p_3, p_4\}) - V(\{v_1^\infty, p_1, p_3, p_4\}), \quad (2.1)$$

where the right hand side of (2.1) is computed by Vinberg's formula (1.11).

In the special case of one of the vertices approaching infinity, our formula

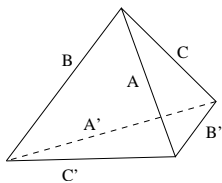


Figure 2.1: Finite hyperbolic tetrahedron $T_0(A, B, C, A', B', C')$

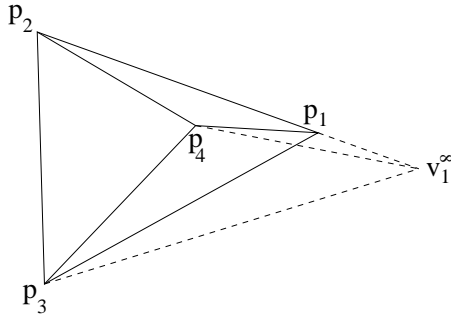


Figure 2.2: Hyperbolic tetrahedron T with one of its edges extended to infinity

reduces to (1.11). In the general case, the formula is a sum of \mathcal{I} applied to non-linear functions of the dihedral angles of the original tetrahedron. One of the byproducts of our formulation is that calculating the dihedral angles of the orthoschemes resulting from the decomposition of an arbitrary tetrahedron takes a few easy extra steps.

2.1 Background

$\mathbb{E}^{n,1}$, the $(n+1)$ -dimensional Minkowski space, is known the space which results from imposing on $\mathbb{R}^{(n+1)}$ the inner product

$$\langle x, y \rangle = -x_0y_0 + x_1y_1 + \cdots + x_ny_n, \quad (2.2)$$

where $x = (x_0, x_1, \dots, x_n)$ and $y = (y_0, y_1, \dots, y_n)$. This inner product determines a positive definite metric when restricted to the set $H = \{x \in \mathbb{R}^{(n+1)} \mid \langle x, x \rangle = -1\}$. Let $\mathbb{R}^{(n+1)+}$ denote the halfspace of $\mathbb{R}^{(n+1)}$ with $x_0 > 0$, and let $H^+ = H \cap \mathbb{R}^{(n+1)+}$. Then H^+ together with (2.2) represent the *hyperboloid model* of hyperbolic space \mathbb{H}^n .

For vectors $u, v \in \mathbb{E}^{n,1}$ of square length ± 1 ,

$$\langle u, v \rangle = \begin{cases} \cos \angle(u^\perp, v^\perp) & \text{if } u, v \text{ have square length } 1 \text{ and } u^\perp \text{ and } v^\perp \\ & \text{intersect} \\ \pm \cosh d(u^\perp, v^\perp) & \text{if } u, v \text{ have square length } 1 \text{ and } u^\perp \text{ and } v^\perp \text{ are} \\ & \text{ultraparallel} \\ \pm \sinh d(u, v^\perp) & \text{if } u \text{ has square length } -1 \text{ and } v \text{ has} \\ & \text{square length } 1 \\ -\cosh d(u, v) & \text{if } u, v \text{ have square length } -1, \end{cases} \quad (2.3)$$

where $\angle(u^\perp, v^\perp)$ denotes angle between the n -dimensional planes u^\perp and v^\perp with their respective orientations induced by u and v , and $d(x, y)$ denotes the distance between x and y for any $x, y \in \mathbb{E}^{n,1}$. The sign ambiguities in (2.3) can be resolved as follows. In the second case, consider Π , the n -dimensional plane spanned by some geodesic connecting u^\perp and v^\perp and the origin. If the respective orientations induced on u^\perp and v^\perp by u and v agree *with respect to* Π , then $\langle u, v \rangle = +\cosh d(u^\perp, v^\perp)$. In the third case the $+$ results if u and v lie in the same half-space of $\mathbb{E}^{n,1}$ with respect to v^\perp . A detailed discussion and proof of the results presented in (2.3) can be found in [15].

In the present work we make use of the hyperboloid model with $n = 3$. Let T be a tetrahedron in \mathbb{H}^3 , and let $\mathcal{P} = \{p_i\}_{i=1}^4$ be the set of position vectors of the vertices of T . \mathcal{P} is indexed so as to induce a positive orientation on T . The following construction is adapted from [16]. Let K be the convex hull of \mathcal{P} and 0 in $\mathbb{E}^{3,1}$. Define the set of normals to T , $\mathcal{N} = \{e_i\}_{i=1}^4$, as the unit vectors outwardly normal to the four three-dimensional faces of K which include the origin. The normals are indexed so that e_i^\perp is spanned by the face of T that is opposite to the vertex p_i and the origin.

Each of the normals e_i is of square length 1 since it is normal to the subspace of $\mathbb{E}^{3,1}$ where the inner product (2.2) is indefinite. Therefore, by (2.3), the matrix

of inner products of $\{e_i\}_{i=1}^4$ is given by

$$G = [-\cos \alpha_{ij}] \quad (2.4)$$

where α_{ij} is the interior dihedral angle between the i -th and j -th faces of the tetrahedron if $i \neq j$ and π otherwise. G is known as the *Gram Matrix* of T .

G not only determines T , but also yields a wealth of quantitative data related to T . This data will be extracted in the sections to follow.

2.2 Exterior Algebra in Minkowski Space

Let $\bigwedge^p \mathbb{E}^{n,1}$ for $p = 0, 1, 2, \dots, n, n+1$ be the space of p -vectors on $\mathbb{E}^{n,1}$. It follows that $\bigwedge^0 \mathbb{E}^{n,1} = \mathbb{R}$, $\bigwedge^{n+1} \mathbb{E}^{n,1} \cong \mathbb{R}$, and $\bigwedge^n \mathbb{E}^{n,1} \cong \mathbb{E}^{n,1}$. We are interested in the case $n = 3$ and the (Hodge) star operator $*$: $\bigwedge^3 \mathbb{E}^{3,1} \longrightarrow \mathbb{E}^{3,1}$.

We choose $\mathcal{N} = \{e_i\}_{i=1}^4$ as the basis for $\mathbb{E}^{3,1}$. It follows that $\{e_1 \wedge e_2 \wedge e_3 \wedge e_4\}$ and $\{e_1 \wedge e_2 \wedge e_3, e_1 \wedge e_4 \wedge e_2, e_1 \wedge e_3 \wedge e_4, e_3 \wedge e_2 \wedge e_4\}$ are bases for $\bigwedge^4 \mathbb{E}^{3,1}$ and $\bigwedge^3 \mathbb{E}^{3,1}$, respectively. Then $*$: $\bigwedge^3 \mathbb{E}^{3,1} \longrightarrow \mathbb{E}^{3,1}$ is defined so that

$$\lambda \wedge e_i = \langle * \lambda, e_i \rangle e_1 \wedge e_2 \wedge e_3 \wedge e_4, \quad (2.5)$$

where λ is an element of $\bigwedge^3 \mathbb{E}^{3,1}$ and $\langle \cdot, \cdot \rangle$ is the inner product defined in (2.2) [7]. It follows from the alternating property of wedge products that $*$ is determined by

$$* : e_j \wedge e_k \wedge e_l \longmapsto (-1)^i e_i^*, \quad (2.6)$$

where $j < k < l$ and i, j, k, l are distinct integers between 1 and 4 and $\{e_i^*\}_{i=1}^4$ is the vector space dual to $\{e_i\}_{i=1}^4$ in the sense that $\langle e_i^*, e_j \rangle = \delta_{ij}$.

Remark 1 *By linearity of the exterior multiplication it follows that $*(x \wedge y \wedge z)$ is normal to x , y , and z for any $x, y, z \in \mathbb{E}^{3,1}$. This is a key property in our development of the formula for the volume of T .*

At this point we can use the exterior algebraic results developed so far to extend the geometric results in §2.1 as follows. For $i = 1, 2, 3, 4$,

$$e_i^* = c_i p_i \quad (2.7)$$

for some negative scalar c_i . This is because $p_i \in e_j^\perp \cap e_k^\perp \cap e_l^\perp$ for distinct i, j, k, l , which is precisely the subspace of $\mathbb{E}^{3,1}$ spanned by e_i^* . Furthermore, c_i must be negative because $\langle e_i^*, e_i \rangle = 1 = c_i \langle p_i, e_i \rangle$, and $\langle p_i, e_i \rangle$ is negative since p_i and e_i are in two different halfspaces of $\mathbb{E}^{3,1}$ with respect to e_i^\perp (see (2.3) and the explanation following it). Now we can use the facts that the Gram matrix of the dual basis is G^{-1} (see [16] or [15]) and that p_i is of square length -1 to conclude that

$$c_i = -\sqrt{-g_{ii}^*/\det G}, \quad (2.8)$$

where g_{kl}^* is the kl -th entry in the matrix of cofactors of $G^* = G^{-1} \det G$.

Remark 2 *At this point, the computation of the volume of T by the method of dissecting T into orthoschemes (see §2.1) becomes quite simple. By (2.3), (2.7), and (2.8), the length of the altitude a_i of T extending from p_i and meeting the i -th face at a right angle is given by*

$$\sinh a_i = -\langle p_i, e_i \rangle = -\frac{1}{c_i} = \sqrt{\frac{-\det G}{g_{ii}^*}}, \quad (2.9)$$

while the length l_{ij} of the edge connecting p_i and p_j is given by

$$\cosh l_{ij} = -\langle p_i, p_j \rangle = \frac{g_{ij}^*}{\sqrt{g_{ii}^* g_{jj}^*}}. \quad (2.10)$$

Let T be decomposed into orthoschemes so that the altitude of T , a_i is dropped from vertex i . We denote the set of six orthoschemes $\{O_{jk}\}$ where j and k are distinct integers between 1 and 4 with $j, k \neq i$. j refers to the face of T whose subset forms a face of O_{jk} , and k refers to the vertex of T shared by O_{jk} . Furthermore, let A_{jk} denote the dihedral angle of O_{jk} at the edge a_i , and let B_{jk} denote the dihedral angle of O_{jk} at the edge joining its vertices i and k . The notation is summarized in Figure 2.3. Then the volume of O_{jk} is given in [16] by

$$\begin{aligned} V(O_{jk}) = \frac{1}{4} [& \mathfrak{L}(A_{jk} + \delta_{jk}) - \mathfrak{L}(A_{jk} - \delta_{jk}) + \mathfrak{L}(\alpha_{ij} + \delta_{jk}) - \mathfrak{L}(\alpha_{ij} - \delta_{jk}) \\ & - \mathfrak{L}(\frac{\pi}{2} - B_{jk} + \delta_{jk}) + \mathfrak{L}(\frac{\pi}{2} - B_{jk} - \delta_{jk}) + 2\mathfrak{L}(\frac{\pi}{2} - \delta_{jk})], \quad (2.11) \end{aligned}$$

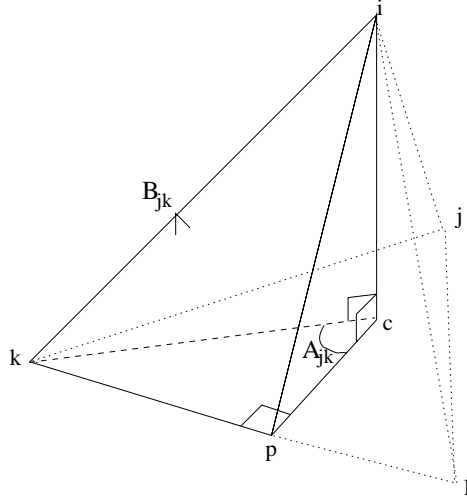


Figure 2.3: Orthoscheme O_{jk} shown as part of the tetrahedron which it is used to decompose. The tetrahedron is drawn with a dotted line

where

$$\delta_{jk} = \tan^{-1} \frac{\sqrt{\cos^2 B_{jk} \sec^2 A_{jk} - \tan^2 A_{jk} \sin^2 \alpha_{ij}}}{\cos \alpha_{ij}} \quad (2.12)$$

We compute A_{jk} by using (2.9), (2.10), and the hyperbolic laws of sines and cosines specialized to right triangles. Referring to Figure 2.3, we have

$$\cosh |kc| = \frac{\cosh l_{ik}}{\cosh a_i}, \quad (2.13)$$

$$\sinh |pc| = \cot \alpha_{ij} \tanh a_i, \quad (2.14)$$

and

$$\cos A_{ij} = \coth |kc| \tanh |pc|. \quad (2.15)$$

Thus

$$A_{jk} = \cos^{-1} \frac{g_{ik}^*}{\sqrt{g_{ik}^{*2} - g_{ii}^* g_{kk}^* + g_{kk}^* \det G}} \frac{\cot \alpha_{ij} \sqrt{-\det G}}{\sqrt{-\cot^2 \alpha_{ij} \det G + g_{ii}^* - \det G}}. \quad (2.16)$$

With the addition of the formula for B_{jk} in [16] we also have

$$B_{jk} = \cot^{-1} \frac{\tan A_{jk} \tanh a_i}{\tanh l_{ik}} \quad (2.17)$$

We finally have

$$V(T(\alpha_{12}, \alpha_{13}, \alpha_{14}, \alpha_{34}, \alpha_{24}, \alpha_{23})) = \sum_{j,k}^4 V(O_{jk}), \quad (2.18)$$

where j, k take on all the distinct integer values between 1 and 4 except i , and $V(O_{jk})$ are given by (2.11)-(2.17).

2.3 Main Theorem

In the hyperboloid model of \mathbb{H}^n each point at infinity corresponds to the span (over \mathbb{R}^+) of a vector of zero length in $\mathbb{E}^{n,1}$. In the following lemma the vectors which represent the endpoints of a given geodesic in \mathbb{H}^n are calculated in terms of the points p_1 and p_2 which determine that geodesic.

Lemma 3 *The endpoints of the geodesic l determined by the oriented geodesic segment (p_1, p_2) in \mathbb{H}^n are represented by the vectors $v_1^\infty = p_1 + \eta p_2$ and $v_2^\infty = p_2 + \eta p_1$, where*

$$\eta = \langle p_1, p_2 \rangle + \sqrt{(\langle p_1, p_2 \rangle)^2 - 1} \quad (2.19)$$

and the orientation of $(v_1^\infty, p_1, p_2, v_2^\infty)$ is consistent with that of (p_1, p_2) .

Proof. v_1^∞ and v_2^∞ are both in the 2-dimensional plane spanned by p_1 and p_2 , and they are each of length 0. Therefore, v_i^∞ for $i = 1, 2$ can be determined by finding the two roots of the quadratic equation $\langle (p_1 + \lambda p_2), (p_1 + \lambda p_2) \rangle = 0$. Assuming $\langle p_i, p_i \rangle = -1$ for $i = 1, 2$, we obtain $\lambda_1 = \langle p_1, p_2 \rangle + \sqrt{(\langle p_1, p_2 \rangle)^2 - 1}$ and $\lambda_2 = \langle p_1, p_2 \rangle - \sqrt{(\langle p_1, p_2 \rangle)^2 - 1} = 1/\lambda_1$ as the two solutions. If p_2 and l are fixed and p_1 moves towards v_1^∞ along l , the distance between p_1 and p_2 tends to infinity. By (2.10), so does $\langle p_1, p_2 \rangle$. It follows easily that λ_1 tends to 0, so that p_1 approaches $p_1 + \lambda_1 p_2$. Therefore, $v_1^\infty = p_1 + \lambda_1 p_2$. By interchanging 1 and 2 we obtain that $v_2^\infty = p_2 + \lambda_1 p_1$. \square

We now describe the the steps of the calculation of the volume of T as they were outlined in the Introduction. As shown in Figure 2.4, we extend the edge

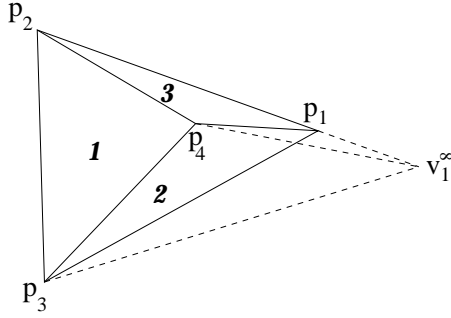


Figure 2.4: Hyperbolic tetrahedron T with one of its edges extended to infinity

connecting p_1 to p_2 to the point at infinity which we call v_1^∞ according to the notation of Lemma 3. In order to calculate the dihedral angles of the tetrahedron T' determined by the points $\{v_1^\infty, p_2, p_3, p_4\}$ we need an expression for Q , the outward unit normal to the face of T' determined by the points $\{v_1^\infty, p_3, p_4\}$. By Remark 1,

$$Q = \frac{*(v_1^\infty \wedge p_4 \wedge p_3)}{\sqrt{*(v_1^\infty \wedge p_4 \wedge p_3), *(v_1^\infty \wedge p_4 \wedge p_3)}} \quad (2.20)$$

But

$$*(v_1^\infty \wedge p_4 \wedge p_3) = *(p_1 \wedge p_4 \wedge p_3) + \eta(*(p_2 \wedge p_4 \wedge p_3)) \quad (2.21)$$

by Lemma 3 and the linearity of the exterior product. Furthermore, by (2.7) and (2.8)

$$p_1 \wedge p_4 \wedge p_3 = -\frac{(\sqrt{-\det G})^3}{\sqrt{g_{11}^* g_{33}^* g_{44}^*}} e_1^* \wedge e_4^* \wedge e_3^* \quad (2.22)$$

and

$$p_2 \wedge p_4 \wedge p_3 = -\frac{(\sqrt{-\det G})^3}{\sqrt{g_{22}^* g_{33}^* g_{44}^*}} e_2^* \wedge e_4^* \wedge e_3^* \quad (2.23)$$

From the definition of $*$ as described by (2.5) it is easy to verify that

$$*(e_1^* \wedge e_4^* \wedge e_3^*) = -e_2 \quad (2.24)$$

and

$$*(e_2^* \wedge e_4^* \wedge e_3^*) = e_1 \quad (2.25)$$

Therefore, by (2.20)-(2.25) and the linearity of $*$

$$Q = \mu(\sqrt{g_{22}^*}e_2 - \eta\sqrt{g_{11}^*}e_1) \quad (2.26)$$

where

$$\mu = \frac{1}{\sqrt{g_{22}^* + \eta^2 g_{11}^* + 2\eta\sqrt{g_{11}^* g_{22}^*} \cos \alpha_{12}}}, \quad (2.27)$$

$$\eta = \frac{-g_{12}^* + \sqrt{g_{12}^{*2} - g_{11}^* g_{22}^*}}{\sqrt{g_{11}^* g_{22}^*}} \quad (2.28)$$

by (2.28) and (2.10), and g_{kl}^* is the kl -th entry in the matrix of cofactors of G . We now use (2.3) to conclude that

$$[p_3, p_4] = \cos^{-1}\langle Q, e_2 \rangle + \alpha_{12} = \cos^{-1}(\mu(\sqrt{g_{22}^*} + \eta\sqrt{g_{11}^*} \cos \alpha_{12})) + \alpha_{12}, \quad (2.29)$$

and

$$\begin{aligned} [p_3, v_1^\infty] &= \pi - \cos^{-1}\langle Q, e_4 \rangle \\ &= \pi - \cos^{-1}(\mu(-\sqrt{g_{22}^*} \cos \alpha_{24} + \eta\sqrt{g_{11}^*} \cos \alpha_{14})), \end{aligned} \quad (2.30)$$

where $[x, y]$ denotes the dihedral angle at the edge connecting the vertices of T' with position vectors x and y . Since T' is uniquely determined by its angles $[p_3, p_4] + \alpha_{12}$, $\pi - \alpha_{24}$, $\pi - \alpha_{23}$, $[p_3, v_1^\infty]$, and α_{34} , we actually do not need $[p_4, v_1^\infty]$ for the final formula, but we compute it by the method developed so far for completeness:

$$\begin{aligned} [p_4, v_1^\infty] &= \pi - \cos^{-1}\langle Q, e_3 \rangle \\ &= \pi - \cos^{-1}(\mu(-\sqrt{g_{22}^*} \cos \alpha_{23} + \eta\sqrt{g_{11}^*} \cos \alpha_{13})). \end{aligned} \quad (2.31)$$

The computations in equations (2.27)-(2.30) are summarized in Table 2.1.

Thus we have proved

Theorem 1 *The volume of a hyperbolic tetrahedron T with all finite vertices and gram matrix $G = [-\cos \alpha_{ij}]$ is given by*

$$\begin{aligned} V &= V(T([p_4, v_1^\infty], [p_3, v_1^\infty], \alpha_{34}, \alpha_{14}, \alpha_{13}, [p_3, p_4])) \\ &\quad - V(T([p_4, v_1^\infty], [p_3, v_1^\infty], \alpha_{34}, \pi - \alpha_{24}, \pi - \alpha_{23}, [p_3, p_4] - \alpha_{12})), \end{aligned} \quad (2.32)$$

where all the relevant quantities are defined in Table 2.1.

1.	Compute $G^* = [g_{ij}^*]$, the matrix of cofactors of G .
2.	Compute $\eta = \frac{-g_{12}^* + \sqrt{g_{12}^{*2} - g_{11}^* g_{22}^*}}{\sqrt{g_{11}^* g_{22}^*}}$
3.	Compute $\mu = \frac{1}{\sqrt{g_{22}^* + \eta^2 g_{11}^* + 2\eta \sqrt{g_{11}^* g_{22}^*} \cos \alpha_{12}}}$
4.	Compute $[p_3, p_4] = \cos^{-1}(\mu(\sqrt{g_{22}^*} + \eta \sqrt{g_{11}^*} \cos \alpha_{12})) + \alpha_{12}$
5.	Compute $[p_3, v_1^\infty] = \pi - \cos^{-1}(\mu(-\sqrt{g_{22}^*} \cos \alpha_{24} + \eta \sqrt{g_{11}^*} \cos \alpha_{14}))$
6.	Compute $[p_4, v_1^\infty] = \pi - \cos^{-1}(\mu(-\sqrt{g_{22}^*} \cos \alpha_{23} + \eta \sqrt{g_{11}^*} \cos \alpha_{13}))$
7.	$V = V(T([p_4, v_1^\infty], [p_3, v_1^\infty], \alpha_{34}, \alpha_{14}, \alpha_{13}, [p_3, p_4]))$ $- V(T([p_4, v_1^\infty], [p_3, v_1^\infty], \alpha_{34}, \pi - \alpha_{24}, \pi - \alpha_{23}, [p_3, p_4] - \alpha_{12}))$, where $V(T(\gamma_1, \gamma_2, \gamma_3, \alpha_3, \alpha_1, \alpha_2))$ is the volume of a hyperbolic tetrahedron with one ideal vertex as defined in (1.11) and \mathcal{L} is the Lobachevsky function as defined in (1.3).

Table 2.1: Procedure for computing the volume V of an arbitrary hyperbolic tetrahedron with Gram matrix $G = [-\cos \alpha_{ij}]$.

2.4 Alternative Approach

The method described above does not require the introduction of a coordinate system and relies entirely on the angle data of a given tetrahedron. We now present a variation on this method which provides a way to calculate a set of coordinates for the vertices of the tetrahedron T in the standard Minkowskian basis and then use these coordinates to calculate the angles $[p_3, p_4]$, $[p_3, v_1^\infty]$, and $[p_4, v_1^\infty]$ described above. The coordinates of p_1 are chosen as $(1, 0, 0, 0)$ and the coordinates of p_2 are chosen as $(a, b, 0, 0)$, where the positive constants a and b are computed by a procedure described below. It then follows immediately that the coordinates of v_1^∞ are $(1, -1, 0, 0)$. Once the coordinates the vertices of T' (the convex hull of the vertices 2,3,4 of T and v_1^∞) are known, the unit normals to the faces of T' are easily computed by exploiting the dual relationship of the normals and the position vectors of the vertices. The computation of the necessary dihedral angles follows from taking the inner products of the normal vectors in question. The alternative method relies on the use of a standard Gram-Schmidt routine such as, for instance, the one in the Mathematica package. The steps of the method are summarized in Table 2.2.

Proof of steps 1-10 in Table 2.2

Steps 1-3.

Recall that G , the Gram matrix of T , is the matrix of the inner products of the outward unit normals of T as given by (2.4). We begin by reversing the order of rows and columns of G to ensure that the coordinates $(1, 0, 0, 0)$ will correspond to vertex 1 of T . Hence we get the matrix \tilde{G} which, together with the standard Minkowskian basis $\mathcal{M} = \{(1, 0, 0, 0), (0, 1, 0, 0), (0, 0, 1, 0), (0, 0, 0, 1)\}$ (i.e the rows of the identity matrix), we input to the Gram-Schmidt routine. The output, W , is a set of four vectors expressed in terms of the basis \mathcal{M} that are orthonormal with respect to the inner product determined by \tilde{G} . Since \tilde{G} represents the Lorentz

	Input	Computation	Output
1.	$G = [-\cos \alpha_{ij}]$	Reverse the order of the rows and columns	\tilde{G}
2.	I_4 and \tilde{G}	Gram-Schmidt procedure with respect to the inner product with matrix \tilde{G}	W
3.	W	Divide the fourth row by i , then reverse the order of the rows	\tilde{W}
4.	\tilde{W} and D	$(D\tilde{W})^T$	U
5.	U	Reverse the order of the rows, normalize each row with respect to the the metric given by $-D$.	\tilde{U} (position vectors of the vertices of T)
6.	\tilde{U}	Replace the first row of \tilde{U} with $(1, -1, 0, 0)$	Z
7.	Z and D	Compute $(DZ^{-1})^T$ and normalize each of its rows with respect to (2.2)	N' (normals to faces of T')
8.	N' and D	Compute $N'D(N')^T$	G'
9.	G'_{12}	$\pi - \cos^{-1} G'_{12}$	$[p_3, p_4]$
10.	G'_{24}	$\pi - \cos^{-1} G'_{24}$	$[p_3, v_1^\infty]$
11.	G'_{23}	$\pi - \cos^{-1} G'_{23}$	$[p_4, v_1^\infty]$
12.	$[p_3, p_4], [p_3, v_1^\infty],$ and $[p_4, v_1^\infty]$	Plug into (2.32)	Volume of T

Table 2.2: Procedure for computing the volume V of an arbitrary hyperbolic tetrahedron with Gram matrix $G = [-\cos \alpha_{ij}]$. D denotes the matrix with diagonal entries -1,1,1,1 and 0 elsewhere, and W has the vectors outputted by the Gram-Schmidt routine as its rows.

inner product given by (2.2) in the basis of the unit normals of T , we should expect that three of these vectors be spacelike and one timelike. Thus, three of the vectors should have square length 1 and one should have square length -1. However, a standard Gram-Schmidt routine will force the fourth vector to have square length 1, and in doing so will produce a fourth vector all of whose components are pure imaginary. Hence we divide the fourth vector of W by i . Subsequently, we reverse the order of the rows of W so that the resulting matrix \widetilde{W} has as its rows vectors that are orthonormal (in the sense of the timelike vector having negative unit length) with respect to the inner product (2.2).

Steps 4-5.

Let $N = \widetilde{W}^{-1}$. Since $D^2 = I_4$, it follows that

$$ND(D\widetilde{W}) = I_4. \quad (2.33)$$

Thus, if n_i is the i -th row of N , and w_j is the j -th row of $D\widetilde{W}$, (2.33) says that $\langle n_i, w_j \rangle = \delta_{ij}$, where $\langle \cdot, \cdot \rangle$ denotes the inner product determined by $D(-1, 1, 1, 1)$. Therefore, when viewed in the framework of §2.2, the rows of N are dual to the columns of $D\widetilde{W}$. Now, the rows of N represent the outward normals of T in terms of the basis determined by the rows of \widetilde{W} . It was shown in §2.2 that the set of normals of T is dual to the set of the position vectors of the vertices of T up to a scalar multiple. Therefore, after normalizing the rows of $(D\widetilde{W})^T$ with respect to the inner product (2.2) we obtain the position vertices of T . Since each row of $(D\widetilde{W})^T$ is a time-like vector, its square length is negative. In order to insure that the normalization scales each row by a positive real number we normalize with respect to the metric given by $-D$. In the resulting matrix the fourth and third rows are $(1, 0, 0, 0)$ and $(a, b, 0, 0)$ with $a, b \in \mathbb{R}^+$, respectively. We end by reversing the order of the rows to insure that these are the respective coordinates of the first and second vertices of T . This reordering has been accounted for in Step 1 by reversing the rows and columns of G to obtain \tilde{G} . Thus \tilde{U} is the 4×4 matrix whose

i -th row describes the position of the i -th vertex of T . In particular, the first row of \tilde{U} is $(1, 0, 0, 0)$, the second row is of the form $(a, b, 0, 0)$ for some positive a and b .

Step 6.

By plotting the coordinates of the first two vertices of T on the hyperbola $x_0^2 - x_1^2 = 1$ in the x_0x_1 plane one can see immediately that the endpoints of the geodesic determined by these vertices will be $(1, -1, 0, 0)$ and $(1, 1, 0, 0)$, where the orientation of the segment (p_1, p_2) is consistent with that imposed by $((1, -1, 0, 0), (1, 1, 0, 0))$. Thus the coordinates of v_1^∞ are $(1, -1, 0, 0)$. For Step 7 we need a matrix whose rows are the position vectors of the vertices of T' . Therefore, we replace the first row of \tilde{U} with the coordinates of v_1^∞ .

Step 7.

As in Step 4, we use the fact that $ZD(DZ^{-1}) = I_4$ and the duality of the normals and position vectors of hyperbolic tetrahedra to determine that normalized columns of DZ^{-1} are the unit normals of T' .

Step 8.

We compute G' , the Gram matrix of T' .

Steps 9-12.

We use the first of the equations (2.3) to find the angles $[p_3, p_4]$, $[p_3, v_1^\infty]$, and $[p_4, v_1^\infty]$. At this point the volume of T can be found from (2.32), (1.11), and (1.3).

2.5 Special Cases

If vertex 1 of T is infinite, i.e. p_1 is of length 0, (2.32) easily reduces to Vinberg's formula (1.11). In this case $g_{11}^* = 0$, so that $[p_3, p_4] = \alpha_{12}$, while $[p_3, v_1^\infty] = \alpha_{24}$, and $[p_4, v_1^\infty] = \alpha_{23}$. If vertex 2 of T is infinite it is necessary to evaluate limits of type $\frac{0}{0}$ in order to use (2.32). In this case (2.32) reduces to a formula for the volume of a tetrahedron with at least one infinite vertex that differs from Vinberg's formula yet outputs the same values. The situation is similar in the case when vertex 3 or vertex 4 is infinite. This points to the general fact that the formula we have developed in Theorem 1 is highly non-symmetric with respect to the four vertices of T . One can easily come up with three more formulas like (2.32) by extending vertices 2,3, or 4 to infinity. All four formulas give the correct answer but are not obviously equivalent. The existence of these various formulas for the volumes of the same tetrahedron apparently has to do with non-linear identities satisfied by \mathcal{H} . In some special cases the equivalence of these formulas for the volume yields some of the Kubert identities.

2.6 A numerical example of the computation of the volume of a hyperbolic tetrahedron using the method outlined in Table 2.2 of §2.4

Suppose we wish to compute the volume of a hyperbolic tetrahedron $T = T_0(\pi/3.5, \pi/3.8, \pi/3.1, \pi/2.2, \pi/2.01, \pi/2.1)$ whose Gram matrix is given by

$$G = \begin{pmatrix} -1 & -\cos(\pi/3.5) & -\cos(\pi/3.8) & -\cos(\pi/3.1) \\ -\cos(\pi/3.5) & -1 & -\cos(\pi/2.1) & -\cos(\pi/2.01) \\ -\cos(\pi/3.8) & -\cos(\pi/2.1) & -1 & -\cos(\pi/2.2) \\ -\cos(\pi/3.1) & -\cos(\pi/2.01) & -\cos(\pi/2.2) & -1 \end{pmatrix}. \quad (2.34)$$

Step 1. We reverse the order of the rows and columns to obtain

$$\tilde{G} = \begin{pmatrix} -1 & -\cos(\pi/2.2) & -\cos(\pi/2.01) & -\cos(\pi/3.1) \\ -\cos(\pi/2.2) & -1 & -\cos(\pi/2.1) & -\cos(\pi/3.8) \\ -\cos(\pi/2.01) & -\cos(\pi/2.1) & -1 & -\cos(\pi/3.5) \\ -\cos(\pi/3.1) & -\cos(\pi/3.8) & -\cos(\pi/3.5) & -1 \end{pmatrix}. \quad (2.35)$$

Step 2. We input the inner product given by \tilde{G} and the basis $\{(1, 0, 0, 0), (0, 1, 0, 0), (0, 0, 1, 0), (0, 0, 0, 1)\}$ into a Gram-Schmidt procedure. The output is

$$W = \begin{pmatrix} 1 & 0 & 0 & 0 \\ 0.143778 & 1.01028 & 0 & 0 \\ 0.0188875 & 0.0776407 & 1.00928 & 0 \\ -1.13184i & -1.42773i & -1.1991i & -1.73789i \end{pmatrix}. \quad (2.36)$$

Step 3. We divide the fourth row of W by i and then reverse the order of the rows to obtain

$$\tilde{W} = \begin{pmatrix} -1.13184 & -1.42773 & -1.1991 & -1.73789 \\ 0.0188875 & 0.0776407 & 1.00928 & 0 \\ 0.143778 & 1.01028 & 0 & 0 \\ 1 & 0 & 0 & 0 \end{pmatrix}. \quad (2.37)$$

Step 4. Let

$$D = \begin{pmatrix} -1 & 0 & 0 & 0 \\ 0 & 1 & 0 & 0 \\ 0 & 0 & 1 & 0 \\ 0 & 0 & 0 & 1 \end{pmatrix}. \quad (2.38)$$

Compute

$$U = (D\tilde{W})^T = \begin{pmatrix} 1.13184 & 0.0188875 & 0.143778 & 1 \\ 1.42773 & 0.0776407 & 1.01028 & 0 \\ 1.991 & 1.00298 & 0 & 0 \\ 1.73789 & 0 & 0 & 0 \end{pmatrix}. \quad (2.39)$$

Step 5. We normalize each row of U with respect to the metric given by $-D$ to obtain

$$\tilde{U} = \begin{pmatrix} 1 & 0 & 0 & 0 \\ 1.82465 & 1.52622 & 0 & 0 \\ 1.41944 & 0.0771901 & 1.00442 & 0 \\ 2.21958 & 0.0370392 & 0.281955 & 1.96104 \end{pmatrix}. \quad (2.40)$$

The rows of \tilde{U} give the coordinates of the respective vertices of T .

Step 6. We replace the first row of \tilde{U} with the coordinates of the point at infinity which is one of the endpoint of the geodesic determined by vertices 1 and two. The rows of the resulting matrix,

$$Z = \begin{pmatrix} 1 & -1 & 0 & 0 \\ 1.82465 & 1.52622 & 0 & 0 \\ 1.41944 & 0.0771901 & 1.00442 & 0 \\ 2.21958 & 0.0370392 & 0.281955 & 1.96104 \end{pmatrix}, \quad (2.41)$$

are the position vectors of T' as shown in Figure 2.4.

Step 7. We compute $(DZ^{-1})^T$ and normalize each of its rows with respect to the inner product given by D to obtain

$$N' = \begin{pmatrix} -0.57541 & -0.687923 & -0.7603 & -0.528964 \\ -0.568213 & 0.568213 & -0.846665 & -0.532127 \\ 0 & 0 & 0.989821 & -0.142315 \\ 0 & 0 & 0 & 1 \end{pmatrix}. \quad (2.42)$$

The rows of N' are the normal vectors to the respective faces of T' .

Step 8. We compute the Gram matrix of T' ,

$$G' = N'D(N')^T = \begin{pmatrix} 1 & 0.207352 & -0.677282 & -0.528964 \\ 0.207352 & 1 & -0.762317 & -0.532127 \\ -0.677282 & -0.762317 & 1 & -0.142315 \\ -0.528964 & -0.532127 & -0.142315 & 1 \end{pmatrix}. \quad (2.43)$$

Steps 9-11. We compute the dihedral angles of T' ,

$$[p_3, p_4] = \pi - \cos^{-1} G'_{12} - \alpha_{12} = 1.77966, \quad (2.44)$$

$$[p_3, v_1^\infty] = \pi - \cos^{-1} G'_{24} = 1.00969, \quad (2.45)$$

and

$$[p_4, v_1^\infty] = \pi - \cos^{-1} G'_{23} = 0.70391. \quad (2.46)$$

Step 12. Plugging $[p_3, p_4]$, $[p_3, v_1^\infty]$, and $[p_4, v_1^\infty]$ into (2.32) gives the final answer of .152838 as the volume of T .

Chapter 3

A scissors congruence proof of the Regge symmetry

The Regge symmetries are a family of involutive linear transformations on the six edges of a tetrahedron. They are defined as follows.

Definition 6 Let $T(A, B, C, A', B', C')$ denote a tetrahedron as shown in Figure 3.1. Define

$$R_a(T(A, B, C, A', B', C')) = T(A, s_a - B, s_a - C, A', s_a - B', s_a - C'), \quad (3.1)$$

where $s_a := (B + C + B' + C')/2$. Similarly, define

$$R_b(T(A, B, C, A', B', C')) := T(s_b - A, B, s_b - C, s_b - A', B', s_b - C'), \quad (3.2)$$

and

$$R_c(T(A, B, C, A', B', C')) := T(s_c - A, s_c - B, C, s_c - A', s_c - B', C'), \quad (3.3)$$

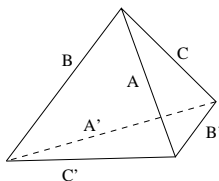


Figure 3.1: Tetrahedron $T(A, B, C, A', B', C')$ with its dihedral angles denoted by letters

where $s_b := (A + C + A' + C')/2$ and $s_c := (A + B + A' + B')/2$. Then R_a , R_b , and R_c generate the family of Regge symmetries of $T(A, B, C, A', B', C')$.

Any two maps out of R_a , R_b , and R_c , together with the tetrahedral symmetries, form a group isomorphic to $S_3 \times S_4$ [13].

The Regge symmetries first arose in conjunction with the $6j$ -symbol, which is a real number that can be associated to a labeling of the six edges of a tetrahedron by irreducible representations of $SU(2)$. In the 1960's, Tullio Regge discovered that the $6j$ -symbols are invariant under the linear transformations generated by R_a , R_b , and R_c . Expanding on his work in [13], Justin Roberts explored the effect of the Regge symmetries on Euclidean tetrahedra associated with the $6j$ -symbols. He found that the volumes of Euclidean tetrahedra as well as their Dehn invariants remain unchanged under the action of the Regge symmetries. Therefore, the Regge symmetries give rise to a family of scissors congruent Euclidean tetrahedra. In the hyperbolic case, it was unknown until now whether the Regge symmetries preserve equidecomposability, since the conjecture concerning the completeness of the volume and Dehn invariant as scissors congruence invariants is still open. In this chapter, we show that the Regge symmetries do indeed generate a family of scissors congruent tetrahedra by an explicit construction. The construction is based on a volume formula for a hyperbolic tetrahedron first developed by Jun Murakami and Masakazu Yano in [12], and later geometrically interpreted and generalized by Gregory Leibon in [9].

3.1 Murakami and Yano's formula for the volume of a hyperbolic tetrahedron

In 2001 Jun Murakami and Masakazu Yano developed the following remarkable new formula for the volume of a hyperbolic tetrahedron.

Theorem 2 (Murakami and Yano) *Let T denote a hyperbolic tetrahedron as shown in Figure 3.1, and let $a = e^{iA}$, $a' = e^{iA'}$, ..., $b' = e^{iB'}$. Let z_1 and z_2 be the*

two solutions of the quadratic equation

$$-\frac{1}{z}((1-z)(1-aba'b')(1-aca'c')(1-bcb'c') - (1+abcz)(1+ab'c'z)(1+ba'c')(1+ca'b'z)) = 0. \quad (3.4)$$

Furthermore, let $Z_1 = \arg z_1$, $Z_2 = \arg z_2$, $W_1 = A+B+C-\pi$, $W_2 = A+B'+C'-\pi$, $W_3 = B+A'+C'-\pi$, and $W_4 = C+A'+B'-\pi$. Define

$$U(T, Z) = \mathfrak{I}\left(\frac{Z}{2}\right) + \mathfrak{I}\left(\frac{Z+W_1+W_4}{2} - C\right) + \mathfrak{I}\left(\frac{Z+W_1+W_3}{2} - B\right) + \mathfrak{I}\left(\frac{Z+W_1+W_2}{2} - A\right) - \mathfrak{I}\left(\frac{Z+W_1}{2}\right) - \mathfrak{I}\left(\frac{Z+W_2}{2}\right) - \mathfrak{I}\left(\frac{Z+W_3}{2}\right) - \mathfrak{I}\left(\frac{Z+W_4}{2}\right), \quad (3.5)$$

$$\tilde{\Delta}(W, A, B, C) = \frac{\mathfrak{I}(W) - \mathfrak{I}(W-A) - \mathfrak{I}(W-B) - \mathfrak{I}(W-C)}{2}, \quad (3.6)$$

and

$$\Delta(T) = \tilde{\Delta}\left(\frac{W_1}{2}, A, B, C\right) + \tilde{\Delta}\left(\frac{W_2}{2}, A, B', C'\right) + \tilde{\Delta}\left(\frac{W_3}{2}, B, A', C'\right) + \tilde{\Delta}\left(\frac{W_4}{2}, C, A', B'\right). \quad (3.7)$$

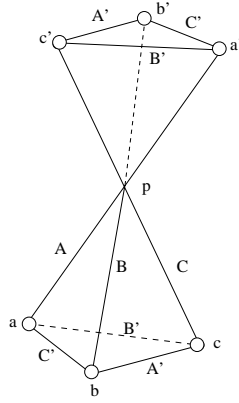
Then the volume of T is given by the absolute value of any of the following three expressions:

$$V(T) = U(T, Z_1) + \Delta(T), \quad (3.8)$$

$$V(T) = U(T, Z_2) + \Delta(T), \quad (3.9)$$

$$V(T) = \frac{U(T, Z_1) - U(T, Z_2)}{2}. \quad (3.10)$$

This was the first formula that produced the volume of the tetrahedron in terms of a sum of the Lobachevsky function (1.3) and was symmetric with respect to the group of symmetries of the tetrahedron. In addition, the action of the Regge symmetries on a tetrahedron merely permutes the terms of $U(z, T)$ and $\Delta(T)$ in equations (3.5) and (3.7). This shows that the Regge symmetries preserve not

Figure 3.2: Polyhedron D

only the volume but also the scissors congruence class of a tetrahedron, provided one can find a geometric interpretation of equations (3.8), (3.9), and (3.10). This geometric interpretation was provided by Gregory Leibon in [9].

3.2 Warm-up for the development Leibon's set of formulas for the volume of a hyperbolic tetrahedron

In this section we develop the basic idea that is central to Leibon's geometrization of Murakami and Yano's formula. We start by revisiting the construction for finding the volume of the tetrahedron $T_3(A, B, C, A', B', C')$ that was presented in §1.3. As before, we extend the three edges meeting at the non-ideal vertex to infinity, and obtain the polyhedron shown in Figure 3.2, which we will call D .

D is symmetric about the point p , so that its volume is twice that of $T_3(A, B, C, A', B', C')$. It will be convenient to view D as a simplicial complex which can be triangulated by oriented simplices as follows.

$$D = \{a, b, c, c'\} + \{a, a', b', c'\} + \{a, b', b, c'\}, \quad (3.11)$$

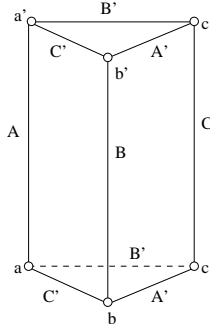


Figure 3.3: An ideal hyperbolic prism

where $\{x_1, x_2, x_3, x_4\}$ denotes the oriented hyperbolic tetrahedron with vertices x_1 , x_2 , x_3 , and x_4 . Now consider the ideal hyperbolic prism, P , shown in Figure 3.3. Viewed as a simplicial complex, P can be triangulated as

$$P = \{a, b, c, c'\} + \{a, a', b', c'\} + \{a, b', b, c'\}. \quad (3.12)$$

Equations (3.11) and (3.12) indicate that P and D are the same object from the point of view of homology. Clearly, P and D are embedded in space differently. In particular, P is convex while D is not. This is accounted for by the term $\{a, b, b', c'\}$ in equations (3.11) and (3.12). In the case of D , $\{a, b', b, c'\}$ represents a simplex with negative volume, while in the case of P , it represents a simplex with positive volume.

Just as D and P are the same object when viewed as simplicial complexes, they are also the same type of object from the point of view of hyperbolic geometry. Both D and P are completely determined by the dihedral angles A , B , and C (angles A' , B' , and C' are determined from the fact that the dihedral angles at any ideal vertex must add up to π , as discussed in §1.3). In the case of D , $A+B+C > \pi$, while in the case of P , $A+B+C < \pi$. P can be obtained by a continuous deformation of D which involves moving the point p outside the sphere at infinity. In the framework of the hyperboloid model of hyperbolic space presented in §2.1, this deformation is equivalent to moving the intersection of the planes which span

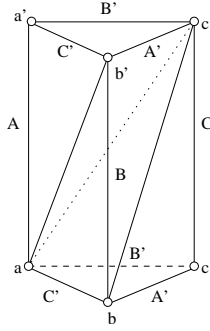


Figure 3.4: A triangulation of an ideal hyperbolic prism

the quadrilateral faces of D from the inside to the outside of the cone $x_0^2 + x_1^2 + x_2^2 = x_3^2$. In this process, the angles A , B , and C decrease. Since the volume of D and P depends only on these three angles, by analytic continuation D and P have the same volume formula. It is easier to see this formula in the case of P , since the three tetrahedra triangulating P do not intersect each other.

Letting $V(\{v_0, v_1, v_2, v_3\})$ represent the signed volume of an oriented simplex $\{v_0, v_1, v_2, v_3\}$, and using the fact that the opposite angles of an ideal hyperbolic tetrahedron are equal, we find that

$$\begin{aligned}
 V(\{a, b, c, c'\}) &= T(A', B', C) \\
 V(\{a, a', b', c'\}) &= T(A, B', C') \\
 V(\{a, b, b', c'\}) &= T(C' - C, B, \pi - B'),
 \end{aligned} \tag{3.13}$$

as shown in Figure 3.4. Applying the condition that the sum of the dihedral angles at an ideal vertex is π , we obtain

$$\begin{aligned}
 A' &= \frac{\pi + A - B - C}{2} \\
 B' &= \frac{\pi + B - A - C}{2} \\
 C' &= \frac{\pi + C - A - B}{2}.
 \end{aligned} \tag{3.14}$$

By (3.12) and (3.13)

$$2V(\{a, b, c, a', b', c'\}) = \mathfrak{L}(A) + \mathfrak{L}(A') + \mathfrak{L}(B) + \mathfrak{L}(B') + \mathfrak{L}(C) + \mathfrak{L}(C') - \mathfrak{L}\left(\frac{\pi + A + B + C}{2}\right), \quad (3.15)$$

where $\{a, b, c, a', b', c'\}$ is either the non-convex prism of Figure 3.2 or the convex prism of Figure 3.3.

3.3 Leibon's formulas for the volume of a hyperbolic tetrahedron

We now extend the ideas developed in §3.2 to a hyperbolic tetrahedron T with finite vertices. We start by extending all the edges of T to infinity. The resulting polyhedron, C , is shown in Figure 3.5. Clearly,

$$\begin{aligned} V(T) &= V(C) \\ &- (V(\{c'_1, a_1, b'_1, p_1\}) + V(\{a'_1, b'_2, c_1, p_2\}) + V(\{a'_2, b_1, c'_2, p_3\}) + V(\{a_2, b_2, c_2, p_4\})) \end{aligned} \quad (3.16)$$

As discussed in §3.2,

$$V(\{c'_1, a_1, b'_1, p_1\}) = V(\{c'_1, a_1, b'_1, c'_2, a_2, b'_2\})/2, \quad (3.17)$$

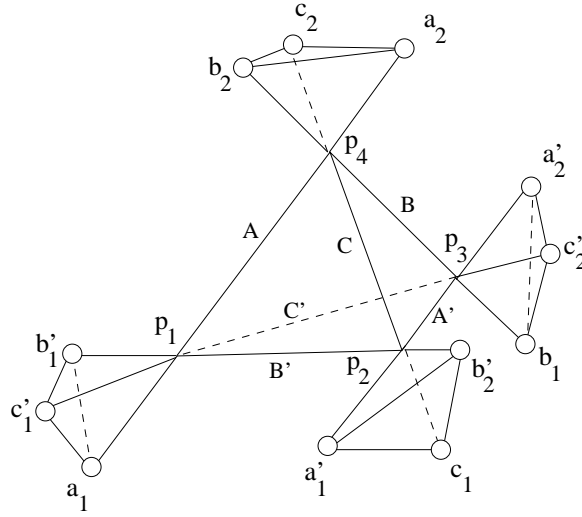
$$V(\{a'_1, b'_2, c_1, p_2\}) = V(\{a'_1, b'_2, c_1, a'_2, b'_1, c_2\})/2, \quad (3.18)$$

$$V(\{a'_2, b_1, c'_2, p_3\}) = V(\{a'_2, b_1, c'_2, a'_1, b_2, c'_1\})/2, \quad (3.19)$$

and

$$V(\{a_2, b_2, c_2, p_4\}) = V(\{a_2, b_2, c_2, a_1, b_1, c_1\})/2. \quad (3.20)$$

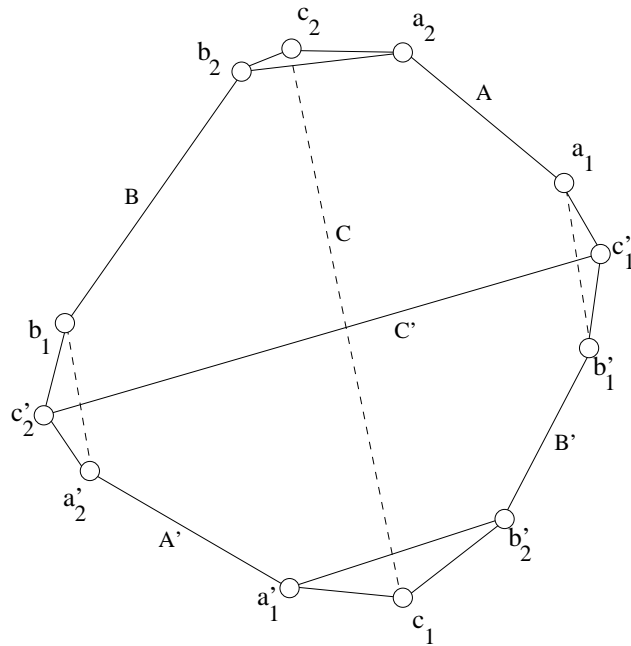
Therefore, we can easily find the volume of T with the help of (3.15) once we know the volume of C . In order to triangulate C , we first note that it is the same object as U (see Figure 3.6) from the point of view of homology, following the method of §3.2. That is, U can be obtained from C by pulling out the

Figure 3.5: Polyhedron C

points p_1 , p_2 , p_3 , and p_4 outside the sphere at infinity. So a triangulation of C by oriented simplices is also a triangulation of U . Under this deformation the non-convex prisms $\{c'_1, a_1, b'_1, c'_2, a_2, b'_2\}$, $\{a'_1, b'_2, c_1, a'_2, b'_1, c_2\}$, $\{a'_2, b_1, c'_2, a'_1, b_2, c'_1\}$, and $\{a_2, b_2, c_2, a_1, b_1, c_1\}$ become convex, but their volume formula stays the same by analytic continuation. Thus, we have established that

$$\begin{aligned}
 V(T) = V(U) &- V(\{c'_1, a_1, b'_1, c'_2, a_2, b'_2\})/2 - V(\{a'_1, b'_2, c_1, a'_2, b'_1, c_2\})/2 \\
 &- V(\{a'_2, b_1, c'_2, a'_1, b_2, c'_1\})/2 - V(\{a_2, b_2, c_2, a_1, b_1, c_1\})/2. \quad (3.21)
 \end{aligned}$$

In order to compute the volume of U we must triangulate it and then compute the volume of each of the simplices in its triangulation using formula (1.2). It turns out that no matter which way U is triangulated, some of the tetrahedra comprising it will have dihedral angles that are affine functions of the dihedral angles of T , while others will not. Leibon has looked at a particular family of 2^6 triangulations of U , each of which divides U up into six tetrahedra with dihedral angles that depend linearly on the dihedral angles of T and one octahedron whose dihedral angles are determined by a quadratic equation that is very similar to (3.4). The number 2^6 comes from the fact that the vertices of the octahedron can be chosen by

Figure 3.6: Polyhedron U

choosing exactly one of the vertices in each pair $\{a_1, a_2\}$, $\{b_1, b_2\}$, $\{c_1, c_2\}$, $\{a'_1, a'_2\}$, $\{b'_1, b'_2\}$, $\{c'_1, c'_2\}$. If one chooses both or neither of the vertices in any pair, then it is impossible to form a non-degenerate octahedron with the remaining vertices.

The 64 ways to cut U down to an octahedron can be grouped in four combinatorially distinct categories. Each category is described by four numbers between 0 and 3, each one of which indicates how many vertices of the octahedron are taken from a group of 3 vertices bounding a triangular face. For example, the octahedron formed by the convex hull of vertices a_2 , b_2 , c_2 , b'_1 , c'_1 , and a'_1 in Figure 3.6 falls into the category 3210, since it has 3 vertices from the group (a_2, b_2, c_2) , 2 from the group (a_1, b'_1, c'_1) , 1 from the group (a'_1, b'_2, c_1) and none from the group (a'_2, b_1, c'_2) . The four categories are 3210, 2211, 2220, and 3111.

The computations of the volume of U for each of the four categories are quite similar. We will illustrate the computation using a 2220 decomposition as an example. Here U is decomposed into a prism and three tetrahedra, and octahedron as shown in Figure 3.7. The prism and three tetrahedra resulting from this decom-

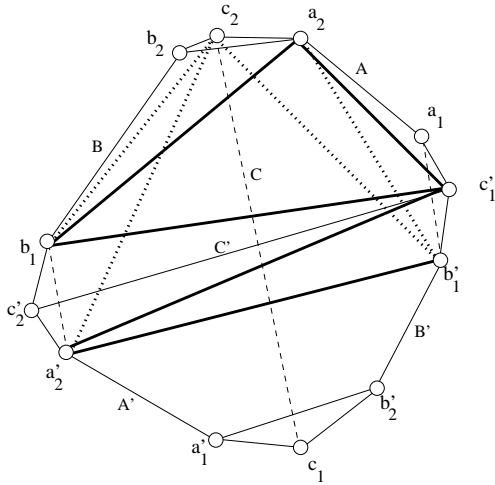


Figure 3.7: Decomposition of polyhedron U via the 2220 method; the edges of U are shown with thin and dashed lines, while the cuts of the decomposition are shown with thicker and dotted lines.

position are shown in Figure 3.8, while the octahedron O is shown in Figure 3.9.

The prism in Figure 3.8 can be decomposed into three ideal tetrahedra, as demonstrated in §3.2. In Figure 3.8, the dihedral angles other than those belonging to the original tetrahedron T were computed with the help of (3.14). For example, the dihedral angle at the edge (a_1, c'_1) was computed by considering the prism $\{c'_1, a_1, b'_1, c'_2, a_2, b'_2\}$. Since the dihedral angles at each pair of opposite edges of an ideal tetrahedron are equal, the labels in Figure 3.8 are enough to completely determine each tetrahedron. The dihedral angles of the octahedron O then follow immediately.

The octahedron in Figure 3.9 can be triangulated by drawing an edge from one of its vertices to a non-adjacent vertex. There are three distinct ways to do this. No matter which way is chosen, the dihedral angles of the resulting four tetrahedra can be determined by a family of 7 linear equations and one quadratic equation.

The following terminology will be used to describe the triangulation of an octahedron.

Definition 7 *The firepole of an octahedron is a segment joining one of its vertices*

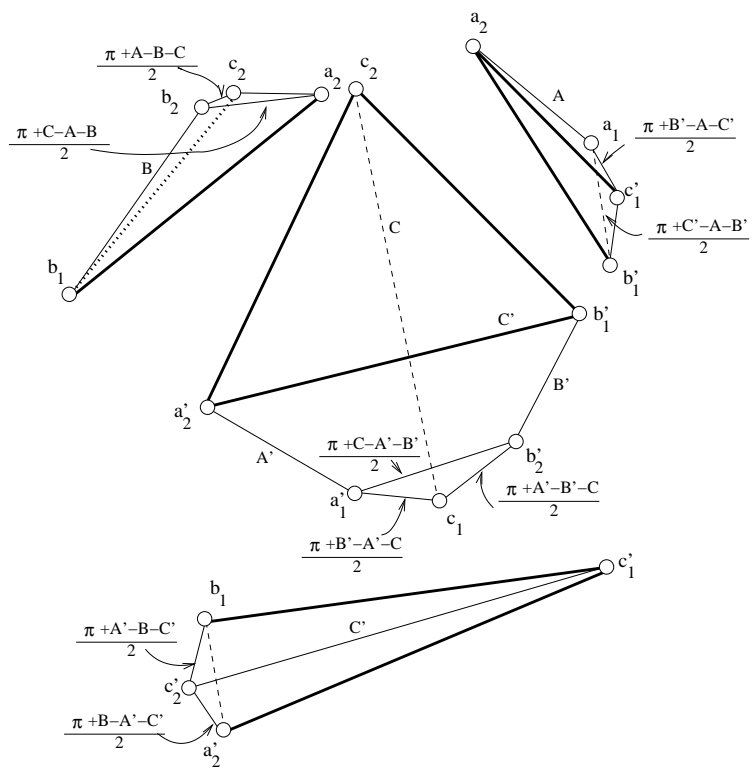


Figure 3.8: Decomposition of polyhedron U , Part I: the tetrahedra

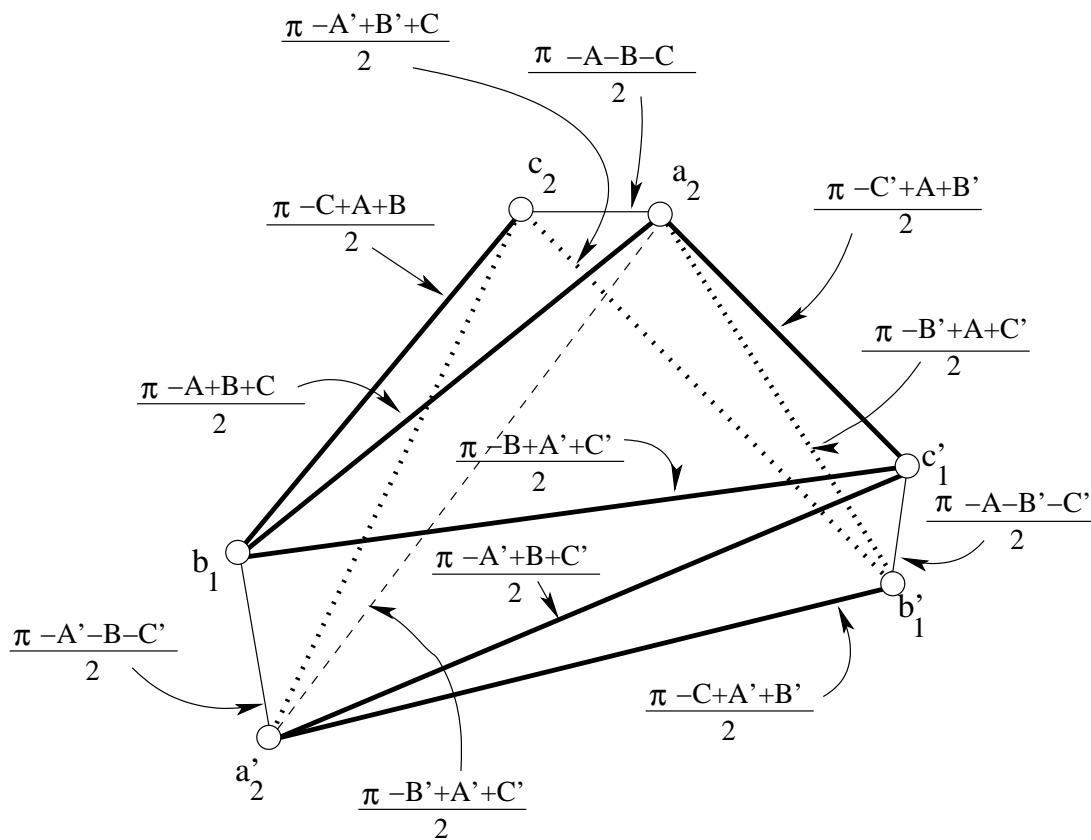
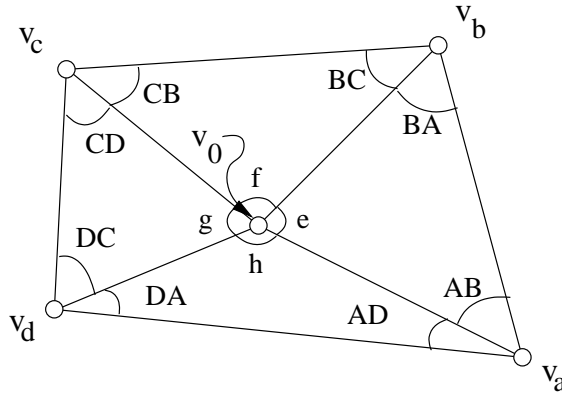


Figure 3.9: Decomposition of polyhedron U , Part II: the octahedron O

Figure 3.10: Octahedron O in the half-space model

with a another non-adjacent vertex.

In Figure 3.9 the firepole is the dashed line connecting the vertices a_2 and a'_2 . At this point it is easier to view O in the half-space model, with one of the ends of its firepole at the point at infinity. This is depicted in Figure 3.10. The segments $\{a_2, c'_1\}$, $\{a_2, b'_1\}$, $\{a_2, c_2\}$, $\{a_2, b_1\}$ become lines perpendicular to the plane at infinity in the half-space model, and their projection is seen in Figure 3.10 as vertices v_A, v_B, v_C , and v_D (these are vertices c'_1, b'_1, c_2 , and b_1 , respectively, in Figure 3.9). The angles of the quadrilateral at each of these vertices are a, b, c , and d , and they are equal to the angles dihedral angles of O at edges $\{v_0, v_a\}$, $\{v_0, v_b\}$, $\{v_0, v_c\}$, and $\{v_0, v_d\}$, since the half-space model is conformal. As seen in Figure 3.9, these angles are

$$\begin{aligned} a &= \frac{\pi - C' + A + B'}{2}; & b &= \frac{\pi - B' + A + C'}{2} \\ c &= \frac{\pi - A - B - C}{2}; & d &= \frac{\pi - A + B + C}{2} \end{aligned} \quad (3.22)$$

The edges with dihedral angles e, f, g, h are opposite to edges $\{v_a, v_b\}$, $\{v_b, v_c\}$, $\{v_c, v_d\}$, $\{v_d, v_a\}$, respectively, and the angles at those edges have already been computed (see Figure 3.9). Using the fact that opposite edges of an ideal tetrahe-

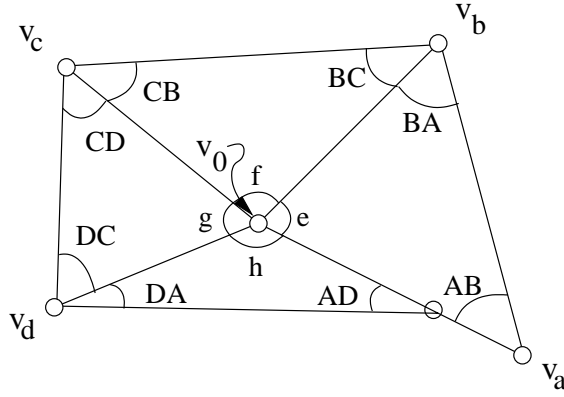


Figure 3.11: Four tetrahedra that satisfy equations (3.24)

dron have equal dihedral angles, we have

$$\begin{aligned}
 e &= \frac{\pi - A - B' - C'}{2}; & f &= \frac{\pi - A' + B' + C}{2} \\
 g &= \frac{\pi - C + A + B}{2}; & h &= \frac{\pi - B + A' + C'}{2}
 \end{aligned}
 \tag{3.23}$$

The unknown angles have been denoted as AB , BA , BC , CB , CD , DC , DA , and AD . These angles are subject to the following linear constraints:

$$\begin{aligned}
 AB + AD &= a; & AB + BA + e &= \pi \\
 BC + BA &= b; & BC + CB + f &= \pi \\
 CD + CB &= c; & CD + DC + g &= \pi \\
 DA + DC &= d; & DA + AD + h &= \pi
 \end{aligned}
 \tag{3.24}$$

The matrix expressing conditions (3.24) has a one-dimensional null space, so one more condition is needed to determine the 8 unknown angles. Geometrically, this last condition insures that the four ideal tetrahedra fit together. In other words, one can always fit together four tetrahedra that satisfy (3.24) as shown in Figure 3.11, since the faces of all ideal tetrahedra are ideal triangles, and, therefore, isometric to one another. In order avoid the situation in Figure 3.11, we need to ensure that once we fit the four tetrahedra together, the length of the segment $\{v_0, v_a\}$ does not change as we go around the quadrilateral $\{v_a, v_b, v_c, v_d\}$.

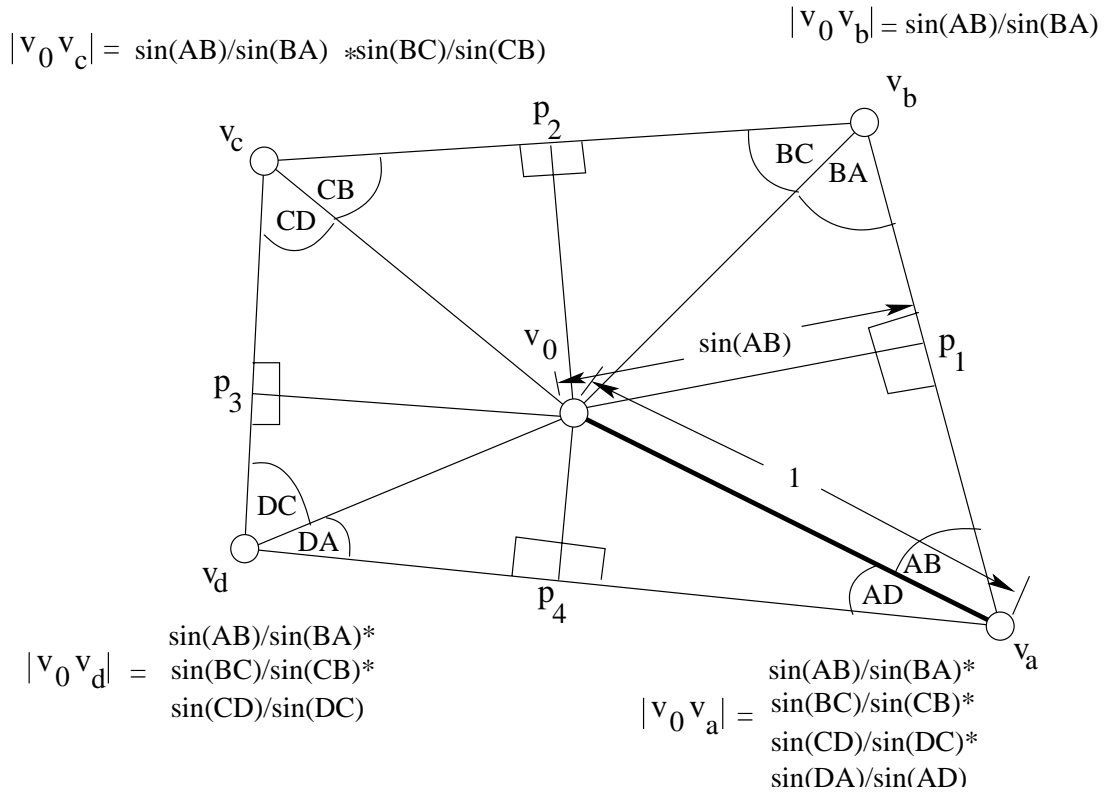


Figure 3.12: Non-linear condition for ensuring that four tetrahedra fit together to make an octahedron

In particular, if we assume that the length of the segment $\{v_0, v_a\}$ is equal to 1, and then express it in terms of the other lengths of the quadrilateral and equate the two quantities, we will get a non-trivial condition that, together with equations (3.24), will determine the unknown angles in Figure 3.10.

The equation we need is

$$\frac{\sin(AB) \sin(BC) \sin(CD) \sin(DA)}{\sin(BA) \sin(CB) \sin(DC) \sin(AD)} = 1, \quad (3.25)$$

and Figure 3.12 suggests how it is obtained. Since scaling is an isometry in hyperbolic space, we may assume without loss of generality that $|v_0 v_a| = 1$. Then by going counter-clockwise around Figure 3.12 and using basic trigonometry we obtain that $|v_0 p_1| = \sin(AB)$, $|v_0 v_b| = |v_0 p_1| / \sin(BA) = \sin(AB) / \sin(BA)$ and so on, until finally we arrive at the two equivalent expressions for $|v_0 v_a|$ in (3.25).

It is easier to solve the system of equations (3.24) and (3.25) if we first come up with a solution in the one-dimensional space that satisfies (3.24) and then use (3.25) to find the remaining unknown. Let $(\overline{AB}, \overline{BA}, \overline{BC}, \overline{CB}, \overline{CD}, \overline{DC}, \overline{DA}, \overline{AD})$ be a solution to the system of equations (3.24). Then there must be a Z such that

$$\begin{aligned}\overline{AB} + Z &= AB; & \overline{BA} - Z &= BA \\ \overline{BC} + Z &= BC; & \overline{CB} - Z &= CB \\ \overline{CD} + Z &= CD; & \overline{DC} - Z &= DC \\ \overline{DA} + Z &= DA; & \overline{AD} - Z &= AD.\end{aligned}\tag{3.26}$$

No matter what the value of Z is, the quantities on the right hand side of equations (3.26) still satisfy equations (3.24), since the sums in those equations are unchanged when Z is added to one summand and subtracted from the other one. After substituting (3.26) into (3.25) and letting $z = \exp iZ$ and

$$\begin{aligned}\alpha_1 &= \exp(i\overline{AB}); & \beta_1 &= \exp(i\overline{BA}) \\ \alpha_2 &= \exp(i\overline{BC}); & \beta_2 &= \exp(i\overline{CB}) \\ \alpha_3 &= \exp(i\overline{CD}); & \beta_3 &= \exp(i\overline{DC}) \\ \alpha_4 &= \exp(i\overline{DA}); & \beta_4 &= \exp(i\overline{AD}),\end{aligned}\tag{3.27}$$

we obtain

$$\begin{aligned}0 &= \frac{1}{\alpha_1\alpha_2\alpha_3\alpha_4} - \beta_1\beta_2\beta_3\beta_4 + z^2\left(-\frac{\alpha_1}{\alpha_2\alpha_3\alpha_4} - \frac{\alpha_2}{\alpha_1\alpha_3\alpha_4} - \frac{\alpha_3}{\alpha_1\alpha_2\alpha_4} - \frac{\alpha_4}{\alpha_1\alpha_2\alpha_3}\right. \\ &\quad \left. + \frac{\beta_1\beta_2\beta_3}{\beta_4} + \frac{\beta_1\beta_2\beta_4}{\beta_3} + \frac{\beta_1\beta_3\beta_4}{\beta_2} + \frac{\beta_2\beta_3\beta_4}{\beta_1}\right) \\ &\quad + z^4\left(\frac{\alpha_1\alpha_2}{\alpha_3\alpha_4} + \frac{\alpha_1\alpha_3}{\alpha_2\alpha_4} + \frac{\alpha_2\alpha_3}{\alpha_1\alpha_4} + \frac{\alpha_1\alpha_4}{\alpha_2\alpha_3} + \frac{\alpha_2\alpha_4}{\alpha_1\alpha_3} + \frac{\alpha_3\alpha_4}{\alpha_1\alpha_2}\right. \\ &\quad \left. - \frac{\beta_1\beta_2}{\beta_3\beta_4} - \frac{\beta_1\beta_3}{\beta_2\beta_4} - \frac{\beta_2\beta_3}{\beta_1\beta_4} - \frac{\beta_1\beta_4}{\beta_2\beta_3} - \frac{\beta_2\beta_4}{\beta_1\beta_3} - \frac{\beta_3\beta_4}{\beta_1\beta_2}\right) \\ &\quad + z^6\left(\frac{\beta_1}{\beta_2\beta_3\beta_4} + \frac{\beta_2}{\beta_1\beta_3\beta_4} + \frac{\beta_3}{\beta_1\beta_2\beta_4} + \frac{\beta_4}{\beta_1\beta_2\beta_3}\right. \\ &\quad \left. - \frac{\alpha_1\alpha_2\alpha_3}{\alpha_4} - \frac{\alpha_1\alpha_2\alpha_4}{\alpha_3} - \frac{\alpha_1\alpha_3\alpha_4}{\alpha_2} - \frac{\alpha_2\alpha_3\alpha_4}{\alpha_1}\right) + z^8\left(\alpha_1\alpha_2\alpha_3\alpha_4 - \frac{1}{\beta_1\beta_2\beta_3\beta_4}\right)\end{aligned}\tag{3.28}$$

By equations (3.24) and (3.26),

$$(\overline{AB} + \overline{BC} + \overline{CD} + \overline{DA}) + (\overline{BA} + \overline{CB} + \overline{DC} + \overline{AD}) = 2\pi,$$

so that

$$\alpha_1\alpha_2\alpha_3\alpha_4 = \frac{1}{\beta_1\beta_2\beta_3\beta_4}$$

by (3.27). This reduces (3.28) to a quadratic equation in z^2 .

Let z_+ (z_-) denote the solution of (3.28) corresponding to adding (subtracting) the square root of the discriminant. Then z_- gives the correct values of the angles of the octahedron O in Figure 3.9, while z_+ is of great significance as well and will be discussed in the next subsection.

3.3.1 Computation of the volume formula using the root z_- of the equation (3.28)

At this point we can write down the volume of the octahedron O (see Figures 3.9 and 3.10) using formula (1.2) for the volume of an ideal hyperbolic tetrahedron):

$$\begin{aligned} V(O) &= V(\{v_a, v_b, v_0, \infty\}) + V(\{v_b, v_c, v_0, \infty\}) + \\ &\quad V(\{v_c, v_d, v_0, \infty\}) + V(\{v_d, v_a, v_0, \infty\}) \\ &= \mathfrak{L}(AB) + \mathfrak{L}(BA) + \mathfrak{L}(e) + \mathfrak{L}(BC) + \mathfrak{L}(CB) + \mathfrak{L}(f) \\ &\quad \mathfrak{L}(CD) + \mathfrak{L}(DC) + \mathfrak{L}(g) + \mathfrak{L}(DA) + \mathfrak{L}(AD) + \mathfrak{L}(h). \end{aligned} \quad (3.29)$$

Substituting (3.26) and (3.23) into (3.29) and setting $Z = \arg z_-$, we have

$$\begin{aligned} V(O) &= \mathfrak{L}(\overline{AB} + \arg z_-) + \mathfrak{L}(\overline{BA} - \arg z_-) + \mathfrak{L}(\overline{BC} + \arg z_-) \\ &\quad + \mathfrak{L}(\overline{CB} - \arg z_-) + \mathfrak{L}(\overline{CD} + \arg z_-) + \mathfrak{L}(\overline{DC} - \arg z_-) \\ &\quad + \mathfrak{L}(\overline{DA} + \arg z_-) + \mathfrak{L}(\overline{AD} - \arg z_-) + \mathfrak{L}\left(\frac{\pi - A - B' - C'}{2}\right) \\ &\quad + \mathfrak{L}\left(\frac{\pi - A' + B' + C}{2}\right) + \mathfrak{L}\left(\frac{\pi - C + A + B}{2}\right) + \mathfrak{L}\left(\frac{\pi - B + A' + C'}{2}\right), \end{aligned} \quad (3.30)$$

where \overline{AB} , etc. are chosen as

$$\begin{aligned}
\overline{AB} &= \frac{A + A' + 2B'}{4}; & \overline{BA} &= \frac{2\pi + A - A' + 2C'}{4} \\
\overline{BC} &= \frac{A + A' - 2B'}{4}; & \overline{CB} &= \frac{2\pi - A + A' - 2C'}{4} \\
\overline{CD} &= \frac{-A - A' - 2B}{4}; & \overline{DC} &= \frac{2\pi - A + A' + 2C}{4} \\
\overline{DA} &= \frac{-A - A' + 2B}{4}; & \overline{AD} &= \frac{2\pi + A - A' - 2C'}{4}.
\end{aligned} \tag{3.31}$$

The volume of the three tetrahedra and prism in Figure 3.8 that comprise $U - O$ can be computed using (1.2) and (3.15).

$$\begin{aligned}
V(U) - V(O) &= V(\{a'_2, b_1, c'_2, c'_1\}) + V(\{c'_1, a_1, b'_1, a_2\}) + \\
&\quad V(\{a_2, b_2, c_2, b_1\}) + V(\{a'_1, b'_2, c_1, a'_2, b'_1, c_2\}) \\
&= \mathfrak{L}(C') + \mathfrak{L}\left(\frac{\pi + B - A' - C'}{2}\right) + \mathfrak{L}\left(\frac{\pi + A' - B - C'}{2}\right) \\
&\quad + \mathfrak{L}(A) + \mathfrak{L}\left(\frac{\pi + B' - A - C'}{2}\right) + \mathfrak{L}\left(\frac{\pi + C' - A - B'}{2}\right) \\
&\quad + \mathfrak{L}(B) + \mathfrak{L}\left(\frac{\pi + A - B - C}{2}\right) + \mathfrak{L}\left(\frac{\pi + C - A - B}{2}\right) \\
&\quad + \mathfrak{L}(A') + \mathfrak{L}(B') + \mathfrak{L}(C) + \mathfrak{L}\left(\frac{\pi + C - A' - B'}{2}\right) \\
&\quad + \mathfrak{L}\left(\frac{\pi + A' - B' - C}{2}\right) + \mathfrak{L}\left(\frac{\pi + B' - A' - C}{2}\right) \\
&\quad - \mathfrak{L}\left(\frac{\pi + A' + B' + C}{2}\right).
\end{aligned} \tag{3.32}$$

Combining equations (3.30) and (3.32), and using the fact that \mathfrak{L} is odd and

π -periodic gives

$$\begin{aligned}
V(U) = & \mathfrak{L}(\overline{AB} + \arg z_-) + \mathfrak{L}(\overline{BA} - \arg z_-) + \\
& \mathfrak{L}(\overline{BC} + \arg z_-) + \mathfrak{L}(\overline{CB} - \arg z_-) + \\
& \mathfrak{L}(\overline{CD} + \arg z_-) + \mathfrak{L}(\overline{DC} - \arg z_-) + \\
& \mathfrak{L}(\overline{DA} + \arg z_-) + \mathfrak{L}(\overline{AD} - \arg z_-) + \\
& + \mathfrak{L}(A) + \mathfrak{L}(A') + \mathfrak{L}(B) + \mathfrak{L}(B') + \mathfrak{L}(C) + \mathfrak{L}(C') \\
& + \mathfrak{L}\left(\frac{\pi - A - B' - C'}{2}\right) + \mathfrak{L}\left(\frac{\pi + A' - B - C'}{2}\right) \\
& + \mathfrak{L}\left(\frac{\pi + B' - A - C'}{2}\right) + \mathfrak{L}\left(\frac{\pi + C' - A - B'}{2}\right) \\
& + \mathfrak{L}\left(\frac{\pi + A - B - C}{2}\right) + \mathfrak{L}\left(\frac{\pi + C - A' - B'}{2}\right) \\
& + \mathfrak{L}\left(\frac{\pi + B' - A' - C}{2}\right) - \mathfrak{L}\left(\frac{\pi + A' + B' + C}{2}\right) \tag{3.33}
\end{aligned}$$

Finally, plugging (3.33) into (3.21) and using formulas (3.15) and (3.14) gives

$$\begin{aligned}
V(T) = & \mathfrak{L}(\overline{AB} + \arg z_-) + \mathfrak{L}(\overline{BA} - \arg z_-) + \mathfrak{L}(\overline{BC} + \arg z_-) \\
& + \mathfrak{L}(\overline{CB} - \arg z_-) + \mathfrak{L}(\overline{CD} + \arg z_-) + \mathfrak{L}(\overline{DC} - \arg z_-) \\
& + \mathfrak{L}(\overline{DA} + \arg z_-) + \mathfrak{L}(\overline{AD} - \arg z_-) + \frac{1}{2} \left[\mathfrak{L}\left(\frac{\pi + A - B - C}{2}\right) \right. \\
& - \mathfrak{L}\left(\frac{\pi + B - A - C}{2}\right) - \mathfrak{L}\left(\frac{\pi + C - A - B}{2}\right) + \mathfrak{L}\left(\frac{\pi + B' - A' - C}{2}\right) \\
& + \mathfrak{L}\left(\frac{\pi + A + B + C}{2}\right) + \mathfrak{L}\left(\frac{\pi + C - A' - B'}{2}\right) + \mathfrak{L}\left(\frac{\pi - A' + B' + C}{2}\right) \\
& - \mathfrak{L}\left(\frac{\pi + A' + B' + C}{2}\right) + \mathfrak{L}\left(\frac{\pi + A' - B - C'}{2}\right) - \mathfrak{L}\left(\frac{\pi + A + B' + C'}{2}\right) \\
& - \mathfrak{L}\left(\frac{\pi + A - B' - C'}{2}\right) + \mathfrak{L}\left(\frac{\pi + B' - A - C'}{2}\right) - \mathfrak{L}\left(\frac{\pi - A' - B + C'}{2}\right) \\
& \left. + \mathfrak{L}\left(\frac{\pi + A' - B - C'}{2}\right) + \mathfrak{L}\left(\frac{\pi + A' + B + C'}{2}\right) + \mathfrak{L}\left(\frac{\pi - A - B' + C'}{2}\right) \right], \tag{3.34}
\end{aligned}$$

where the quantities with bars are given by (3.31), and z_- is the solution of the quadratic equation (3.28) with the negative square root.

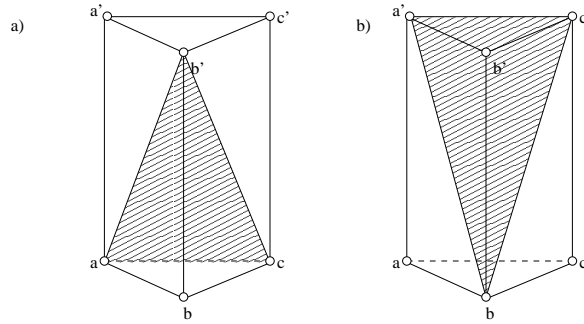


Figure 3.13: A triangular prism divided into two parts

3.3.2 Computation of the volume formula using the root z_+ of the equation (3.28)

When z_- is replaced by z_+ in equation (3.34) one gets $-V(T)$ instead of $V(T)$. This surprising result has a very concrete geometrical explanation. The main idea is that the octahedron O has a dual octahedron O' associated with it, and that $V(T)$ can be expressed in terms of either O or O' . It will be shown below that the solution z_+ of (3.28) solves the angles of a triangulation of the octahedron O' .

To begin with, let us go back to the triangular prism. A plane determined by any of the 3 vertices of the prism divides it into two polyhedra (one of these could be the degenerate flat polyhedron); for example, see Figure 3.13. One way we could express half of the volume of the prism is by averaging the volumes of $\{a, b, c, b'\}$ and $\{a, c, c', a', b'\}$, as suggested in Figure 3.13a), so that

$$\frac{V(P)}{2} = \frac{V(\{a, b, c, b'\}) + V(\{a, c, c', a', b'\})}{2}. \quad (3.35)$$

Due to the symmetry of the prism, $\{a, b, c, b'\}$ is isometric to $\{a', b', c', b\}$, and $\{a, c, c', a', b'\}$ is isometric to $\{a', c', c, a, b\}$. Thus we can rewrite (3.35) as

$$\frac{V(P)}{2} = \frac{|V(\{a, b, c, b'\})| + |V(\{a, c, c', a', b'\})|}{2}. \quad (3.36)$$

Let us introduce the following notation in order to generalize this discussion.

Definition 8 Let P be a triangular prism with vertices $V_P = \{a, b, c, a', b', c'\}$, and

let $H_P = \{v_i\}$, where $v_i \in V_P$. Then H_P^c is the reflection of $P - H_P$ in the plane of symmetry P . It follows that $|V(H_P)| + |V(H_P^c)| = 2V(P)$.

In the above definition, $\{a, b, c, b'\}_P = \{a, c, c', a', b'\}_P^c$ and $\{a', b', c', b\}_P = \{a, c, c', a', b'\}_P^c$.

We will now show how to recast equation (3.21) in terms of this basic idea. First, let us recall the construction of the octahedron O . As described earlier, O (see Figure 3.9) was constructed by selecting one vertex from each edge of U (see Figure 3.7). It follows that each of the four hexagonal faces of U coincides with a face of O . There is a one-to-one correspondence between the other four faces of O and the four prisms

$$\begin{aligned} P_1 &= \{c'_1, a_1, b'_1, c'_2, a_2, b'_2\} \\ P_2 &= \{a'_1, b'_2, c_1, a'_2, b'_1, c_2\} \\ P_3 &= \{a'_2, b_1, c'_2, a'_1, b_2, c'_1\} \\ P_4 &= \{a_2, b_2, c_2, a_1, b_1, c_1\} \end{aligned}$$

To be more precise, given each prism, there is exactly one face of the octahedron O that divides it into two polyhedra in the manner of Figure 3.13 are divided. For example, P_1 is divided into $\{c'_1, a_1, b'_1, a_2\}$ and $\{c'_1, b'_1, b'_2, c'_2, a_2\}$.

Let the four subsets of prisms in Figure 3.8 be labeled as

$$\begin{aligned} H_{P_1} &= \{c'_1, a_1, b'_1, a_2\} \\ H_{P_2} &= \{a'_1, b'_2, c_1, a'_2, b'_1, c_2\} \\ H_{P_3} &= \{a'_2, b_1, c'_2, c'_1\} \\ H_{P_4} &= \{a_2, b_2, c_2, b_1\}. \end{aligned}$$

Then we can rewrite equation (3.21) as follows:

$$\begin{aligned}
V(T) &= V(U) - V(P_1)/2 - V(P_2)/2 - V(P_3)/2 - V(P_4)/2 \\
&= V(O) + V(H_{P_1}) + V(H_{P_2}) + V(H_{P_3}) + V(H_{P_4}) \\
&\quad - V(P_1)/2 - V(P_2)/2 - V(P_3)/2 - V(P_4)/2 \\
&= V(O) + V(H_{P_1}) + V(H_{P_2}) + V(H_{P_3}) + V(H_{P_4}) \\
&\quad - \frac{V(H_{P_1}) + V(H_{P_1}^c)}{2} - \frac{V(H_{P_2}) + V(H_{P_2}^c)}{2} \\
&\quad - \frac{V(H_{P_3}) + V(H_{P_3}^c)}{2} - \frac{V(H_{P_4}) + V(H_{P_4}^c)}{2} \\
&= V(O) + \frac{V(H_{P_1}) - V(H_{P_1}^c)}{2} + \frac{V(H_{P_2}) - V(H_{P_2}^c)}{2} \\
&\quad + \frac{V(H_{P_3}) - V(H_{P_3}^c)}{2} + \frac{V(H_{P_4}) - V(H_{P_4}^c)}{2} \tag{3.37}
\end{aligned}$$

We now introduce O' , the octahedron dual to O . With Figure 3.7 in mind, one can visualize sliding the vertices of O , $\{a_2, c_2, b_1, a'_2, b'_1, c'_1\}$, along the respective edges labeled as A, C, B, A', B', C' until they hit the vertex at the end of that edge. The resulting octahedron is O' . In other words O' is the convex hull of the vertices $\{a_1, c_1, b_2, a'_1, b'_2, c'_2\}$. Now we can express the volume of U as

$$V(U) = V(O') + V(H_{P_1}^c) + V(H_{P_2}^c) + V(H_{P_3}^c) + V(H_{P_4}^c), \tag{3.38}$$

so that

$$\begin{aligned}
V(T) &= V(U) - \frac{V(H_{P_1}) + V(H_{P_1}^c)}{2} - \frac{V(H_{P_2}) + V(H_{P_2}^c)}{2} \\
&\quad - \frac{V(H_{P_3}) + V(H_{P_3}^c)}{2} - \frac{V(H_{P_4}) + V(H_{P_4}^c)}{2} \\
&= V(O') + V(H_{P_1}^c) + V(H_{P_2}^c) + V(H_{P_3}^c) + V(H_{P_4}^c) \\
&\quad - \frac{V(H_{P_1}) + V(H_{P_1}^c)}{2} - \frac{V(H_{P_2}) + V(H_{P_2}^c)}{2} \\
&\quad - \frac{V(H_{P_3}) + V(H_{P_3}^c)}{2} - \frac{V(H_{P_4}) + V(H_{P_4}^c)}{2} \\
&= V(O') - \frac{V(H_{P_1}) - V(H_{P_1}^c)}{2} - \frac{V(H_{P_2}) - V(H_{P_2}^c)}{2} \\
&\quad - \frac{V(H_{P_3}) - V(H_{P_3}^c)}{2} - \frac{V(H_{P_4}) - V(H_{P_4}^c)}{2} \tag{3.39}
\end{aligned}$$

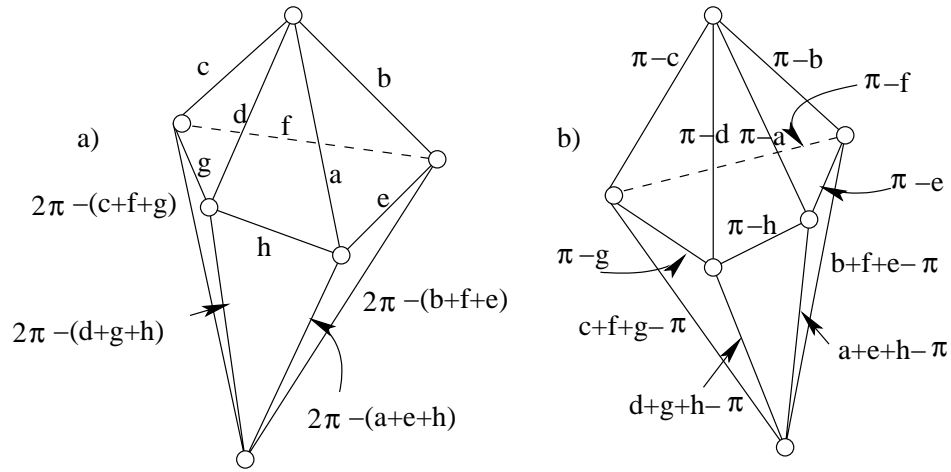


Figure 3.14: a) The original octahedron O with its dihedral angles labeled. b) The dual octahedron O'

Comparing equations (3.37) and (3.39) shows that if $V(O)$ is replaced with $-V(O')$, one gets $-V(T)$ instead of $V(T)$.

The only thing remaining to be shown is that by replacing z_- with z_+ in (3.34) one is swapping $V(O)$ for $-V(O')$. To see this, let us examine the quantitative relationship of O and O' .

Recall Figure 3.13, where we saw that $\{a, b, c, b'\}$ is isometric to $\{a', b', c', b\}$. As stated earlier, we can visualize the process of getting from Figure 3.13a) to Figure 3.13b) as sliding the vertices a, b', c along the edges $\{a, a'\}$, $\{b, b'\}$, $\{c, c'\}$, respectively. If measure the change in the angle θ between the oriented faces $\{a, c, b'\}$ and $\{a, b, c'\}$ during this process, we find that θ changes to $\pi - \theta$ in Figure 3.13b). Extending this process to O and O' , we see that dihedral angles of O and O' add up to π , as shown in the Klein model drawings in Figure 3.14. Finding the dihedral angles of the four tetrahedra that triangulate O' results in a

set of linear constraints similar to (3.24):

$$\begin{aligned}
AB + AD &= \pi - a; & AB + BA + \pi - e &= \pi \\
BC + BA &= \pi - b; & BC + CB + \pi - f &= \pi \\
CD + CB &= \pi - c; & CD + DC + \pi - g &= \pi \\
DA + DC &= \pi - d; & DA + AD + \pi - h &= \pi
\end{aligned} \tag{3.40}$$

We can choose a solution $(\widetilde{AB}, \widetilde{BA}, \widetilde{BC}, \widetilde{CB}, \widetilde{CD}, \widetilde{DC}, \widetilde{DA}, \widetilde{AD})$ to equations (3.40) such that

$$\widetilde{AB} = -\overline{AB}; \quad \widetilde{BC} = -\overline{BC}; \quad \widetilde{CD} = -\overline{CD}; \quad \widetilde{DA} = -\overline{DA} \tag{3.41}$$

and

$$\widetilde{BA} = \pi - \overline{BA}; \quad \widetilde{CB} = \pi - \overline{CB}; \quad \widetilde{DC} = \pi - \overline{DC}; \quad \widetilde{AD} = \pi - \overline{AD}, \tag{3.42}$$

where the \overline{AB} , etc. were defined in (3.31). With a, b, c , and d defined by (3.22) and e, f, g, h defined by (3.23), one can easily see that the quantities defined by equations (3.41) and (3.42) satisfy (3.40). As in the case of O earlier, we need to find W such that

$$\begin{aligned}
\widetilde{AB} + W &= AB; & \widetilde{BA} - W &= BA \\
\widetilde{BC} + W &= BC; & \widetilde{CB} - W &= CB \\
\widetilde{CD} + W &= CD; & \widetilde{DC} - W &= DC \\
\widetilde{DA} + W &= DA; & \widetilde{AD} - W &= AD.
\end{aligned} \tag{3.43}$$

Proceeding in the manner of §3.3.1, we find that W is determined by equations (3.43) and the equation

$$\frac{\sin(\widetilde{AB} + W) \sin(\widetilde{BC} + W) \sin(\widetilde{CD} + W) \sin(\widetilde{DA} + W)}{\sin(\widetilde{BA} - W) \sin(\widetilde{CB} - W) \sin(\widetilde{DC} - W) \sin(\widetilde{AD} - W)} = 1. \tag{3.44}$$

After we substitute the values from equations (3.41) and (3.42) and use the oddness and periodicity of \sin , (3.44) becomes

$$\frac{\sin(\overline{AB} - W) \sin(\overline{BC} - W) \sin(\overline{CD} - W) \sin(\overline{DA} - W)}{\sin(\overline{BA} + W) \sin(\overline{CB} + W) \sin(\overline{DC} + W) \sin(\overline{AD} + W)} = 1. \tag{3.45}$$

After substituting equations (3.27) into (3.45) and letting $z = \exp(-iW)$ we see that (3.45) becomes the same equation as (3.28). This explains why the second root of (3.28) solves for the unknown angles of the triangulation of O' .

Now let us see what volume we actually compute when we replace z_- with z_+ in (3.30). With this change, the right hand side of (3.30) becomes

$$\begin{aligned} & \mathfrak{L}(\overline{AB} + \arg z_+) + \mathfrak{L}(\overline{BA} - \arg z_+) + \mathfrak{L}(\overline{BC} + \arg z_+) \\ & \quad + \mathfrak{L}(\overline{CB} - \arg z_+) + \mathfrak{L}(\overline{CD} + \arg z_+) + \mathfrak{L}(\overline{DC} - \arg z_+) \\ & \quad + \mathfrak{L}(\overline{DA} + \arg z_+) + \mathfrak{L}(\overline{AD} - \arg z_+) + \mathfrak{L}\left(\frac{\pi - A - B' - C'}{2}\right) \\ & \quad + \mathfrak{L}\left(\frac{\pi - A' + B' + C}{2}\right) + \mathfrak{L}\left(\frac{\pi - C + A + B}{2}\right) + \mathfrak{L}\left(\frac{\pi - B + A' + C'}{2}\right) \end{aligned} \quad (3.46)$$

Substituting (3.41), (3.42) and $W = \arg z_+$ gives

$$\begin{aligned} & \mathfrak{L}(-\widetilde{AB} - W) + \mathfrak{L}(\pi - \widetilde{BA} + W) + \mathfrak{L}(-\widetilde{BC} - W) \\ & \quad + \mathfrak{L}(\pi - \widetilde{CB} + W) + \mathfrak{L}(-\widetilde{CD} - W) + \mathfrak{L}(\pi - \widetilde{DC} + W) \\ & \quad + \mathfrak{L}(-\widetilde{DA} - W) + \mathfrak{L}(\pi - \widetilde{AD} + W) + \mathfrak{L}\left(\frac{\pi - A - B' - C'}{2}\right) \\ & \quad + \mathfrak{L}\left(\frac{\pi - A' + B' + C}{2}\right) + \mathfrak{L}\left(\frac{\pi - C + A + B}{2}\right) + \mathfrak{L}\left(\frac{\pi - B + A' + C'}{2}\right) \end{aligned} \quad (3.47)$$

Using the π -periodicity and oddness of \mathfrak{L} and rewriting the last 4 terms of (3.47) in terms of equations (3.23), we see that the expression (3.47) is none other than the negative of the volume of O' :

$$\begin{aligned} -V(O') &= -\mathfrak{L}(\widetilde{AB} + W) - \mathfrak{L}(\widetilde{BA} - W) - \mathfrak{L}(\widetilde{BC} + W) - \mathfrak{L}(\widetilde{CB} - W) \\ & \quad - \mathfrak{L}(\widetilde{CD} + W) - \mathfrak{L}(\widetilde{DC} - W) - \mathfrak{L}(\widetilde{DA} + W) - \mathfrak{L}(\widetilde{AD} - W) \\ & \quad - \mathfrak{L}(\pi - e) - \mathfrak{L}(\pi - f) - \mathfrak{L}(\pi - g) - \mathfrak{L}(\pi - h), \end{aligned} \quad (3.48)$$

where $W = -\arg z_+$ and e, f, g, h are given by (3.23).

Thus, we have shown that one of the roots of (3.28) gives $V(T)$ when used in (3.34), while the other root gives $-V(T)$. This is analogous to Murakami and

Yano's formulas (3.8) and (3.9). Looking back at equations (3.37) and (3.39), we see that their sum gives

$$2V(T) = V(O) + V(O'). \quad (3.49)$$

Substituting expressions (3.30) and (3.48) into (3.49) gives

$$\begin{aligned} 2V(T) = & \mathfrak{L}(\overline{AB} + \arg z_-) + \mathfrak{L}(\overline{BA} - \arg z_-) + \mathfrak{L}(\overline{BC} + \arg z_-) \\ & + \mathfrak{L}(\overline{CB} - \arg z_-) + \mathfrak{L}(\overline{CD} + \arg z_-) + \mathfrak{L}(\overline{DC} - \arg z_-) \\ & + \mathfrak{L}(\widetilde{DA} + \arg z_-) + \mathfrak{L}(\widetilde{AD} - \arg z_-) + \mathfrak{L}(\widetilde{AB} + \arg z_+) \\ & + \mathfrak{L}(\widetilde{BA} - \arg z_+) + \mathfrak{L}(\widetilde{BC} + \arg z_+) + \mathfrak{L}(\widetilde{CB} - \arg z_+) \\ & + \mathfrak{L}(\widetilde{CD} + \arg z_+) + \mathfrak{L}(\widetilde{DC} - \arg z_+) + \mathfrak{L}(\widetilde{DA} + \arg z_+) \\ & + \mathfrak{L}(\widetilde{AD} - \arg z_+), \quad (3.50) \end{aligned}$$

which is analagous to Murakami and Yano's (3.10).

Thus we have demonstrated that twice a hyperbolic tetrahedron is scissors congruent to two octahedra, O and O' . This formula will be used extensively in the next section to prove that the Regge symmetry is a scissors congruence.

3.4 A scissors congruence proof of the Regge symmetry

Based on the formula (3.50) we can now construct a simple proof that $2T$ is scissors congruent to $2R(T)$, where R denotes any composition of R_a , R_b , and R_c as defined in (3.1), (3.2), and (3.3).

Recall Figure 3.10, which shows a triangulation of O in the half-space model. In other words,

$$O = \{v_a, v_b, v_0, \infty\} + \{v_b, v_c, v_0, \infty\} + \{v_c, v_d, v_0, \infty\} + \{v_d, v_a, v_0, \infty\}. \quad (3.51)$$

We will now subdivide each of the tetrahedra $\{v_a, v_b, v_0, \infty\}$, $\{v_b, v_c, v_0, \infty\}$, $\{v_c, v_d, v_0, \infty\}$, and $\{v_d, v_a, v_0, \infty\}$ into three tetrahedra, as described in §1.2 and

illustrated in Figure 1.2. In fact, this subdivision was implicitly done in §3.3, since it is used to derive formula (1.2). This formula was used to write down the volume of O . This time the construction will be used explicitly to show the scissors congruence.

Recall that in order to subdivide an ideal hyperbolic tetrahedron as shown in Figure 1.2, we drop a perpendicular from one of its vertices to the opposite face. If we are in the half-space model and the vertex from which we drop the perpendicular is the point at infinity, the perpendicular must meet the plane at infinity at the center of the hemisphere that determines the opposite face. In other words, the projection of this configuration onto the plane at infinity must look like Figure 1.3, where the end of the perpendicular coincides with the circumcenter of the triangle determined by 3 vertices of the tetrahedron. We now apply this construction to the 4 tetrahedra that triangulate the octahedron in Figure 3.9, ending up with 12 tetrahedra each of which has 3 ideal vertices and 1 non-ideal vertex. The projection of this construction onto the plane at infinity is shown in Figure 3.15. In that figure, the projections of the vertices p_e , p_f , p_g , and p_h are the respective circumcenters of the triangles $v_a v_b v_0$, $v_b v_c v_0$, $v_c v_d v_0$, and $v_d v_a v_0$. The actual positions of the vertices p_e , p_f , p_g , and p_h are on the planes determined by the respective triangles. The dashed lines are the edges of the new triangulation, and they coincide with the planes determined by the triangles.

Remark 3 *As Figure 3.15 indicates, the vertex p_h is outside of the triangle $v_d v_a v_0$. As one might expect, formula (1.2) still applies to the tetrahedron $\{v_d, v_a, v_0, \infty\}$. Since the angle h exceeds $\pi/2$, $\mathfrak{I}(h) < 0$. So in the formula*

$$V(\{v_d, v_a, v_0, \infty\}) = \mathfrak{I}(AD) + \mathfrak{I}(DA) + \mathfrak{I}(h),$$

the first two terms correspond to the volumes of the tetrahedra $\{v_a, v_0, p_h, \infty\}$ and $\{v_0, v_d, p_h, \infty\}$, while the last term corresponds to the negative volume of the tetrahedron $\{v_a, p_h, v_d, \infty\}$. Thus one can see how formula (1.2) still makes geometric as well as analytic sense in the case of a tetrahedron such as $\{v_d, v_a, v_0, \infty\}$.

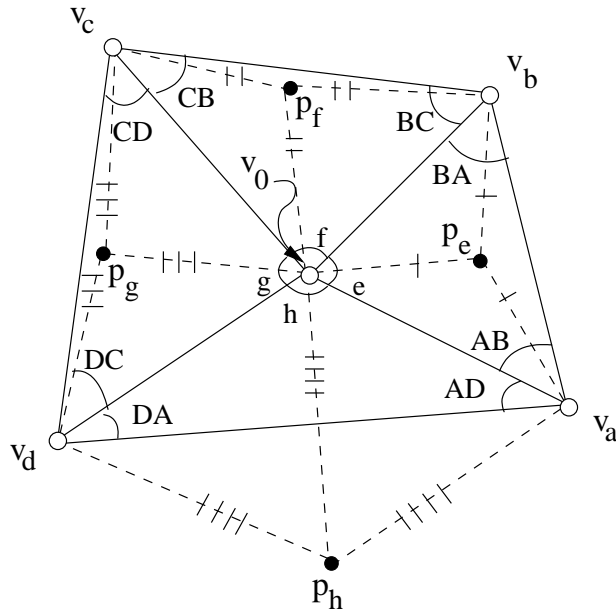


Figure 3.15: Octahedron O in the half-space model, triangulated according to the construction in §1.2

Looking back at formula (3.50), and formulas (3.49), (3.29) and (3.48), we see that the terms $\mathfrak{I}(e)$, $\mathfrak{I}(f)$, $\mathfrak{I}(g)$, $\mathfrak{I}(h)$ corresponding to tetrahedra $\{v_a, v_b, p_e, \infty\}$, $\{v_b, v_c, p_f, \infty\}$, $\{v_c, v_d, p_g, \infty\}$, and $\{v_d, v_a, p_h, \infty\}$ in Figure 3.16 cancel in the formula for the volume of T . Therefore, in our scissors congruence proof we will only be concerned with the tetrahedra $\{v_0, v_a, p_e, \infty\}$, $\{v_b, v_0, p_e, \infty\}$, $\{v_0, v_b, p_f, \infty\}$, $\{v_c, v_0, p_f, \infty\}$, $\{v_0, v_c, p_g, \infty\}$, $\{v_d, v_0, p_g, \infty\}$, $\{v_0, v_d, p_h, \infty\}$, $\{v_a, v_0, p_h, \infty\}$, and their counterparts in O' .

With this in mind, we redraw those tetrahedra in the new triangulation of O that are involved in the scissors congruence proof in Figure 3.16. These tetrahedra correspond to the first 4 terms in formula (3.50). Triangulating O' in the same way as O , we get the tetrahedra corresponding to the last 8 terms in formula (3.50), shown in Figure 3.17.

We have found that certain permutations of the tetrahedra in Figure 3.16 (and corresponding permutations of the tetrahedra in Figure 3.17) give us new octahedra that correspond to $R_b(T)$ and $R_c(T)$. In other words, given that $2T$ is

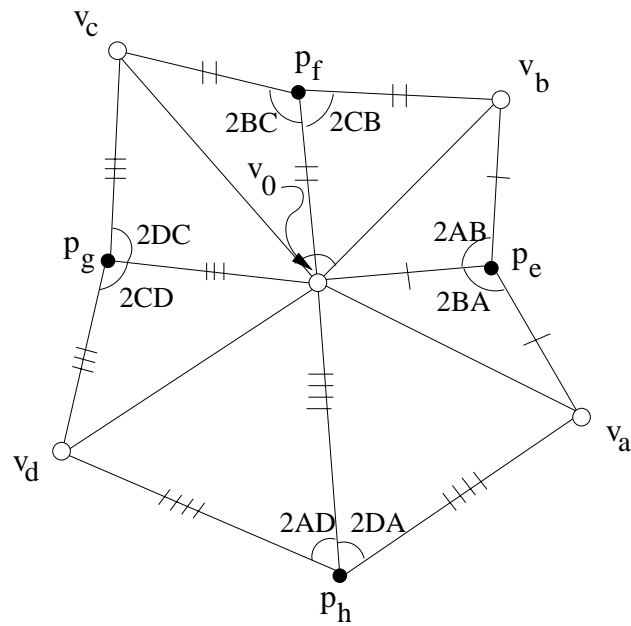


Figure 3.16: Tetrahedra in the triangulation of the octahedron O that correspond to the first 8 terms in formula (3.50)

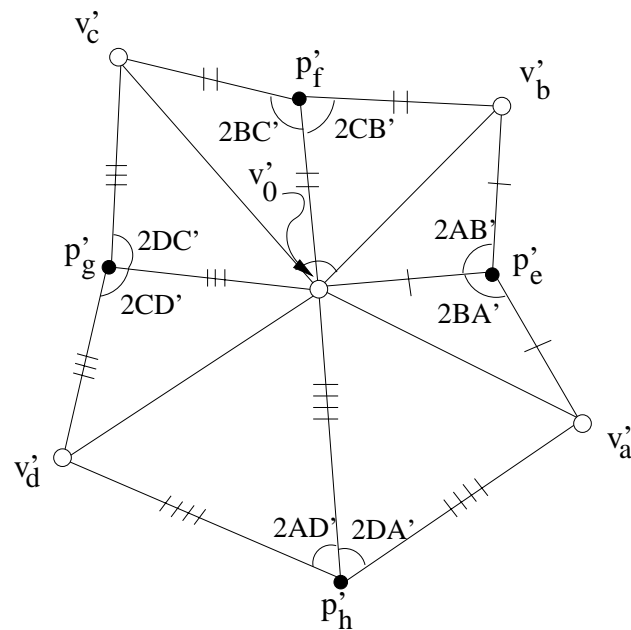


Figure 3.17: Tetrahedra in the triangulation of the octahedron O' that correspond to the last 8 terms in formula (3.50)

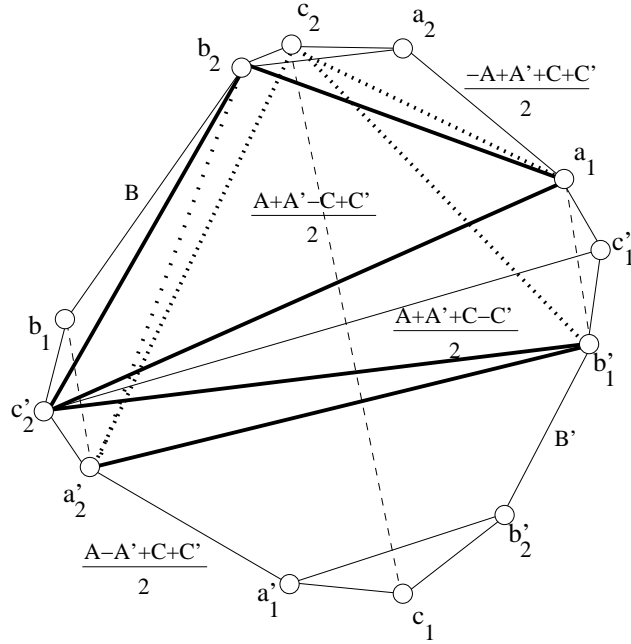
scissors congruent to $O + O'$, we have found that $2R_b(T)$ is scissors congruent to $P(O) + P(O')$, where $P(O)$ and $P(O')$ are the octahedra obtained by permuting the tetrahedra in the triangulations of O and O' .

Before stating this fact and its proof formally, we address the fact that there are no permutations of the tetrahedra that give us $R_a(T)$. This can be traced back to the choice of the firepole (see Definition 7) in triangulating O . The firepole, as shown in Figure 3.9, connects the vertices a_2 and a'_2 . From the position of these vertices in Figure 3.6, we see that this choice of the firepole “favors” the pair of opposite edges A and A' . Similarly, the Regge symmetry R_a is singles out the edge A and its opposite, as seen in Definition 6. The other two choices of the firepole for O are the segments $[b_1, b'_1]$ and $[c'_1, c_2]$, which have preferred pairs of edges B, B' and C, C' . The first of these choices yields a triangulation of O that admits permutations that correspond to $R_a(T)$ and $R_c(T)$, while the second allows permutations that give $R_a(T)$ and $R_b(T)$. In fact, no matter which of the 2^6 possible decomposition one uses to cut down to octahedron, it is always true that for every choice of a firepole that prefers a certain pair of opposite edges one cannot obtain the octahedron corresponding to exactly one of the Regge symmetries R_a , R_b or R_c by simply permuting tetrahedra.

The formal statement of the results obtained is as follows.

Theorem 3 *Let $T = T(A, B, C, A', B', C')$ be a hyperbolic tetrahedron, and let $R_b(T) = T(s_b - A, B, s_b - C, s_b - A', B', s_b - C')$ denote the action on T of one of the Regge symmetries, as defined in Definition 6. Then $2T$ is scissors congruent to $2R_b(T)$.*

Proof. Let O_T denote the octahedron obtained from T by the construction in §3.3, and let O'_T denote the corresponding dual tetrahedron. As shown in §3.3.2, $2T$ is scissors congruent to $O_T + O'_T$. We apply the construction described in §3.3 to $R_b(T)$ by first extending its edges to infinity and obtaining the octahedron $U_{R_b(T)}$ shown in Figure 3.18. Then we triangulate $U_{R_b(T)}$ so that $O_{R_b(T)}$ has as its vertices the points $\{a_1, b'_1, a'_2, c'_2, b_2, c_2\}$, while $O'_{R_b(T)}$ has vertices the points

Figure 3.18: Polyhedron $U_{R_b(T)}$

$\{a_2, b'_2, a'_1, c'_1, b_1, c_1\}$. $O_{R_b(T)}$ is depicted in Figure 3.19. $O'_{R_b(T)}$ has dihedral edges that are π -dihedral edges of $O_{R_b(T)}$, as shown in §3.3.2. Just as in the case of T , $2R_b(T)$ is scissors congruent to $O_{R_b(T)} + O'_{R_b(T)}$. What remains to be shown is that $O_T + O'_T$ is scissors congruent to $O_{R_b(T)} + O'_{R_b(T)}$. This is done as follows.

Let O be triangulated as shown in Figure 3.15. We need not consider the tetrahedra $\{v_a, v_b, p_e, \infty\}$, $\{v_b, v_c, p_f, \infty\}$, $\{v_c, v_d, p_g, \infty\}$, and $\{v_d, v_a, p_h, \infty\}$ as they cancel when O is added to O' . Therefore, it is sufficient to consider the polyhedron shown in Figure 3.16. The scissors congruence move consists of interchanging the tetrahedra $\{v_a, p_e, v_0, \infty\}$ and $\{v_0, v_c, p_g, \infty\}$, while leaving all the other tetrahedra in place. The resulting polyhedron is shown in Figure 3.20, where the tetrahedra that were moved are shaded. The pieces in the resulting figure still fit together (i.e. the situation depicted in Figure 3.11 does not occur) because the new polyhedron satisfies equation (3.25). In fact, the permutation merely interchanges the terms $\sin(BA)$ and $\sin(DC)$ in (3.25). As a final step, we translate the 8 tetrahedra making up the polyhedron of Figure 3.20 to obtain the mirror image of that polyhedron.

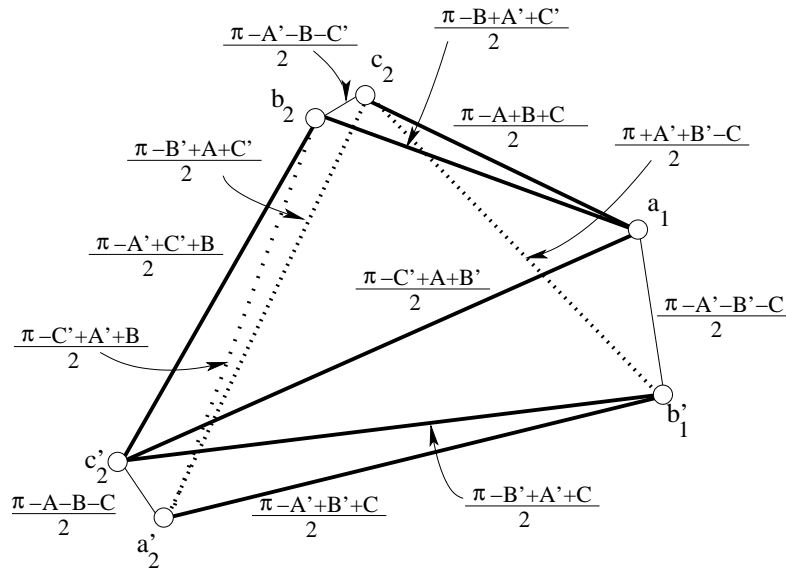


Figure 3.19: Octahedron $O_{R_i}(T)$

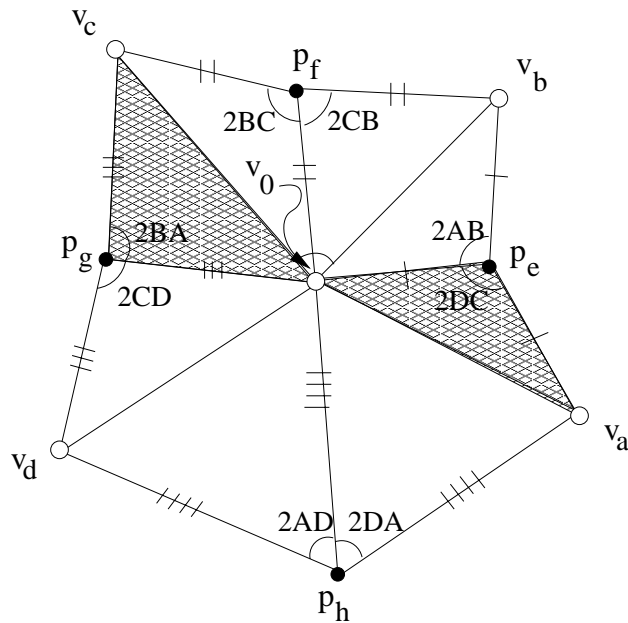


Figure 3.20: Polyhedron of Figure 3.16 with two tetrahedra interchanged. These two tetrahedra have been shown as shaded

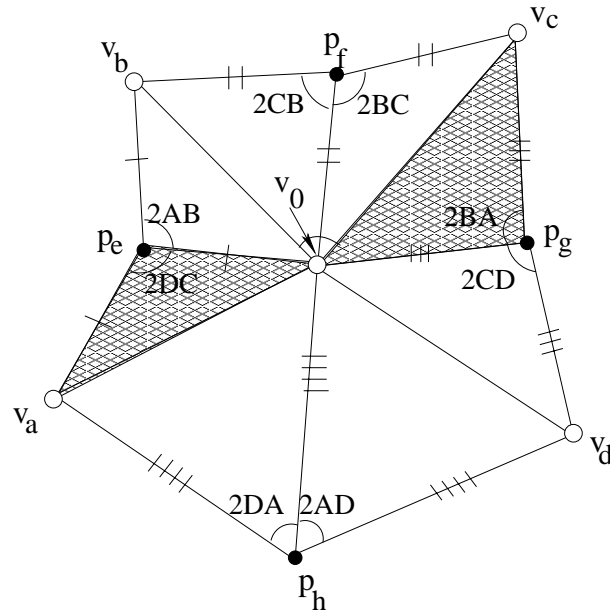


Figure 3.21: Mirror image of the polyhedron of Figure 3.20

The result is shown in Figure 3.21. After adding the tetrahedra $\{v_a, v_b, p_e, \infty\}$, $\{v_b, v_c, p_f, \infty\}$, $\{v_c, v_d, p_g, \infty\}$, and $\{v_d, v_a, p_h, \infty\}$ to the polyhedron in Figure 3.21 (these tetrahedra will subsequently cancel) we obtain the octahedron $P(O)$ shown in Figure 3.22. The angles in Figure 3.22 were given in equations (3.26), (3.23) and (3.31). Using these equations in adding up the dihedral angles at the edges, we obtain the Klein model picture of $P(O)$ shown in Figure 3.23. It is isometric to the octahedron $O_{R(T)}$ depicted in Figure 3.19. The discussion above applies verbatim to the dual octahedra. Since their dihedral angles are dependent on the dihedral angles of the original tetrahedra, we need to perform the same permutation on the tetrahedra making up O' as we did on the tetrahedra making up O . In other words we interchange the tetrahedra $\{v'_a, p'_e, v'_0, \infty\}$ and $\{v'_0, v'_c, p'_g, \infty\}$ in Figure 3.17 and take the mirror image of the result. The result is shown in Figure 3.24. Adding in the tetrahedra $\{v'_a, v'_b, p'_e, \infty\}$, $\{v'_b, v'_c, p'_f, \infty\}$, $\{v'_c, v'_d, p'_g, \infty\}$, and $\{v'_d, v'_a, p'_h, \infty\}$ gives the octahedron shown in Figure 3.25. Recall from §3.3.2 that

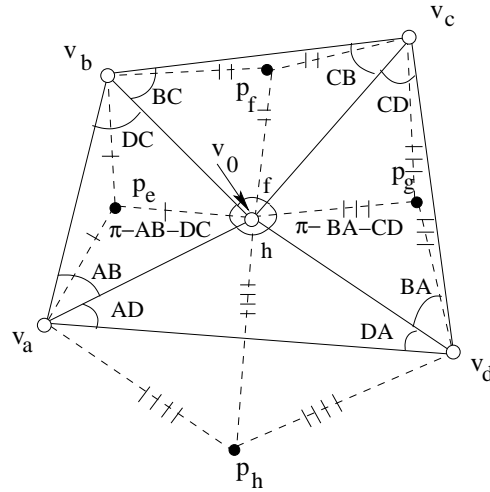


Figure 3.22: Octahedron $P(O)$

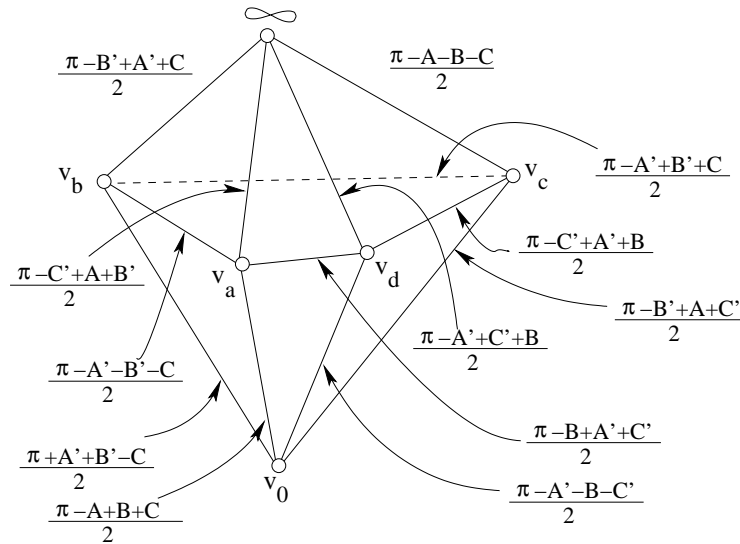


Figure 3.23: Octahedron $P(O)$ in the Klein model

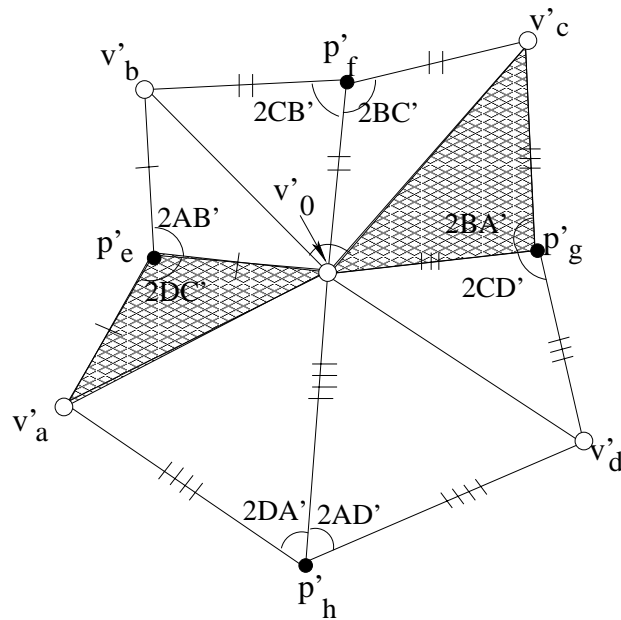


Figure 3.24: Mirror image of the polyhedron of Figure 3.17 where the interchanged tetrahedra have been shown as shaded

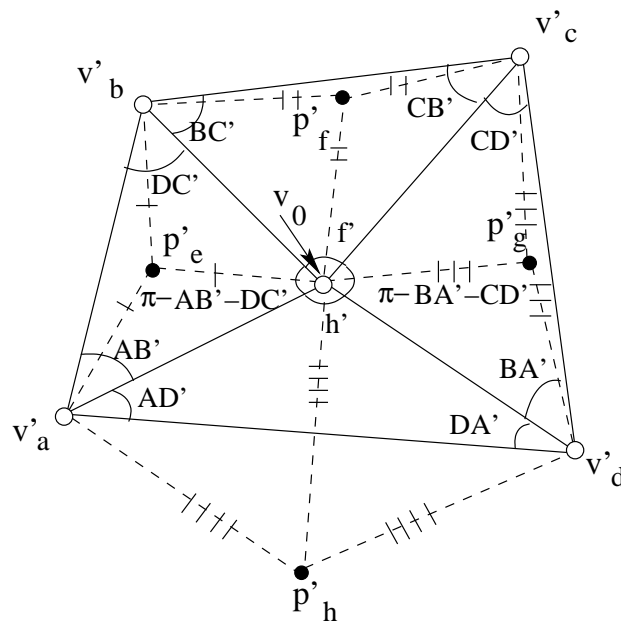
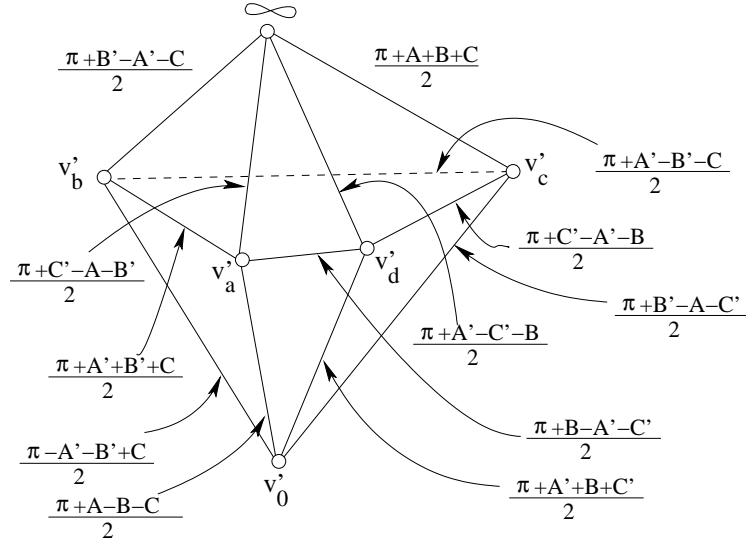


Figure 3.25: Octahedron $P(O')$

Figure 3.26: Octahedron $P(O')$ in the Klein model

$$\begin{aligned}
\widetilde{AB} + W &= AB'; & \widetilde{BA} - W &= BA' \\
\widetilde{BC} + W &= BC'; & \widetilde{CB} - W &= CB' \\
\widetilde{CD} + W &= CD'; & \widetilde{DC} - W &= DC' \\
\widetilde{DA} + W &= DA'; & \widetilde{AD} - W &= AD',
\end{aligned} \tag{3.52}$$

where the \widetilde{AB} , etc. are given by (3.41) and (3.42) and W is one of the solutions to (3.45). Using these values, we find that the Klein model of the octahedron in Figure 3.25 is the octahedron in Figure 3.26. Comparing the octahedra in Figure 3.23 and Figure 3.26, we see that their dihedral angles add up to π . Therefore, the octahedron in Figure 3.26 is isometric to $O'_{R(T)}$. Thus we have shown that $O + O'$ is scissors congruent to $O_{R(T)} + O'_{R(T)}$ by a permutation. This completes the proof. \square

Corollary 1 *Let T and $R_b(T)$ be hyperbolic tetrahedra as defined in Theorem 3. Then T is scissors congruent to $R_b(T)$.*

Proof. The fact that we can “divide by 2” the construction that led to the proof of Theorem 3 follows from Dupont’s result of unique divisibility in [3]. Dupont

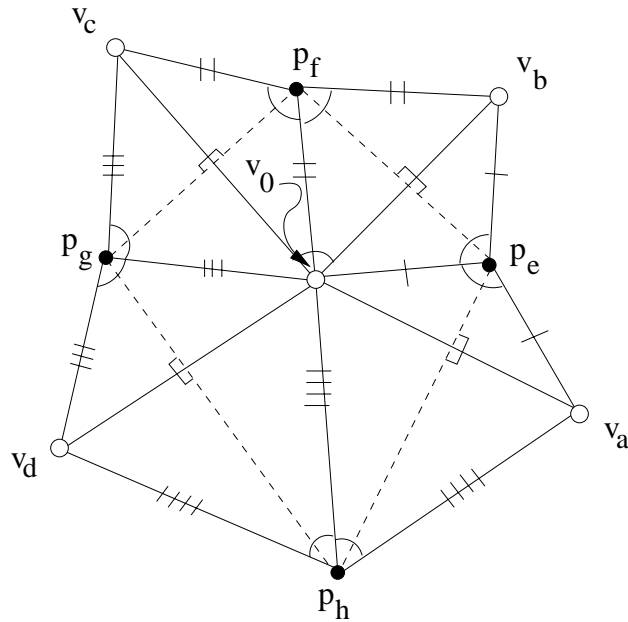


Figure 3.27: Dividing the polyhedron of Figure 3.16 into two scissors congruent parts

shows how an ideal hyperbolic tetrahedron can be divided into two parts that are scissors congruent to one another (this is expressed in (4.75) in the next chapter). The fact that this 2-divisibility is unique means that it is well-defined with respect to the different ways to divide a tetrahedron into 2 scissors congruent sets of polyhedra. In other words, suppose we find that $T = A \sqcup B$, where A and B is each a collection of polyhedra found by means of (4.75). Now suppose that we can also express T as $T = A' \sqcup B'$, where A' and B' are also scissors congruent to one another. Then by unique 2-divisibility, A , A' , B , and B' are all scissors congruent to one another.

We saw in the proof of Theorem 3 that $2T$ is scissors congruent to $\tilde{O} + \tilde{O}'$, where \tilde{O} is the polyhedron in Figure 3.16 and \tilde{O}' is the polyhedron in Figure 3.17. We now divide each of the 8 tetrahedra comprising \tilde{O} into two scissors congruent (in fact, congruent) halves as shown in Figure 3.27. The result is the polyhedron $\tilde{O}/2$ shown in Figure 3.28. We perform the same division by 2 procedure on \tilde{O}' to obtain $\tilde{O}'/2$, as depicted in Figure 3.29.

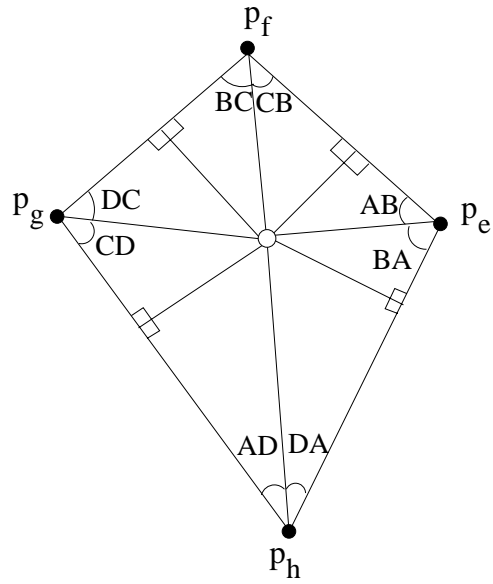


Figure 3.28: One of the two congruent halves comprising the polyhedron of Figure 3.16

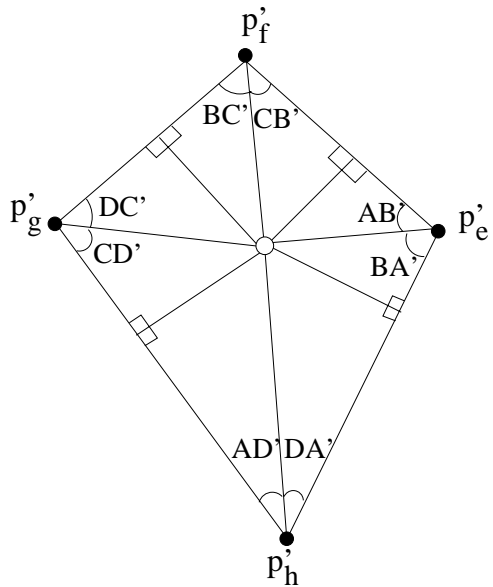


Figure 3.29: One of the two congruent halves comprising the polyhedron of Figure 3.17

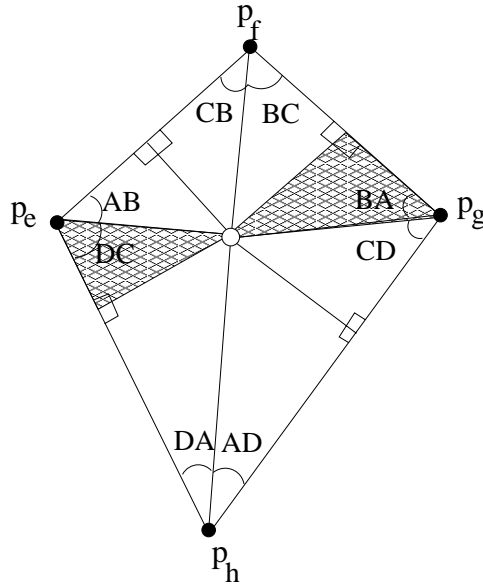


Figure 3.30: One of the two congruent halves comprising the polyhedron of Figure 3.21

By Dupont's unique 2-divisibility result, T is scissors congruent to $\tilde{O}/2 + \tilde{O}'/2$, that is to the sum of the octahedra in Figures 3.28 and 3.29. Permuting the indicated tetrahedra in $\tilde{O}/2$ and $\tilde{O}'/2$ results in $\tilde{O}_{R(T)}/2$ and $\tilde{O}'_{R(T)}/2$, shown in Figures 3.30 and 3.31. $\tilde{O}_{R(T)}/2$ ($\tilde{O}'_{R(T)}/2$) is one of the two congruent halves of $\tilde{O}_{R(T)}$ ($\tilde{O}'_{R(T)}$), obtained the same way as $\tilde{O}/2$ and $\tilde{O}'/2$ were. Thus $R_b(T)$ is scissors congruent to $\tilde{O}_{R(T)}/2 + \tilde{O}'_{R(T)}/2$. Since $\tilde{O}/2 + \tilde{O}'/2$ is scissors congruent to $\tilde{O}_{R(T)}/2 + \tilde{O}'_{R(T)}/2$ by a permutation of tetrahedra, it follows that T is scissors congruent to $R_b(T)$. \square

Corollary 2 *All the tetrahedra in the family generated by the Regge symmetries are scissors congruent to one another.*

Proof. By Theorem 3, the tetrahedron T is scissors congruent to $R_b(T)$. By applying the construction in the proof of that theorem to the rigid rotations of T we can prove that T is scissors congruent to $R_a(T)$ and $R_c(T)$. The corollary then follows from the fact that any two maps out of $R_a(T)$, $R_b(T)$ and $R_c(T)$ generate

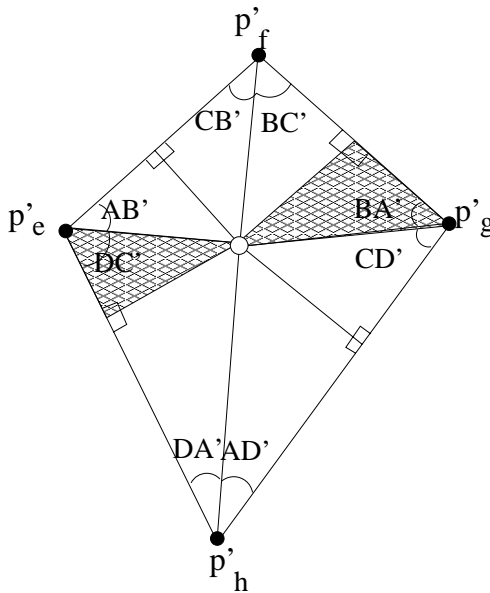


Figure 3.31: One of the two congruent halves comprising the polyhedron of Figure 3.24

the group of Regge symmetries, so we can obtain any member of the family of Regge symmetric tetrahedra by a sequence of procedures described in the proof of Theorem 3. \square

Remark 4 *Alternatively to the above corollary, it can be proved directly that T is scissors congruent to $R_c(T)$ by slightly altering the proof of Theorem 3. The change consists of rotating the polyhedron $U_{R_b(T)}$ of Figure 3.18 so that the face $\{a, b', c\}$ is replaced by the face $\{a, c', b\}$. One can then proceed with the rest of the proof.*

Chapter 4

On the geometric proof that the Lobachevsky function satisfies the Kubert identities

The Kubert identities are equations of the form

$$f(x) = m^{s-1} \sum_{n=0}^{m-1} f((x+n)/m), \quad (4.1)$$

where m can be any positive integer, x is a real number, and s is some fixed complex parameter. In [11] Milnor shows that for every s there are exactly two linearly independent functions, defined and continuous on $(0, 1)$ that satisfy the identities (4.1). These two functions can be chosen so that one is even and one is odd. We will be interested in the case $s = 2$, where the odd function that satisfies the Kubert identities is $\mathcal{J}(\pi\theta) = -\int_0^{\pi\theta} \log 2|\sin u| du$ which was introduced in §1.2. Rewriting the Kubert identities of order 2 for the \mathcal{J} function, we have

$$\mathcal{J}(n\theta) = n \sum_{k=0}^{n-1} \mathcal{J}(\theta + k\pi/n). \quad (4.2)$$

The even function is the Bernoulli polynomial

$$\beta_2(x) = x^2 - x + \frac{1}{6}, \dots$$

and will not be studied here. Henceforth the special case (4.2) of (4.1) will be referred to as the Kubert identities. The importance of the Kubert identities can be seen in the following easy lemma:

Lemma 4 *The assumptions that a function L is odd, π -periodic, and satisfies (4.2) are sufficient to determine L up to a constant.*

Proof. Since L is odd and π -periodic, it is also odd about $\pi/2$, so we can assume that its Fourier series is

$$L(x) = \sum_{n=1}^{\infty} b_{2n} \sin 2nx, \quad (4.3)$$

where

$$b_{2n} = \frac{1}{\pi} \int_{-\pi}^{\pi} L(x) \sin 2nx \, dx. \quad (4.4)$$

Equation (4.3) gives

$$L(mx) = \sum_{n=1}^{\infty} b_{2n} \sin 2mnx \quad (4.5)$$

where m is any natural number. On the other hand, by (4.2)

$$\begin{aligned} L(mx) &= m \sum_{k=0}^{m-1} L(x + k\pi/m) \\ &= \sum_{n=1}^{\infty} c_{2n} \sin 2nx, \end{aligned} \quad (4.6)$$

where

$$c_{2n} = \frac{m}{\pi} \int_{-\pi}^{\pi} \left[\sum_{k=0}^{m-1} L(x + k\pi/m) \right] \sin 2nx \, dx. \quad (4.7)$$

Note that for any real constant a and any integer n

$$\frac{1}{\pi} \int_{-\pi}^{\pi} L(x + a) \sin 2nx \, dx = b_{2n} \cos 2na.$$

Therefore, (4.7) becomes

$$c_{2n} = mb_{2n} \sum_{k=0}^{m-1} \cos \frac{2\pi kn}{m}. \quad (4.8)$$

Thus

$$c_{2n} = \begin{cases} m^2 b_{2n} & \text{if } m \text{ divides } n \\ 0 & \text{otherwise.} \end{cases} \quad (4.9)$$

We can now rewrite (4.6) as

$$L(mx) = \sum_{n=1}^{\infty} m^2 b_{2mn} \sin 2mnx. \quad (4.10)$$

Comparing (4.5) and (4.10) gives

$$b_{2mn} = b_{2n}/m^2$$

for all natural numbers m . In particular,

$$b_{2m} = b_2/m^2.$$

Plugging this result into expression (4.3) gives

$$L(x) = b_2 \sum_{n=1}^{\infty} \frac{\sin 2nx}{n^2}. \quad (4.11)$$

The constant b_2 can be found by evaluating $L(x)$ at a point. \square

The above lemma provides some of the motivation for finding a geometric construction that proves the Kubert identities. The other motivation is to provide some evidence for the yet unproved conjecture that the volume and Dehn invariants form a complete system of invariants for the scissors congruence class of hyperbolic polyhedra. Why we should expect the conjecture to apply in this case will be shown in the sections to follow.

4.1 Analytic proof of the Kubert identities

We present the straightforward analytic proof of the Kubert identities which can be found in [10]. We start with the identities

$$|z^n - 1| = \prod_{k=0}^{n-1} |z - e^{2\pi ik/n}|,$$

where we consider small positive values of θ . The general result follows by analytic continuation. Substituting $z = e^{-2i\theta}$ gives

$$|e^{-2in\theta} - 1| = \prod_{k=0}^{n-1} |e^{-2i\theta} - e^{2\pi ik/n}|,$$

and factoring out some expressions of modulus 1 gives

$$|e^{-in\theta}| |e^{-in\theta} - e^{in\theta}| = \prod_{k=0}^{n-1} |e^{-i(\theta-\pi k/n)}| |e^{-i(\theta+\pi k/n)} - e^{i(\theta+\pi k/n)}|. \quad (4.12)$$

The result is the cyclotomic identities

$$2|\sin n\theta| = \prod_{k=0}^{n-1} 2|\sin(\theta + \pi k/n)|. \quad (4.13)$$

Taking the negative log of both sides and integrating gives

$$\mathfrak{L}(n\theta)/n = \sum_{k=0}^{n-1} \mathfrak{L}(\theta + \pi k/n) + C, \quad (4.14)$$

where the constant C can be determined by substituting $\theta = 0$ in the $n = 2$ case,

$$\mathfrak{L}(2\theta)/2 = \mathfrak{L}(\theta) + \mathfrak{L}(\theta + \pi/2) + C. \quad (4.15)$$

Since $\mathfrak{L}(\pi/2) = 0$ as shown in §1.2, $C = 0$.

4.2 The Kubert identities viewed as identities on simplices; the Dehn invariant

We saw in §1.2 that $\mathfrak{L}(\theta)$ is half of the volume of an isosceles ideal tetrahedron with apex angle 2θ . Recall that in Figure 1.2b) of §1.2, $\mathfrak{L}(\gamma)$ was the volume of the tetrahedron $\{a, b, p, O'\}$, whose projection onto the plane at infinity in the half-space model can be seen in Figure 1.3. Let us adopt the notation of [5] and refer to such a tetrahedron as $\mathcal{L}(\gamma)$. With this in mind, we see that the left hand side of (4.2) is the volume of $\mathcal{L}(n\theta)$, while each term on the right hand side is the

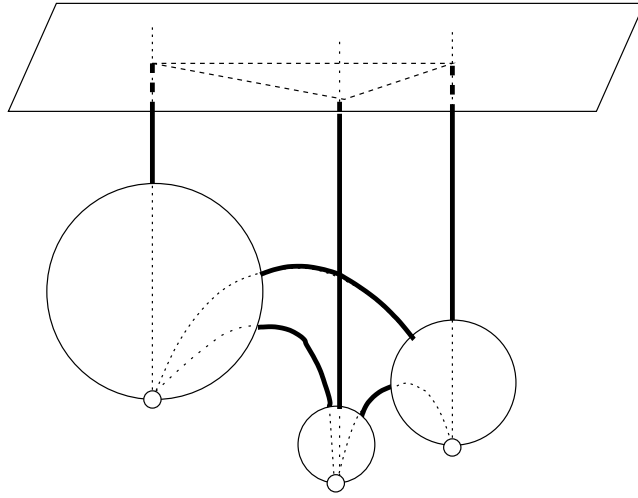


Figure 4.1: Calculation of the Dehn invariant of an ideal hyperbolic tetrahedron

volume of $\mathcal{L}(\theta + k\pi/n)$ for $k = 0, 1, \dots, n-1$. It is then natural to wonder whether one can assemble the simplex $\mathcal{L}(n\theta)$ by cutting and pasting the n^2 simplices on the right hand side of (4.2). Certainly the volumes of both groups of simplices agree. So do the Dehn invariants, as we will now see.

The Dehn invariant of a polyhedron P was defined in §1.1 as

$$D(P) = \sum_{\text{edges of } P} l(E) \otimes (\theta(E)/\pi), \quad (4.16)$$

where $l(E)$ and $\theta(E)$ are the respective lengths and dihedral angles at edge E , and D takes values in the tensor product $\mathbb{R} \otimes_{\mathbb{Z}} (\mathbb{R}/(\pi\mathbb{Z}))$. The definition applies to polyhedra in any geometry, but in the case of hyperbolic polyhedra with an infinite vertex one runs into a potential problem since all the edges meeting at such a vertex have infinite lengths. The solution given by Thurston consists of excising a horospherical neighborhood around each infinite vertex and applying (4.16) to the remaining lengths. For example, if we wish to compute the Dehn invariant of an ideal hyperbolic tetrahedron we need only consider the lengths of the thickly outlined segments in Figure 4.1. Thurston's modified definition of the Dehn invariant is well defined with respect to the choice of diameters of the

horospheres. For if we consider horospheres of diameters d_1 and d_2 around a given ideal point with $d_1 > d_2$, the difference in the edge lengths chopped off by the corresponding spheres is $d_1 - d_2$ for every edge that meets at that ideal point. So the difference in the value of the Dehn invariant would be $(d_1 - d_2) \otimes \sum \theta_i$, where θ_i is the dihedral angle at each edge. But we saw earlier that in the case of a tetrahedron $\sum \theta_i = \pi$. The argument in §1.2 that was used to prove this fact can be applied to deduce that in the case of an arbitrary polyhedron $\sum \theta_i = n\pi$ for some natural number n . Since integral multiples of π are 0 in the group $\mathbb{R}/(\pi\mathbb{Z})$, $(d_1 - d_2) \otimes \sum \theta_i$ has no effect on the Dehn invariant for any values of d_1 and d_2 .

Using a construction similar to that of Figure 4.1 along with some basic trigonometry, Dupont and Sah [5] derive the Dehn invariant of $\mathcal{L}(\theta)$ to be

$$D(\mathcal{L}(\theta)) = 2 \log 2 \sin \theta \otimes (\theta/2\pi). \quad (4.17)$$

Applying (4.17) to the tetrahedra in (4.2) we have

$$\begin{aligned} D(\mathcal{L}(n\theta)) &= 2 \log 2 \sin(n\theta) \otimes (n\theta/2\pi) \\ &= 2n \log 2 \sin(\theta) \otimes (\theta/2\pi) \end{aligned} \quad (4.18)$$

and

$$\begin{aligned} D\left(n \sum_{k=0}^{n-1} \mathcal{L}(\theta + k\pi/n)\right) &= n \sum_{k=0}^{n-1} 2 \log 2 \sin(\theta + k\pi/n) \otimes ((\theta + k\pi/n)/2\pi) \\ &= n \sum_{k=0}^{n-1} 2 \log 2 \sin(\theta + k\pi/n) \otimes (\theta/2\pi) \\ &= 2n \log \prod_{k=0}^{n-1} 2 \sin(\theta + k\pi/n) \otimes (\theta/2\pi) \\ &= 2n \log 2 \sin(n\theta) \otimes (\theta/2\pi), \end{aligned} \quad (4.19)$$

where the last equality follows by the cyclotomic identities (4.13). Thus,

$$D(\mathcal{L}(n\theta)) = D\left(n \sum_{k=0}^{n-1} \mathcal{L}(\theta + k\pi/n)\right).$$

4.3 Attempts and obstacles in the geometric proof of the Kubert identities

The geometric proof of the Kubert identity in the case $n = 2$ follows immediately from applying the construction in Figure 1.2 to an isosceles ideal tetrahedron with apex angle 2θ , $T(2\theta, \pi/2 - \theta, \pi/2 - \theta)$. From that construction, we see that

$$T(2\theta, \pi/2 - \theta, \pi/2 - \theta) = \mathcal{L}(2\theta) + 2\mathcal{L}(\pi/2 - \theta). \quad (4.20)$$

On the other hand,

$$T(2\theta, \pi/2 - \theta, \pi/2 - \theta) = 2\mathcal{L}(\theta). \quad (4.21)$$

Since $V(\mathcal{L}(\alpha)) = \mathcal{I}(\alpha)$, (4.20) and (4.21) give

$$2\mathcal{I}(\theta) = \mathcal{I}(2\theta) + 2\mathcal{I}(\pi/2 - \theta). \quad (4.22)$$

By the oddness and periodicity of \mathcal{I} , $\mathcal{I}(\pi/2 - \theta) = -\mathcal{I}(\theta + \pi/2)$, so that equation (4.22) is equivalent to the Kubert identity in the case $n = 2$.

4.3.1 Two geometric proofs of the Kubert identity in the case $n = 3$

As n increases, the proofs rapidly get more difficult. In [14] Sah proved the $n = 3$ case using a rather complicated geometrical construction due to Thurston that did not lead to an obvious generalization for higher n . The details of Thurston's construction can be found in [14], but we attempt to present the gist of it here. Consider the ideal prism $\{v_1^-, v_2^-, v_3^-, v_1^+, v_2^+, v_3^+\}$ in Figure 4.2. The horizontal plane of symmetry of the prism intersects in an equilateral hyperbolic triangle. Because of this symmetry, the volume of the prism is 3 times the volume of the polyhedron $Q = \{p^+, p^-, v_1^+, v_1^-, v_2^+, v_2^-\}$. In addition, Sah considers the isometric tetrahedra $R^+ = \{p^+, q^+, v_1^+, v_2^+\}$ and $R^- = \{q^-, p^-, v_1^-, v_2^-\}$. The essence of Sah's proof consists of noting that R^- is also isometric to $\{p^-, q^+, v_1^-, v_2^-\}$ by reflection in

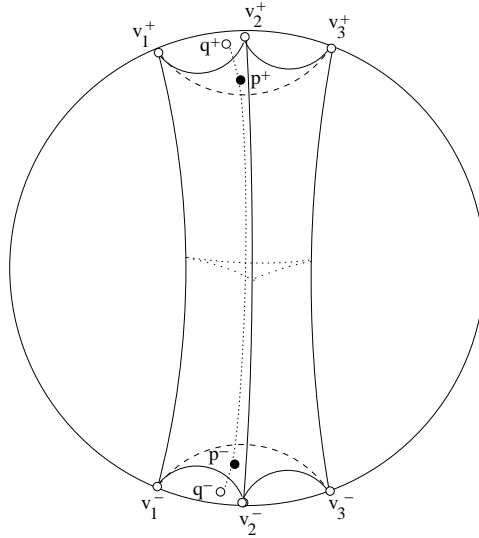


Figure 4.2: A geometric proof of the Kubert identity in the case $n = 3$ based on a construction by Thurston

the plane $\{v_1^-, v_2^-, v_3^-\}$, and writing down the volumes of both sides of the following equality:

$$Q \amalg R^+ = \{q^+, p^-, v_1^-, v_2^-\} \amalg \{q^+, v_1^+, v_2^+, v_1^-, v_2^-\}.$$

An alternative way to prove the $n = 3$ Kubert identity that also does not seem to generalize but is much simpler than Thurston's construction involves the tetrahedron T depicted in Figure 4.3. On the one hand, the volume of T , as given by

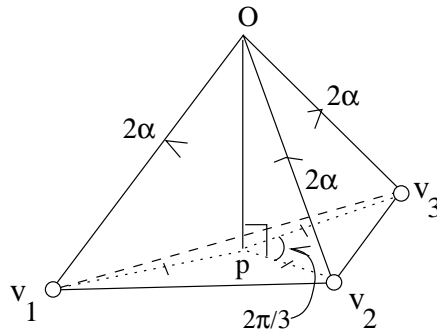


Figure 4.3: A geometric proof of the Kubert identity in the case $n = 3$

(1.10), is

$$V(T) = \frac{1}{2}[3\mathcal{L}(2\alpha) + 3\mathcal{L}(\frac{\pi}{2} - \alpha) - \mathcal{L}(\frac{\pi}{2} + 3\alpha)]. \quad (4.23)$$

On the other hand, the volume of T is 3 times the volume of the tetrahedron $\{v_1, v_2, p, O\}$, and

$$V(\{v_1, v_2, p, O\}) = \frac{1}{2}[2\mathcal{L}(2\alpha) + \mathcal{L}(\frac{5\pi}{6} - \alpha) + \mathcal{L}(\frac{\pi}{6} - \alpha)] \quad (4.24)$$

by formula (1.11). Equating (4.23) with 3 times (4.24), and using the $n = 2$ Kubert identity along with the oddness and π -periodicity of \mathcal{L} gives the $n = 3$ Kubert identity.

4.3.2 The geometric proof of the cyclotomic identities

Another approach to the geometric proof of the Kubert identities is to take the cyclotomic identities (4.13) as a starting point, just as was done in the analytic proof of §4.1. The idea here is to first produce a geometric proof of the cyclotomic identities, and then extend that proof to \mathbb{H}^3 .

The geometric proof of the n -th cyclotomic identity is accomplished by gluing together n isosceles triangles with apex angles $2\theta, 2\theta + 2\pi/n, 2\theta + 2(2)\pi/n, \dots, 2\theta + 2(n-1)\pi/n$. The result is a polygon whose side lengths indicate that the right and left hand sides of (4.13) are equal to one another. For the $n = 2$ case, the situation is depicted in Figure 4.4. Assuming $|OB| = 1$ and considering the isosceles triangle OBA , we have that

$$|AB| = 2 \sin 2\theta. \quad (4.25)$$

On the other hand, we can also calculate $|AB|$ in terms of $|CB|$. The isosceles triangle ABC has apex angle $\pi - 2\theta$, so $|AB| = |CB|(2 \sin(\pi/2 - \theta)) = 2|CB| \sin(\theta + \pi/2)$. By considering the isosceles triangle OBC , we see that $|CB| = 2 \sin \theta$. Therefore,

$$|AB| = (2 \sin \theta)(2 \sin(\theta + \pi/2)). \quad (4.26)$$

Equating (4.25) and (4.26) gives the $n = 2$ cyclotomic identity.

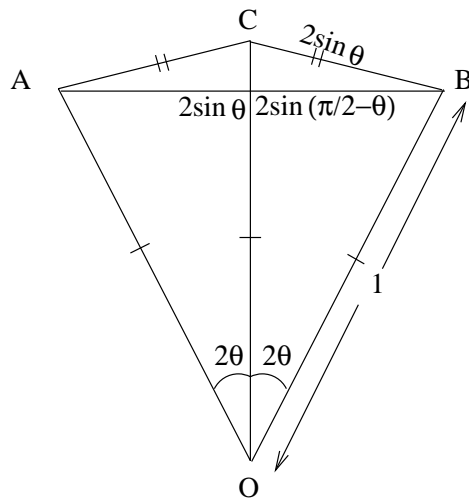


Figure 4.4: A geometric proof of the identity $2 \sin 2\theta = (2 \sin \theta)(2 \sin(\theta + \pi/2))$

We can repeat this procedure in the case of the $n = 3$ cyclotomic identity, continuing to glue the side of each isosceles triangle to the base of the preceding one, keeping the same orientation of the apex angle throughout the construction. The result is shown in Figure 4.5. It must be noted that the order in which the triangles are glued does not matter, since it only affects the order of the terms in the right hand side of (4.13). In the next section it will become clear how to generalize this proof for higher n .

4.3.3 Obstacles in extending the geometric proof of the cyclotomic identities to a geometric proof of the Kubert identities

In order to extend the results of the preceding subsection to a geometric proof of the Kubert identities, we consider the vertices in Figures 4.4 and 4.5 as ideal vertices at the plane at infinity in the half-space model, and the edges in those figures as projections of geodesics onto the plane at infinity. So we now view the polygons as faces of polyhedra. In addition, we consider the point at infinity and

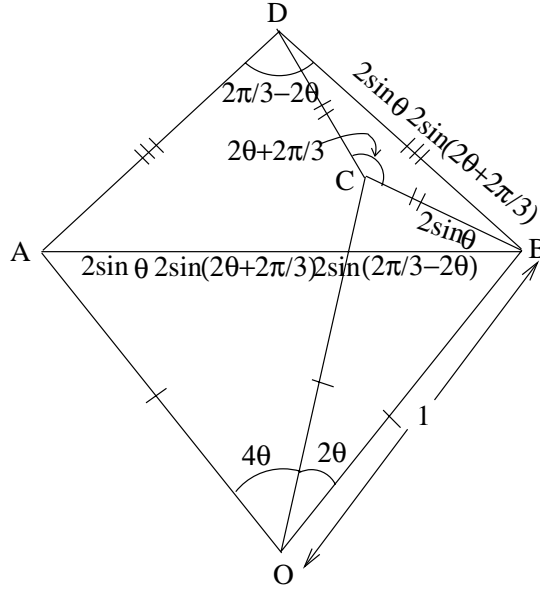


Figure 4.5: A geometric proof of the identity $2 \sin 3\theta = (2 \sin \theta)(2 \sin(\theta + 2\pi/3))(2 \sin(\theta + 4\pi/3))$

the polyhedron G that results from taking the convex hull of the vertices plus the point at infinity. The Kubert identities then arise from equating two different triangulations of G .

Let us take a closer look at how this works in the cases $n = 2$ and $n = 3$. In Figure 4.4

$$G = \{O, B, C, \infty\} + \{O, C, A, \infty\}. \quad (4.27)$$

A different triangulation yields

$$G = \{O, B, C, A\} + \{O, B, A, \infty\} + \{A, B, C, \infty\}. \quad (4.28)$$

It is evident from Figure 4.4 that

$$\{O, B, C, \infty\} = \{O, C, A, \infty\} = 2\mathcal{L}(\theta), \quad (4.29)$$

and

$$\{O, B, A, \infty\} = 2\mathcal{L}(2\theta); \quad \{A, B, C, \infty\} = 2\mathcal{L}(\pi/2 - \theta) \quad (4.30)$$

We calculate the dihedral angles of $\{O, B, C, A\}$ using the following lemma.

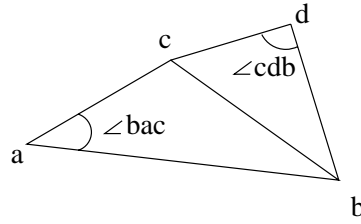


Figure 4.6: Calculating the dihedral angle between two planes in \mathbb{H}^3

Lemma 5 *The angle between two ideal hyperbolic triangles in $\{a, b, c\}$ and $\{c, b, d\}$ in \mathbb{H}^3 whose projection onto the plane at infinity in the half-space model is shown in Figure 4.6 is $\angle bac + \angle cdb$.*

Proof. The angle between the hyperbolic triangles $\{a, b, c\}$ and $\{c, b, d\}$ is the sum of the angle between $\{a, b, c\}$ and $\{b, c, \infty\}$ and the angle between $\{c, b, d\}$ and $\{b, c, \infty\}$. Considering the ideal hyperbolic tetrahedron $\{a, b, c, \infty\}$, we see that by Lemma 1 in §1.2, the angle between $\{a, b, c\}$ and $\{b, c, \infty\}$ is equal to $\angle bac$, since they are angles at opposite edges of $\{a, b, c, \infty\}$. Similarly, the angle between $\{c, b, d\}$ and $\{b, c, \infty\}$ is equal to $\angle cdb$. This proves the lemma. \square

Remark 5 *The above lemma depends on the orientation of the triangles and their angles, which has been encoded in the notation. For example, reflecting $\{c, b, d\}$ about the segment $\{c, b\}$ negates the sign of $\angle cdb$.*

With the help of the above lemma, we can easily calculate that

$$\begin{aligned} \{O, B, C, A\} &= T(\pi - 2\theta, \theta, \theta) \\ &= 2\mathcal{L}(\pi/2 - \theta). \end{aligned} \tag{4.31}$$

Equations (4.27)-(4.31) yield

$$2\mathcal{L}(\theta) = \mathcal{L}(2\theta) + 2\mathcal{L}(\pi/2 - \theta). \tag{4.32}$$

Since $V(\mathcal{L}(\theta)) = \mathcal{I}(\theta)$, (4.32) is equivalent to the Kubert identity in the case $n = 2$. For the $n = 3$ Kubert identity, we consider Figure 4.5 with $G = \{A, B, C, D, O, \infty\}$. Adding the edge connecting points A and C completes the triangulation of G .

On the one hand,

$$\begin{aligned}
G &= \{O, B, C, \infty\} + \{O, C, A, \infty\} + \{C, B, D, \infty\} + \{A, C, D, \infty\} \\
&= 2\mathcal{L}(\theta) + 2\mathcal{L}(2\theta) + 2\mathcal{L}\left(\theta + \frac{\pi}{3}\right) + T\left(\frac{\pi}{6}, \frac{\pi}{2} - \theta, \frac{\pi}{3} + \theta\right) \\
&= 2\mathcal{L}(\theta) + 2\mathcal{L}(2\theta) + 2\mathcal{L}\left(\theta + \frac{\pi}{3}\right) + \mathcal{L}\left(\frac{\pi}{6}\right) + \mathcal{L}\left(\frac{\pi}{2} - \theta\right) + \mathcal{L}\left(\frac{\pi}{3} + \theta\right). \quad (4.33)
\end{aligned}$$

On the other hand, $G = \{O, A, B, C, D\} + \{A, B, D, \infty\} + \{A, O, B, \infty\}$. Since $\{O, A, B, C, D\} = \{O, A, C, B\} + \{A, B, C, D\}$ we have

$$\begin{aligned}
G &= \{O, A, C, B\} + \{A, B, C, D\} + \{A, B, D, \infty\} + \{A, O, B, \infty\} \\
&= T(\pi - 3\theta, 2\theta, \theta) + T\left(\frac{\pi}{2} + \theta, \frac{\pi}{3} - \theta, \frac{\pi}{6}\right) + 2\mathcal{L}\left(\frac{\pi}{3} - \theta\right) + 2\mathcal{L}(3\theta) \\
&= \mathcal{L}(\pi - 3\theta) + \mathcal{L}(2\theta) + \mathcal{L}(\theta) + \mathcal{L}\left(\frac{\pi}{2} + \theta\right) + \mathcal{L}\left(\frac{\pi}{3} - \theta\right) + \mathcal{L}\left(\frac{\pi}{6}\right) \\
&\quad + 2\mathcal{L}\left(\frac{\pi}{3} - \theta\right) + 2\mathcal{L}(3\theta) \\
&= \mathcal{L}(2\theta) + \mathcal{L}(\theta) + \mathcal{L}\left(\frac{\pi}{2} + \theta\right) + 3\mathcal{L}\left(\frac{\pi}{3} - \theta\right) + \mathcal{L}\left(\frac{\pi}{6}\right) + \mathcal{L}(3\theta). \quad (4.34)
\end{aligned}$$

Equating (4.33) and (4.34) gives

$$\mathcal{L}(\theta) + \mathcal{L}(2\theta) + 3\mathcal{L}\left(\theta + \frac{\pi}{3}\right) + \mathcal{L}\left(\frac{\pi}{2} - \theta\right) = \mathcal{L}\left(\frac{\pi}{2} + \theta\right) + 3\mathcal{L}\left(\frac{\pi}{3} - \theta\right) + \mathcal{L}(3\theta). \quad (4.35)$$

Now, $\mathcal{L}\left(\frac{\pi}{2} - \theta\right) = -\mathcal{L}\left(\theta + \frac{\pi}{2}\right)$, and $\mathcal{L}\left(\frac{\pi}{3} - \theta\right) = -\mathcal{L}\left(\theta + \frac{2\pi}{3}\right)$. By Kubert $n = 2$ identity,

$$\mathcal{L}(2\theta) = 2\mathcal{L}(\theta) + 2\mathcal{L}\left(\theta + \frac{\pi}{2}\right), \quad (4.36)$$

So (4.35) is equivalent to

$$3\mathcal{L}(\theta) + 3\mathcal{L}\left(\theta + \frac{\pi}{3}\right) + 3\mathcal{L}\left(\theta + \frac{2\pi}{3}\right) = \mathcal{L}(3\theta), \quad (4.37)$$

which is the Kubert $n = 3$ identity.

One can start to see the difficulties in generalizing this method for higher n in the $n = 4$ case. The geometric proof of the cyclotomic identities in this case is shown in Figure 4.7 in solid lines. The difficulties arise when we try to triangulate the polyhedron $\{A, B, C, D, E\}$. After we add the dashed edge $\{C, D\}$ and then try to calculate the dihedral angles of the tetrahedron $\{C, B, E, D\}$, we find that

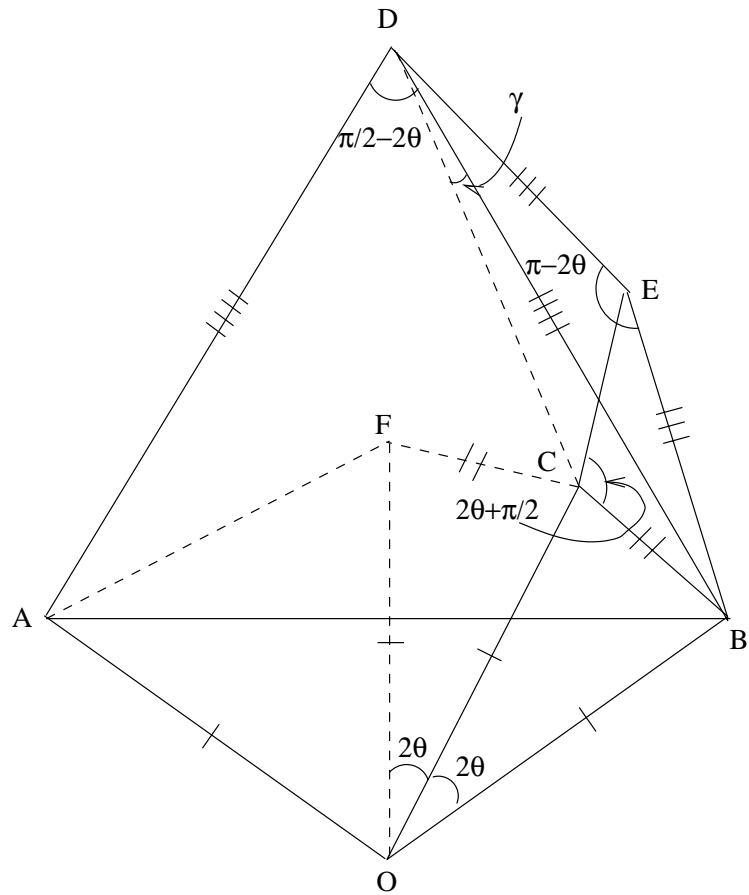


Figure 4.7: A geometric proof of the identity $n = 4$ cyclotomic identity shown in solid lines. The dashed lines are needed in addition to the solid lines to prove the Kubert $n = 4$ identities

the angle γ is a non-linear function of the angle θ . This means that when we write down the two different triangulations of $G = \{A, B, C, D, E, O, \infty\}$, we can hope to get the Kubert $n = 4$ identity only if all the terms involving γ cancel each other!

It turns out that if we triangulate $\{A, B, C, D, E\}$ by simply adding the edges $\{C, D\}$ and $\{C, A\}$ and carry out the calculations similar to the ones in the $n = 2$ and $n = 3$ cases, the terms involving γ will *not* cancel. The problem is solved by introducing the point F . In light of the $n = 2$ and $n = 3$ cases, both of which had n isosceles triangles with apex angle 2θ glued to one another, this is a natural point to consider. We then express the polyhedron $G = \{A, B, C, D, E, F, O, \infty\}$ as follows.

$$\begin{aligned}
G &= \{A, F, D, \infty\} + \{F, C, D, \infty\} + \{C, B, E, \infty\} + \{C, E, D, \infty\} \\
&\quad + \{A, O, F, \infty\} + \{F, O, C, \infty\} + \{C, O, B, \infty\} \\
&= 2\mathcal{L}(\theta + \frac{\pi}{4}) + T(\frac{\pi}{4} - \theta - \gamma, \frac{\pi}{2} + \theta, \frac{\pi}{4} + \gamma) + 2\mathcal{L}(\theta + \frac{\pi}{4}) \\
&\quad + T(\theta + \gamma, \frac{3\pi}{4} - \theta, \frac{\pi}{4} - \gamma) + 2\mathcal{L}(2\theta) + 4\mathcal{L}(\theta) \\
&= 2\mathcal{L}(\theta + \frac{\pi}{4}) + \mathcal{L}(\frac{\pi}{4} - \theta - \gamma) + \mathcal{L}(\frac{\pi}{2} + \theta) + \mathcal{L}(\frac{\pi}{4} + \gamma) + 2\mathcal{L}(\theta + \frac{\pi}{4}) \\
&\quad + \mathcal{L}(\theta + \gamma) + \mathcal{L}(\frac{3\pi}{4} - \theta) + \mathcal{L}(\frac{\pi}{4} - \gamma) + 2\mathcal{L}(2\theta) + 4\mathcal{L}(\theta) \\
&= 4\mathcal{L}(\theta + \frac{\pi}{4}) + \mathcal{L}(\frac{\pi}{4} - \theta - \gamma) + \mathcal{L}(\frac{\pi}{2} + \theta) + \mathcal{L}(\frac{\pi}{4} + \gamma) \\
&\quad + \mathcal{L}(\theta + \gamma) + \mathcal{L}(\frac{3\pi}{4} - \theta) + \mathcal{L}(\frac{\pi}{4} - \gamma) + 2\mathcal{L}(2\theta) + 4\mathcal{L}(\theta) \\
&= 4\mathcal{L}(\theta + \frac{\pi}{4}) + \mathcal{L}(\frac{\pi}{4} - \theta - \gamma) + 5\mathcal{L}(\frac{\pi}{2} + \theta) + \mathcal{L}(\frac{\pi}{4} + \gamma) \\
&\quad + \mathcal{L}(\theta + \gamma) + \mathcal{L}(\frac{3\pi}{4} - \theta) + \mathcal{L}(\frac{\pi}{4} - \gamma) + 8\mathcal{L}(\theta), \tag{4.38}
\end{aligned}$$

where the last equality was obtained by applying the $n = 2$ Kubert identity.

Alternatively,

$$\begin{aligned}
G &= \{C, B, E, D\} + \{F, B, C, D\} + \{A, B, F, D\} + \{O, B, C, F\} \\
&\quad + \{O, B, F, A\} + \{O, B, A, \infty\} + \{A, B, D, \infty\} + \{D, B, E, \infty\} \\
&= T\left(\frac{\pi}{2} + \theta, \frac{\pi}{4} + \gamma, \frac{\pi}{4} - \theta - \gamma\right) + T\left(\frac{3\pi}{4} - \theta, \frac{\pi}{4} - \gamma, \theta + \gamma\right) + 2\mathcal{L}\left(\frac{\pi}{4} - \theta\right) \\
&\quad + 2\mathcal{L}\left(\frac{\pi}{2} - \theta\right) + 2\mathcal{L}\left(\frac{\pi}{2} - 2\theta\right) + 2\mathcal{L}(4\theta) + 2\mathcal{L}\left(\frac{\pi}{4} - \theta\right) + 2\mathcal{L}\left(\frac{\pi}{2} - \theta\right) \\
&= \mathcal{L}\left(\frac{\pi}{2} + \theta\right) + \mathcal{L}\left(\frac{\pi}{4} + \gamma\right) + \mathcal{L}\left(\frac{\pi}{4} - \theta - \gamma\right) + \mathcal{L}\left(\frac{3\pi}{4} - \theta\right) + \mathcal{L}\left(\frac{\pi}{4} - \gamma\right) + \\
&\quad \mathcal{L}(\theta + \gamma) + 2\mathcal{L}\left(\frac{\pi}{4} - \theta\right) + 2\mathcal{L}\left(\frac{\pi}{2} - \theta\right) + 2\mathcal{L}\left(\frac{\pi}{2} - 2\theta\right) + 2\mathcal{L}(4\theta) \\
&\quad + 2\mathcal{L}\left(\frac{\pi}{4} - \theta\right) + 2\mathcal{L}\left(\frac{\pi}{2} - \theta\right) \\
&= \mathcal{L}\left(\frac{\pi}{2} + \theta\right) + \mathcal{L}\left(\frac{\pi}{4} + \gamma\right) + \mathcal{L}\left(\frac{\pi}{4} - \theta - \gamma\right) + \mathcal{L}\left(\frac{3\pi}{4} - \theta\right) + \mathcal{L}\left(\frac{\pi}{4} - \gamma\right) \\
&\quad + \mathcal{L}(\theta + \gamma) + 4\mathcal{L}\left(\frac{\pi}{4} - \theta\right) + 4\mathcal{L}\left(\frac{\pi}{2} - \theta\right) + 2\mathcal{L}\left(\frac{\pi}{2} - 2\theta\right) + 2\mathcal{L}(4\theta) \\
&= \mathcal{L}\left(\frac{\pi}{2} + \theta\right) + \mathcal{L}\left(\frac{\pi}{4} + \gamma\right) + \mathcal{L}\left(\frac{\pi}{4} - \theta - \gamma\right) + 5\mathcal{L}\left(\frac{3\pi}{4} - \theta\right) + \mathcal{L}\left(\frac{\pi}{4} - \gamma\right) \\
&\quad + \mathcal{L}(\theta + \gamma) + 8\mathcal{L}\left(\frac{\pi}{4} - \theta\right) + 4\mathcal{L}\left(\frac{\pi}{2} - \theta\right) + 2\mathcal{L}(4\theta), \tag{4.39}
\end{aligned}$$

where the last equality was obtained by applying the $n = 2$ Kubert identity. Comparing equations (4.38) and (4.39), we see that all the terms involving γ cancel each other, and we are left with the $n = 4$ Kubert identity.

This fortuitous turn of events does not occur in the $n = 5$ case. Of all the points that were added to the cyclotomic $n = 5$ proof, every one resulted in a number of angles such as γ , and the terms involving them in the triangulation of G did not cancel. This indicates that one needs a further algebraic insight into this problem in order to solve it for the general n . This insight was provided by Dupont and Sah in [5].

4.4 A scissors congruence proof of the Kubert identities based on the algebraic proof of Dupont and Sah

4.4.1 Dupont and Sah's proof of the Kubert identities

In [5] Dupont and Sah give an algebraic proof of a slightly generalized form of the Kubert identities. In fact, they show that $\mathcal{L}(n\theta)$ is scissors congruent to $n \sum_{j=0}^{n-1} \mathcal{L}(\theta + j\pi/n)$ using purely algebraic techniques.

In order to state their result we first need to introduce some notation. Consider an ideal tetrahedron in the half-space model, and identify the half-space model with the extended complex plane $\mathbb{C} \cup \infty$. Then this tetrahedron can be determined up to orientation by the cross ratio of the complex coordinates of its vertices, which is defined as follows.

Definition 9 *Let $a, b, c, d \in \mathbb{C} \cup \infty$. Then the cross ratio of a, b, c, d , denoted as (a, b, c, d) , is defined as $\frac{(a-c)(b-d)}{(a-d)(b-c)}$.*

Following the convention in [5], we will denote the ideal tetrahedron with vertices $\{\infty, 0, 1, z\}$ whose projection onto the plane at infinity is shown in Figure 4.8a) as $\{z\}$. This tetrahedron can also be represented as $\{1/(1-z)\}$ or $\{(z-1)/z\}$ as shown in Figure 4.8. The tetrahedron in b) was obtained by scaling the tetrahedron in a) by a factor of $1/z$ and rotating it, and the tetrahedron in c) is a result of scaling the tetrahedron in a) by a factor of $1/(1-z)$ and rotating it. Since scaling and rotation are hyperbolic isometries, all three tetrahedra are isometric to each other.

Note that $-\{1/z\} = \{z\}$ in the sense that $\{1/z\}$ is isometric to $\{z\}$ by an orientation reversing isometry. This can be seen in Figure 4.9a), which shows that the tetrahedron $-\{1/z\} = \{\infty, 1/z, 1, 0\}$ can be obtained from the tetrahedron $\{z\} = \{\infty, 0, 1, z\}$ by multiplication by z , which is an orientation-preserving isometry. Similarly, Figure 4.9b) shows that $-\{1-z\} = \{z\}$.

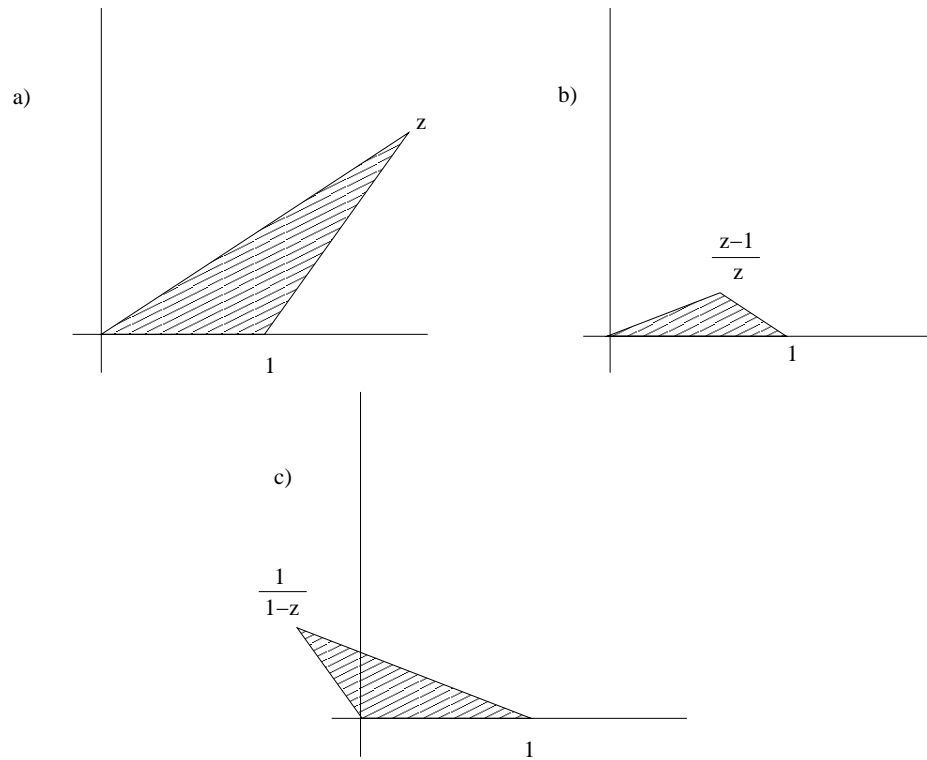


Figure 4.8: An illustration of the three ways to describe an ideal hyperbolic tetrahedron by its cross ratio. The triangles in a), b) and c) are all similar to each other.

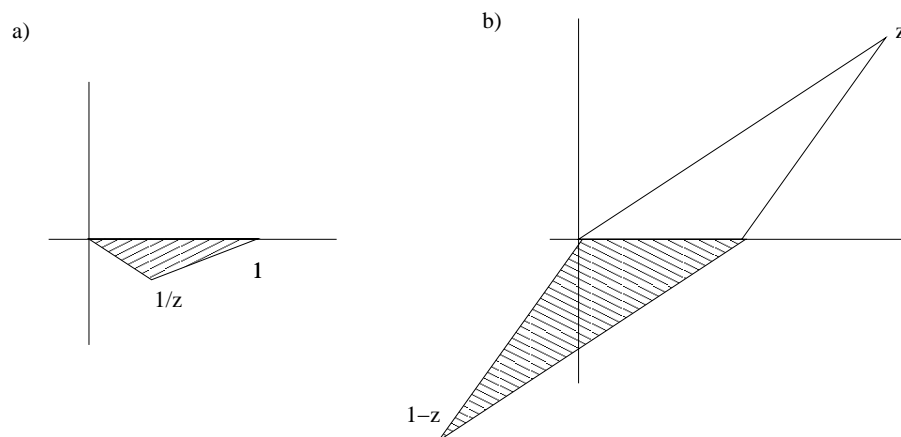


Figure 4.9: The triangle of Figure 4.8 scaled by $1/z$

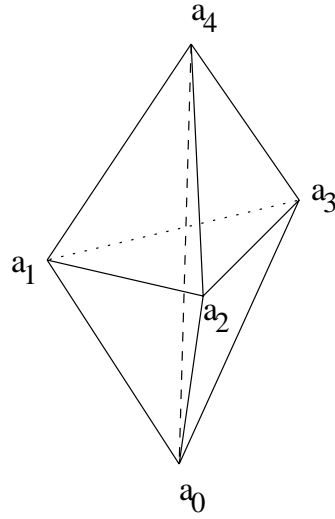


Figure 4.10: Geometric interpretation in the Klein model of the cocycle relation as stating that the union along faces of two hyperbolic tetrahedra can be divided into three tetrahedra

The cross ratio is subject to the *cocycle* relation:

$$\sum_{j=1}^4 (-1)^j \{a_0 : \cdots : \tilde{a}_j : \cdots : a_4\} = 0, \quad (4.40)$$

for any $a_j \in \mathbb{C} \cup \infty$. One can interpret (4.40) as stating that there are two ways to triangulate a the convex hull of 5 distinct points in hyperbolic space, as shown in Figure 4.10. The five tetrahedra on the left hand side (4.40) can be viewed as the boundary of a 4-simplex that has been collapsed to 3-space. The cocycle relation is key in the proof of the following theorem of Dupont and Sah.

Theorem 4 (Dupont-Sah)

$$\{z^n\} = n \sum_{j=0}^{n-1} \{\xi^j z\}, \quad (4.41)$$

where ξ is a primitive n -th root of unity.

When $z = e^{i2\pi\theta}$, $\{z\}$ is an isosceles ideal tetrahedron with apex angle $\arg z$. In that case the left hand side of (4.41) becomes $\mathcal{L}(n\theta)$, while the right hand side

becomes $n \sum_{j=0}^{n-1} \mathcal{L}(\theta + j\pi/n)$. However, $|z| = 1$ need not be true for (4.41) to hold. So (4.41) is a generalization of the Kubert identities.

We now give an outline of Dupont and Sah's proof. Details can be found in [5] and [4]. Following Bloch in [1], Dupont and Sah define the operation $*$ on two rational functions in $\mathbb{C}(x)$ as follows:

Let $f(t) = a \prod (\alpha_i - t)^{d(i)}$, and $g(t) = b \prod (\beta_i - t)^{e(i)}$, $d(i) \in \mathbb{Z}$, where $d(i), e(i) \in \mathbb{Z}$, the $\alpha_i \in \mathbb{C}$ are distinct, and the $\beta_i \in \mathbb{C}$ distinct. Then define

$$f^- * g = \sum_{i,j} d(i)e(j) \{\alpha_i^{-1} \beta_j\}, \quad (4.42)$$

where the sum extends over i and j and the expression is 0 if f or $g \in \mathbb{C}$. $f^- * g$ is clearly bmultiplicative (that is, $f^- * (gh) = f^- * g^- * h$) and, in view of the fact that $-\{1/z\} = -\{z\}$, alternating. The key ingredient in the proof of Theorem 4 is the fact that

$$f^- * (1 - f) = \{f(0)\} - \{f(\infty)\} \quad (4.43)$$

for all $f \in \mathbb{C}(t)$. We will assume this fact for now, and return to its proof shortly.

Next, we consider

$$f(t) = \frac{1 - t^n}{1 - z^n}.$$

Since ξ is a primitive n -th root of unity, we can write

$$f(t) = \frac{\prod_{0 \leq j \leq n-1} (\xi^j - t)}{1 - z^n},$$

so that

$$1 - f(t) = \frac{\prod_{0 \leq j \leq n-1} (\xi^j z - t)}{z^n - 1}.$$

Then by the definition (4.42),

$$f^- * (1 - f) = n \sum_{0 \leq j \leq n-1} \{\xi^j z\}, \quad (4.44)$$

while by Theorem 4

$$f^- * (1 - f) = \{f(0)\} - \{f(\infty)\} = \left\{ \frac{1}{1 - z^n} \right\} - \{\infty\} = \{z^n\}. \quad (4.45)$$

Comparing equations (4.44) and (4.45) proves the theorem.

The proof of the identity (4.43) ultimately boils down to induction on the maximum degree of the numerator and denominator of f , which is done in [4]. To begin with, Dupont and Sah define the set $H = \{f \in \mathbb{C} \mid f \text{ obeys (4.43)}\}$ and prove that H has the following three properties:

- (i) $(at + b)/(ct + d) \in H$ for all $a, b, c, d \in \mathbb{C}$ with $ct + d \neq 0$.
- (ii) $f \in H$ implies that $1 - f \in H$ and that $f^{-1} \in H$ when $f \neq 0$.
- (iii) If $f_1, f_2, f_2/f_1$, and $(1 - f_2)/(1 - f_1) \in H$, then $(1 - f_2)f_1/((1 - f_1)f_2) \in H$.

Proof of property (i). Let $f(t) = (at + b)/(ct + d)$, so that $1 - f(t) = ((c - a)t + (d - b))/(ct + d)$. Then

$$\begin{aligned} f^- * (1 - f) &= \left\{ \frac{(d - b)a}{(c - a)b} \right\} - \left\{ \frac{(d - b)c}{(c - a)d} \right\} + \left\{ \frac{bc}{da} \right\} \\ &= \left\{ \frac{z_1(1 - z_2)}{z_2(1 - z_1)} \right\} - \left\{ \frac{1 - z_2}{1 - z_1} \right\} + \left\{ \frac{z_2}{z_1} \right\}, \end{aligned} \quad (4.46)$$

where $z_1 = a/c$ and $z_2 = b/d$. On the other hand,

$$\begin{aligned} \{f(0)\} - \{f(\infty)\} &= \{b/d\} - \{a/c\} \\ &= \{z_2\} - \{z_1\} \end{aligned} \quad (4.47)$$

But

$$\{z_1\} - \{z_2\} + \left\{ \frac{z_1(1 - z_2)}{z_2(1 - z_1)} \right\} - \left\{ \frac{1 - z_2}{1 - z_1} \right\} + \left\{ \frac{z_2}{z_1} \right\} = 0 \quad (4.48)$$

by the cocycle relation (4.40), where

$$\{a_0, a_1, a_2, a_3, a_4\} = \{\infty, 0, 1, z_1, z_2\}$$

for some $z_1, z_2 \in \mathbb{C}$. Property (i) then follows from the cocycle relation.

Proof of property (ii). Define $L(f) = f^- * (1 - f)$ and $R(f) = \{f(0)\} - \{f(\infty)\}$.

Then

$$L(f) + L(f^{-1}) = 0 \text{ and } L(f) + L(1 - f) = 0 \quad (4.49)$$

easily follow from the fact that $f^- * g$ is alternating. Letting $R(f) = \{f(0)\} - \{f(\infty)\}$, we see that

$$R(f) + R(f^{-1}) = 0 \text{ and } R(f) + R(1 - f) = 0, \quad (4.50)$$

since, as noted earlier, $\{z\} = -\{1/z\} = -\{1 - z\}$. Equations (4.49) and (4.50) imply that if $L(f) = R(f)$, then $L(1 - f) = R(1 - f)$ and $L(f^{-1}) = R(f^{-1})$. This proves property (ii).

Proof of property (iii). Using just the fact that $f^- * g$ is bimultiplicative and alternating, Dupont and Sah prove that for any $f_1, f_2 \in \mathbb{C}(t)$

$$L(f_1) - L(f_2) + L(f_2/f_1) - L((1-f_2)/(1-f_1)) + L((1-f_2)f_1/(1-f_1)f_2) = 0. \quad (4.51)$$

The reader is referred to the proof of Lemma 5.17 in [5] for details. Relation (4.51) holds equally well if L is replaced by R , as can be easily verified by using (4.48). Property (iii) then follows.

What remains to be shown is

$$H = \mathbb{C}(t). \quad (4.52)$$

A generalization of this result is proved by Dupont and Poulsen in [4]. The outline of their proof goes as follows.

Let $\deg(P)$ denote the degree of a polynomial $P = P(x)$, and define

$$H_k = \{f = P/Q \in H \mid \deg(P) \leq k, \deg(Q) \leq k\}. \quad (4.53)$$

Dupont and Poulsen then proceed to show that $H_k \subset H$ by induction on k . The base case of the induction was already proved by Property (i) above, which showed that all linear fractional transformations are in H . For the induction step, assume that $H \subset M$ for $k \geq 1$, and consider $f \in H_{k+1}$ of the form P/Q with $\deg P = \deg Q$. It is sufficient to consider only f of this form by Property (ii). Let

$$f(x) = \frac{P_1(x)(x - a)}{Q_1(x)(x - b)}, \quad (4.54)$$

where $\deg(P_1) = \deg(Q_1) = k$, $a \neq b$, and $Q_1(a) \neq 0$. The authors then give a procedure for finding polynomials $f_1, f_2 \in H_k$ such that

$$f = \frac{f_1(1 - f_2)}{f_2(1 - f_1)}. \quad (4.55)$$

They choose f_1 and f_2 of the form

$$f_1(x) = \frac{P_1(x)}{R(x)(x - d)}, \quad f_2(x) = c \frac{x - b}{x - d}, \quad (4.56)$$

where c , d , and the polynomial R are determined from the equation $f = f_1(1 - f_2)/[f_2(1 - f_1)]$ using f , f_1 and f_2 from (4.54) and (4.56). After making the necessary substitutions we see that the condition we need is

$$c(x - a)(x - d)R(x) = [(x - d) - c(x - b)]Q_1(x) + c(x - a)P_1(x). \quad (4.57)$$

Equation (4.57) can only hold if d is a root of the right hand side. That is, as long as $c \neq 0$, we should have

$$(d - b)Q_1(d) = (d - a)P_1(d). \quad (4.58)$$

Looking back at (4.54), we see that d must be chosen to satisfy

$$f(d) = 1. \quad (4.59)$$

If there does not exist d that satisfies (4.59), f can be replaced by $F = f \circ \varphi$, where $\varphi(x) = 1/x$. In that case, $F(0) = 1$. It then follows by a Lemma in [4] that $f = F \circ \varphi \in H$. Therefore, we can assume, without the loss of generality, that a solution to (4.59) does exist. We find the constant c that appears in (4.57) by enforcing the condition that the right hand side of (4.57) must vanish when $x = a$. This leads to

$$[(a - d) - c(a - b)]Q_1(a) = 0. \quad (4.60)$$

Since $Q_1(a) \neq 0$ and $a \neq b$, c is determined by

$$c = (a - d)/(a - b). \quad (4.61)$$

Once d and c have been determined such that they are both roots of the right hand side of (4.57), R is uniquely determined as a polynomial of degree at most $k - 1$, and the proof is complete. Note that in general there is more than one way to find R since if the numerator or the denominator of f is of degree at least 2, one makes a choice in picking the a or the b in (4.54).

4.4.2 The method used to apply Dupont and Sah's proof to a get a geometric proof of the Kubert identities

In order to use the proof in §4.4.1 to produce a picture of how the various tetrahedra in the Kubert identities fit together, we go through all the steps of the proof Theorem 4 using

$$f(t) = \frac{t^n z^n - 1}{t^n - 1} \quad (4.62)$$

in place of Dupont and Sah's $f(t) = \frac{1-t^n}{1-z^n}$. The f in (4.62) has the property

$$f^- * (1 - f) = -n \sum_{j=0}^{n-1} \{\xi^j z\},$$

and its numerator and denominator are of equal degrees. Therefore, we can show that $f \in H = \{f \in \mathbb{C} \mid f \text{ obeys (4.43)}\}$ by going through the steps of the inductive proof of Dupont and Poulsen, as described in §4.4.1. We illustrate the process in the cases $n = 2, 3, 4$ of the Kubert identities.

4.4.3 “Geometrization” of Dupont and Sah's proof of the Kubert identity n=2

We wish to see the geometry underlying Dupont and Sah's proof of the Kubert identity in the case $n = 2$. This is equivalent to the geometry in the proof of $f^- * (1 - f) = \{f(0)\} - \{f(\infty)\}$ when

$$f(x) = \frac{x^2 z^2 - 1}{x^2 - 1}. \quad (4.63)$$

Following the proof of Dupont and Poulsen described in §4.4.1, we write

$$f(x) = \frac{P_1(x)(x - 1/z)}{Q_1(x)(x - 1)},$$

where

$$P_1(x) = z^2(x + 1/z) \text{ and } Q_1(x) = x + 1. \quad (4.64)$$

This is similar to (4.54) with

$$a = 1/z \text{ and } b = 1. \quad (4.65)$$

Solving (4.59) with f given by (4.63), we have

$$d = 0. \quad (4.66)$$

Equation (4.61) gives

$$c = \frac{1}{1 - z}. \quad (4.67)$$

Substituting (4.64)-(4.67) into (4.57) gives

$$R(x) = z^2 - z. \quad (4.68)$$

It follows by (4.56) that

$$\begin{aligned} f_1(x) &= \frac{P_1(x)}{R(x)(x - d)} \\ &= \frac{zx + 1}{(z - 1)x} \end{aligned} \quad (4.69)$$

and

$$\begin{aligned} f_2(x) &= c \frac{x - b}{x - d} \\ &= \frac{1 - x}{(z - 1)x}. \end{aligned} \quad (4.70)$$

Therefore,

$$\frac{f_1}{f_2} = \frac{1 + xz}{1 - x} \quad (4.71)$$

h	$h(0)$	$h(\infty)$
$f_1 = (zx + 1)/[(z - 1)x]$	∞	$z/(z - 1)$
$f_2 = (1 - x)/[(z - 1)x]$	∞	$1/(1 - z)$
$f_1/f_2 = (1 + xz)/(1 - x)$	1	$-z$
$(1 - f_2)/(1 - f_1) = (1 - xz)/(1 + x)$	1	$-z$
$f_1(1 - f_2)/[f_2(1 - f_1)] = (x^2 z^2 - 1)/(x^2 - 1)$	1	z^2

Table 4.1: Values of f_1 , f_2 , f_1/f_2 , $(1 - f_2)/(1 - f_1)$, $f_1(1 - f_2)/f_2(1 - f_1)$ at 0 and ∞

and

$$\frac{1 - f_2}{1 - f_1} = -\frac{1 - xz}{1 + x}. \quad (4.72)$$

From the equations (4.69)-(4.72) one can easily figure out the values in Table 4.1.

Recalling the definition $R(f) = \{f(0)\} - \{f(\infty)\}$ and (4.63) we find that

$$R(f) = \{1\} - \{z^2\} = -\{z^2\} \quad (4.73)$$

On the other hand, we see from Table 4.1 that

$$\begin{aligned} R(f_1) - R(f_2) - R\left(\frac{f_1}{f_2}\right) - R\left(\frac{1 - f_2}{1 - f_1}\right) &= \left\{\frac{z}{z - 1}\right\} - \left\{\frac{1}{1 - z}\right\} - \{-z\} - \{-z\} \\ &= -2\{z\} - 2\{-z\}. \end{aligned} \quad (4.74)$$

By (4.48) and (4.55), the left hand sides of (4.73) and (4.74) are equal to each other. Therefore,

$$\{z^2\} = 2\{z\} + 2\{-z\}, \quad (4.75)$$

which is the generalized Kubert identity in the case $n = 2$. Note that in this case there was no need to go further in the induction process by proving that f_1 , f_2 , f_1/f_2 , and $(1 - f_2)/(1 - f_1)$ all obey (4.43) since this is evident by simply applying the definition (4.42).

The above proof shows that the generalized $n = 2$ Kubert identity can be proved using only the relation (4.48) with $z_1 = z_2 = z$. The half-plane model of the proof can be seen in Figure 4.11. In that figure, $\{\infty : 0 : 1 : z^2\} = \{z^2\} = \{f(\infty)\}$, with f defined in (4.63). The other 4 tetrahedra in the figure

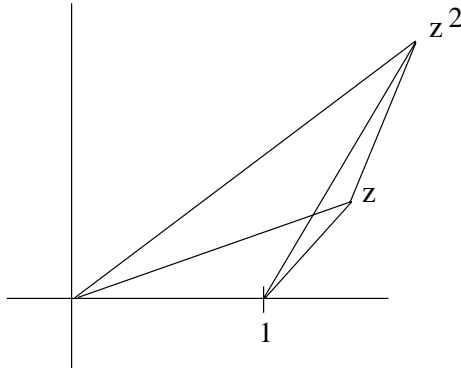


Figure 4.11: A geometric proof of the generalized Kubert identity $\{z^2\} = 2\{z\} + 2\{-z\}$

are $\{\infty : 0 : 1 : z\} = \{z\} = -\{f_1(\infty)\}$, $\{\infty : 0 : z : z^2\} = \{z\} = \{f_2(\infty)\}$, $\{1 : z^2 : z : 0\} = \{-z\} = \{f_1(\infty)/f_2(\infty)\}$, and $\{z : \infty : z^2 : 1\} = \{-z\} = \{(1 - f_2(\infty))/(1 - f_1(\infty))\}$. (Admittedly, there were some arbitrary choices made in matching a given tetrahedron with the terms on the left hand side of (4.74).) Thus, the identity (4.75) can be read off Figure 4.11. In the case $|z| = 1$, Figure 4.11 becomes Figure 4.4, up to rotation. In fact, if one views Figure 4.11 as living in the Euclidean plane, it becomes a geometric proof of the exponential version of the cyclotomic identity

$$z^2 - 1 = (z + 1)(z - 1). \quad (4.76)$$

For if we think of complex numbers as vectors, Figure 4.11 shows that the vector $\overrightarrow{1z^2}$ (representing the complex number $z^2 - 1$) equals $\overrightarrow{1z} + z\overrightarrow{z^2} = \overrightarrow{1z} + z(\overrightarrow{1z})$, which, by the distributive property, is equivalent to $(z + 1)(z - 1)$. Thus Figure 4.11 can be viewed as a graphical representation of multiplication of complex numbers, Figure 4.4 is a special case of Figure 4.11 when $|z| = 1$.

4.4.4 “Geometrization” of Dupont and Sah’s proof of the Kubert identity $n=3$

In order to use Dupont and Sah’s result to produce a geometric proof of the $n = 3$ Kubert identity, the cocycle relation (4.48) needs to be applied repeatedly. We give a brief overview of this process before describing it in detail. To begin with, the cocycle relation states that the tetrahedron $\{z^3\}$ equals 4 other tetrahedra. Then we apply the cocycle relation to 3 of those 4 tetrahedra as follows: we attach a new tetrahedron to one of the 4 tetrahedra, and we divide the union of 2 tetrahedra into 3 in the manner of Figure 4.10. We continue this process of replacing a tetrahedron by 4 other tetrahedra as dictated by the cocycle relation until we arrive at equation (4.41) in the case $n = 3$. Our goal is to come up with a concrete simplicial chain comprised by the tetrahedra $3\{z\}$, $3\{\exp(2\pi i/3)z\}$, and $3\{\exp(4\pi i/3)z\}$ whose boundary equals to the boundary of the tetrahedron $\{z^3\}$.

In this process following Dupont and Poulsen’s induction proof one has to make certain choices. For example, any time one writes

$$f(x) = \frac{x^3 z^3 - 1}{x^3 - 1}.$$

as

$$f(x) = \frac{P_1(x)(x - a)}{Q_1(x)(x - b)},$$

one needs to choose which of the 3 roots of unity to make a and b . As expected, the choice of a primitive root of unity is unimportant because it corresponds to the order in which one multiplies the terms $z - \omega$ and $z - \omega^2$ with $\omega = \exp(2\pi i/3)$. The more difficult choice one must make is to which face of a given tetrahedron one should attach a new tetrahedron. Once a face is fixed, there is only one way a new tetrahedron can be attached in order to get the correct 5-term relation. So, for instance, in Figure 4.10 if only the bottom tetrahedron were rotated so that the vertices a_1 , a_2 , and a_3 were acted on by the permutation $(1\ 2\ 3)$, and then glued back to the top one, the line $\{a_0, a_4\}$ would divide the resulting polyhedron into 3 tetrahedra that are completely different from the original 3 tetrahedra

$\{a_0, a_1, a_2, a_4\}$, $\{a_0, a_2, a_3, a_4\}$, $\{a_0, a_3, a_1, a_4\}$.

Given any one of the 4 faces of $\{a_0, a_1, a_2, a_3\}$ there is exactly one way to glue to it the tetrahedron $\{a_1, a_2, a_3, a_4\}$ so that the result is isometric to the polyhedron in Figure 4.10. This is due to the fact that the dihedral angles at each vertex of an ideal hyperbolic tetrahedron are the same, as discussed in §1.2.

The steps of the Dupont-Poulsen-Sah proof specify which new tetrahedra need to be attached, and how they need to be attached, but they do not specify which face they need to be attached to. Certainly, the choice of the face does not affect the validity of the proof, so that one could program a computer to generate a (possibly very messy) diagram that embodies the Dupont-Poulsen-Sah proof. However, with a proper choice of faces, it can be demonstrated that the geometric version of the proof of Theorem 4 is based on and implies the geometric proof of the cyclotomic identities that was presented in §4.3.2. We will now demonstrate how this works.

We start out with

$$f(x) = \frac{x^3 z^3 - 1}{x^3 - 1}. \quad (4.77)$$

Since $f(0) = 1$,

$$d = 0. \quad (4.78)$$

We write

$$f(x) = \frac{P_1(x)(x - a)}{Q_1(x)(x - b)},$$

and choose

$$a = 1/z \text{ and } b = 1. \quad (4.79)$$

Then (4.61) gives

$$c = 1/(1 - z). \quad (4.80)$$

Also, we have

$$P_1(x) = (x - \omega/z)(x - \omega^2/z)z^3 \quad (4.81)$$

and

$$Q_1(x) = (x - \omega)(x - \omega^2), \quad (4.82)$$

h	$h(0)$	$h(\infty)$
$f_1 = \frac{z^2(x-\omega/z)(x-\omega^2/z)}{x(z-1)(1+x+xz)}$	∞	$z^2/(z^2-1)$
$f_2 = \frac{x-1}{x(1-z)}$	∞	$1/(1-z)$
$\frac{f_1}{f_2} = -\frac{z^2(x-\omega/z)(x-\omega^2/z)}{(x-1)(1+x+xz)}$	1	$-z^2/(z+1)$
$\frac{1-f_2}{1-f_1} = -\frac{z(z+1)(x+1/(z+1))(x-1/z)}{(x-\omega)(x-\omega^2)}$	1	$-z(z+1)$
$\frac{f_1(1-f_2)}{f_2(1-f_1)} = \frac{x^3z^3-1}{x^3-1}$	1	z^3

Table 4.2: Values of f_1 , f_2 , f_1/f_2 , $(1-f_2)/(1-f_1)$, $f_1(1-f_2)/f_2/(1-f_1)$ at 0 and ∞

where $\omega = \exp(2\pi i/3)$ for the rest of this subsection. Then by (4.57)

$$R(x) = (z-1)z(1+x+xz), \quad (4.83)$$

and by (4.56)

$$f_1(x) = \frac{z^2(x-\omega/z)(x-\omega^2/z)}{x(z-1)(1+x+xz)} \quad (4.84)$$

and

$$f_2(x) = \frac{x-1}{x(1-z)}. \quad (4.85)$$

It follows that

$$\frac{f_1}{f_2} = -\frac{z^2(x-\omega/z)(x-\omega^2/z)}{(x-1)(1+x+xz)} \quad (4.86)$$

and

$$\frac{1-f_2}{1-f_1} = -\frac{z(z+1)(x+1/(z+1))(x-1/z)}{(x-\omega)(x-\omega^2)}. \quad (4.87)$$

Using equations (4.84)-(4.87) we generate the data in Table 4.2. Using the values in Table 4.2 and the fact that

$$R(f) = -R(f_1) + R(f_2) + R\left(\frac{f_1}{f_2}\right) + R\left(\frac{1-f_2}{1-f_1}\right), \quad (4.88)$$

where $R(f) = \{f(0)\} - \{f(\infty)\}$, we get the relation

$$\{z^3\} = -\left\{\frac{z^2}{z^2-1}\right\} + \left\{\frac{1}{1-z}\right\} + \left\{-\frac{z^2}{z+1}\right\} + \{-z(z+1)\}. \quad (4.89)$$

Figure 4.12a) shows the simplices corresponding to each term in the equation above. The correspondence is $\{z^2/(z^2-1)\} = \{\infty, 0, z, z^3\}$, $\{1/(1-z)\} =$

$\{\infty, 1, 0, z\}$, $\{-z^2/(z+1)\} = \{0, z, 1, z^3\}$, and $\{-z(z+1)\} = \{\infty, 1, z, z^3\}$. Thus we can now convert (4.89) into a statement involving simplicial complexes:

$$\{\infty, 1, 0, z^3\} = -\{\infty, 0, z, z^3\} + \{\infty, 1, 0, z\} + \{0, z, 1, z^3\} + \{\infty, 1, z, z^3\}. \quad (4.90)$$

Taking the boundary of a 3-simplex using the formula

$$\partial(\{v_0, v_1, v_2, v_3\}) = \sum_{i=0}^3 \{v_0, \dots, \hat{v}_i, \dots, v_3\}, \quad (4.91)$$

we can easily compute the boundaries of both sides of (4.90) and see that they are equal.

Proceeding with the iterative proof, we now need to show that f_1 , f_2 , f_1/f_2 , and $(1-f_2)/(1-f_1)$ all satisfy (4.43). For $f_1 = (z^2(x-\omega/z)(x-\omega^2/z))/(x(z-1)(1+x+xz))$ we repeat the procedure that was just used for f . The auxiliary functions used in the following proof will be denoted as $P_1(f_1)$, $f_1(f_1)$, etc.

$f_1(x) = 1$ has solutions ω and ω^2 . We choose

$$d = \omega. \quad (4.92)$$

Then we choose

$$a = \omega/z \text{ and } b = 0, \quad (4.93)$$

so that by (4.61)

$$c = 1 - z. \quad (4.94)$$

Then

$$P_1(f_1)(x) = (x - \omega^2/z)z^2 \quad (4.95)$$

and

$$Q_1(f_1)(x) = (z-1)(1+x+xz), \quad (4.96)$$

and, by (4.57),

$$R(x) = -z. \quad (4.97)$$

It follows by (4.56)

$$f_1(f_1)(x) = -\frac{z(x - \omega^2/z)}{x - \omega} \quad (4.98)$$

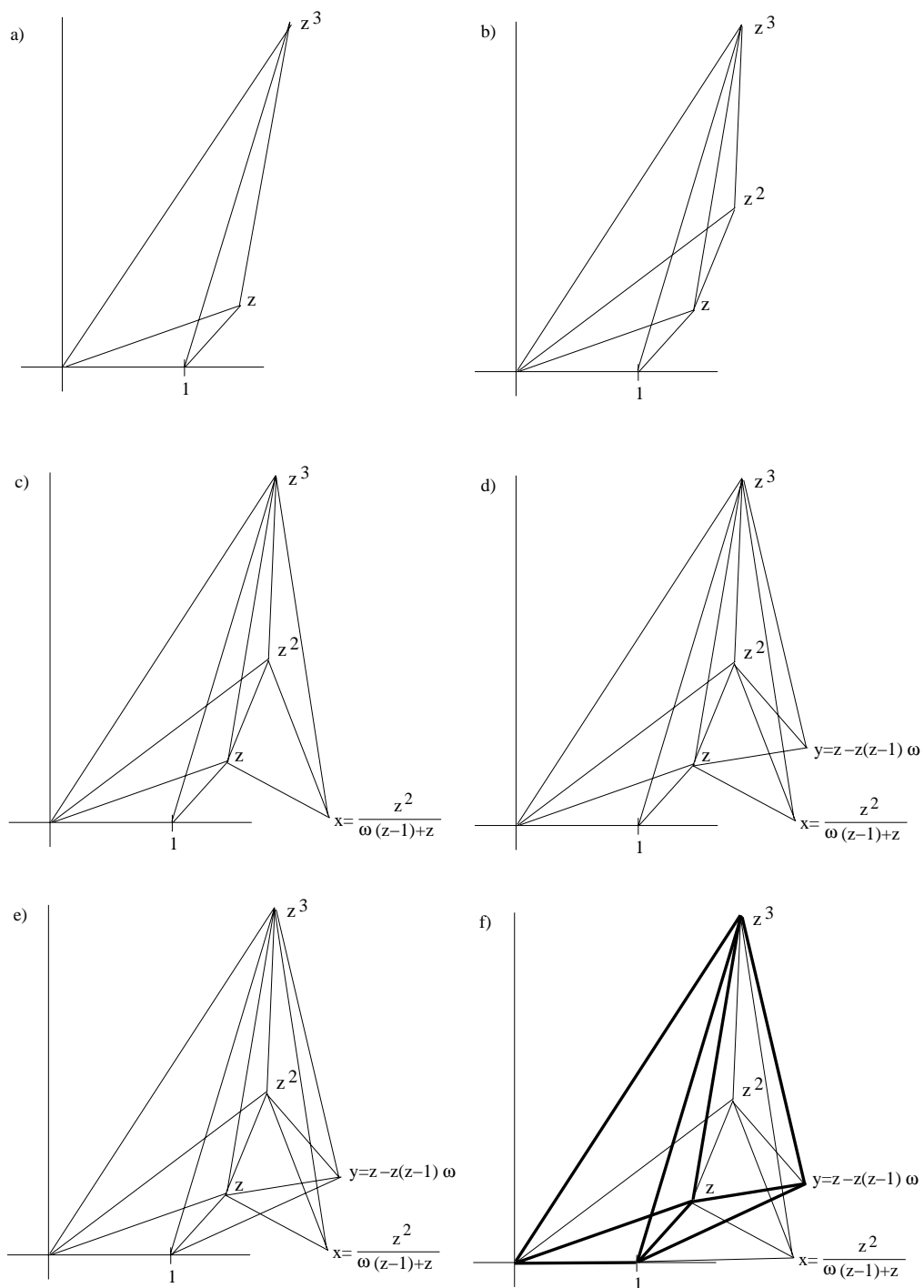


Figure 4.12: A geometric proof of the generalized Kubert identity $\{z^3\} = 3\{z\} + 3\{\omega z\} + 3\{\omega^2 z\}$, where $\omega = \exp(2\pi i/3)$

h	$h(0)$	$h(\infty)$
$f_1(f_1) = \frac{-z(x-\omega^2/z)}{x-\omega}$	$-\omega$	$-z$
$f_2(f_1) = \frac{x(1-z)}{x-\omega}$	0	$1-z$
$\frac{f_1(f_1)}{f_2(f_1)} = \frac{z(x-\omega^2/z)}{x(z-1)}$	∞	$\frac{z}{z-1}$
$\frac{1-f_2(f_1)}{1-f_1(f_1)} = \frac{z(x-\omega/z)}{1+x+xz}$	$-\omega$	$z/(z+1)$
$\frac{f_1(1-f_2(f_1))}{f_2(1-f_1(f_1))} = \frac{z^2(x-\omega/z)(x-\omega^2/z)}{x(z-1)(1+x+xz)}$	∞	$\frac{z^2}{z^2-1}$

Table 4.3: Values of $f_1(f_1)$, $f_2(f_1)$, $f_1(f_1)/f_2(f_1)$, $(1-f_2(f_1))/(1-f_1(f_1))$, $f_1(1-f_2)/f_2/(1-f_1)$ at 0 and ∞

and

$$f_2(f_1)(x) = \frac{x(1-z)}{x-\omega}. \quad (4.99)$$

Then

$$\frac{f_1(f_1)(x)}{f_2(f_1)(x)} = \frac{z(x-\omega^2/z)}{x(z-1)} \quad (4.100)$$

and

$$\frac{1-f_2(f_1)(x)}{1-f_1(f_1)(x)} = \frac{z(x-\omega/z)}{1+x+xz}. \quad (4.101)$$

We now have all the data necessary to generate Table 4.3. Applying (4.88) to the values in Table 4.3, we get

$$\left\{ \frac{z^2}{z^2-1} \right\} = -\{-z\} + \{1-z\} + \left\{ \frac{z}{z-1} \right\} + \left\{ \frac{z}{z+1} \right\} \quad (4.102)$$

Therefore, we can now replace $\left\{ \frac{z^2}{z^2-1} \right\}$ in (4.89) with the right hand side of (4.102). This brings us a step closer to proving (4.41) for the case $n=3$, since the terms $-\{1-z\} = -\left\{ \frac{z}{z-1} \right\} = \{z\}$ actually appear on the right hand side of (4.41).

In order to implement this move geometrically, we need to attach one of the four simplices on the right hand side of (4.102) to the simplex $\left\{ \frac{z^2}{z^2-1} \right\}$ in such a way that the resulting two tetrahedra triangulate to give the 3 simplices that are left over. In Figure 4.12a) it is the tetrahedron $\{\infty, 0, z, z^3\}$ that has cross ratio $\frac{z^2}{z^2-1}$. We find that attaching to it the tetrahedron $\{0, z, z^2, z^3\} = \{-z\}$ as shown in Figure 4.12b) gives us the simplicial chain version of (4.102),

$$\{\infty, z, 0, z^3\} = -\{0, z^2, z, z^3\} + \{\infty, 0, z, z^3\} + \{\infty, 0, z^2, z^3\} + \{\infty, z^2, z, z^3\}, \quad (4.103)$$

since $\{\infty, 0, z, z^2\} = \{1 - z\}$, $\{\infty, 0, z^2, z^3\} = \{z/(z - 1)\}$, and $\{\infty, z^2, z, z^3\} = z/(z + 1)$.

The next step in the iterative process is to show that $f_1(f_1) = -z(x - \omega^2/z)/(x - \omega)$ satisfies (4.43). Since $f_1(f_1)$ is just a linear fractional transformation, we can use the proof of Property(i) in §4.4.1 for this. That proof tells us that for f of the form $f(x) = (ax + b)/(cx + d)$,

$$f(\infty) = \left\{\frac{a}{c}\right\} = -\left\{\frac{(d-b)a}{(c-a)b}\right\} + \left\{\frac{(d-b)c}{(c-a)d}\right\} + \left\{\frac{da}{bc}\right\} + \left\{\frac{b}{d}\right\} \quad (4.104)$$

Substituting $a = -z$, $b = \omega^2$, $c = 1$, and $d = -\omega$ gives the relation

$$\{-z\} = -\left\{-\frac{\omega z}{z+1}\right\} + \left\{\frac{-\omega^2}{z+1}\right\} + \{\omega^2 z\} + \{-\omega\}. \quad (4.105)$$

We implement (4.105) in terms of simplicial complexes by gluing the tetrahedron $\{z, z^2, z^3, x\}$, where $x = z/(\omega(z-1)+z)$, on to the face $\{z, z^2, z^3\}$ of the tetrahedron $\{0, z, z^2, z^3\}$. This is shown in Figure 4.12c). Applying the cocycle relation to these two tetrahedra gives

$$\{0, z^2, z, z^3\} = -\{0, z^3, z, x\} + \{z^3, z, z^2, x\} + \{0, z^3, z^2, x\} + \{0, z^2, z, x\}. \quad (4.106)$$

Why we chose to attach $\{z, z^3, z^2, x\}$ to this particular face of $\{0, z^2, z, z^3\}$ will become clear later.

Coming back to the expression for $f_2(f_1)$ given in (4.99), we find that $f_2(f_1)$ satisfies (4.43) just by definition. Therefore, we need not construct any simplices to prove this geometrically. The same goes for $f_1(f_1)/f_2(f_1)$ given by (4.100). As for $(1 - f_2(f_1))/(1 - f_1(f_1))$, it is a linear fractional transformation, as shown by (4.101). So we prove that it satisfies (4.43) the same way as we did for $f_1(f_1)$. Applying (4.104) with $a = z$, $b = -\omega$, $c = z + 1$ and $d = 1$, we have

$$\left\{\frac{z}{z+1}\right\} = -\{\omega z\} + \{-\omega^2(z+1)\} + \left\{-\frac{\omega^2 z}{z+1}\right\} + \{-\omega\}. \quad (4.107)$$

The simplicial complex version of (4.107) is

$$\{\infty, z^2, z, z^3\} = -\{\infty, y, z^2, z^3\} + \{\infty, y, z, z^3\} + \{y, z^2, z, z^3\} + \{\infty, z, y, z^2\}, \quad (4.108)$$

where $y = z - z(z - 1)\omega$. The simplices in (4.108) are shown in Figure 4.12d).

It remains to be shown that f_1/f_2 and $(1 - f_2)/(1 - f_1)$ satisfy (4.43) (f_2 satisfies (4.43) by definition). This will require two applications of the cocycle equation. The unexpected result is that we need not introduce any more points in order to implement these two cocycle equations in terms of simplices. This is not at all obvious! Certainly, we could get a valid geometric proof of the generalized Kubert identity by introducing two more new points, just as we introduced the points z^2 , $x = z^2/(\omega(z - 1) + z)$, and $y = z - z(z - 1)\omega$. However, if we attach the new tetrahedra in a certain way, the introduction of new points will be avoided. Thus, in the end we will need only the vertices of the polygon in Figure 4.12f). In the case $|z| = 1$ this diagram is none other than the rotated diagram of Figure 4.5 with vertices z^2 and x added. The correspondence between the vertices other than these two in the two diagrams is

$$O \longleftrightarrow 0; \quad B \longleftrightarrow 1; \quad C \longleftrightarrow z; \quad A \longleftrightarrow z^3; \quad D \longleftrightarrow y$$

The fact that Figure 4.5 is just a special case of Figure 4.12f) means that Figure 4.5, and hence Dupont and Sah's proof of the generalized Kubert identities actually implies the trigonometric cyclotomic identities. This fact can be easily proved analytically by simply differentiating both sides of (4.2) with respect to θ and then exponentiating both sides. Figure 4.12f) is a geometric proof of this fact.

We now finish the geometrization of Dupont's and Sah's proof by showing that f_1/f_2 and $(1 - f_2)/(1 - f_1)$ satisfy (4.43). We spare the reader of any more tedious computations and summarize the relevant data. For f_1/f_2 (see (4.86)) we choose $a = \omega/z$ and $b = 1$. For $(1 - f_2)/(1 - f_1)$ (see (4.87)) we choose $a = 1/z$ and $b = \omega$. Both (4.86) and (4.87) have value 1 only when $x = 0$, so we choose $d = 0$ for both f_1/f_2 and $(1 - f_2)/(1 - f_1)$.

The rest of the information we need is contained in the first columns of Table 4.4 and Table 4.5. All the linear fractional transformations in Tables 4.4 and 4.5 satisfy the relation (4.43) by definition, so we need not introduce any simplices in addition to the ones listed in these tables.

h	$h(0)$	$h(\infty)$	Simplex representing $\{h(\infty)\}$ in Fig. 4.12e)
$f_1\left(\frac{f_1}{f_2}\right) = -\frac{(x-\omega^2/z)z}{x(-\omega^2+\omega z)}$	∞	$\frac{1}{1+(z+1)/\omega z}$	$\{0, z, z^3, x\}$
$f_2\left(\frac{f_1}{f_2}\right) = \frac{\omega(x-1)}{x(\omega-z)}$	∞	$\frac{1}{1-\omega^2 z}$	$\{0, z, 1, x\}$
$f_1\left(\frac{f_1}{f_2}\right)/f_2\left(\frac{f_1}{f_2}\right) = \frac{\omega x z - 1}{x - 1}$	1	ωz	$\{0, x, 1, z^3\}$
$\frac{1-f_2\left(\frac{f_1}{f_2}\right)}{1-f_1\left(\frac{f_1}{f_2}\right)} = \frac{1-\omega^2 x z}{1+x+x z}$	1	$\frac{-\omega^2 z}{z+1}$	$\{1, z, z^3, x\}$
$\frac{f_1\left(\frac{f_1}{f_2}\right)(1-f_2\left(\frac{f_1}{f_2}\right))}{f_2\left(\frac{f_1}{f_2}\right)(1-f_1\left(\frac{f_1}{f_2}\right))} = -\frac{(x-\omega/z)(x-\omega^2/z)z^2}{(x-1)(1+x+x z)}$	1	$-\frac{z^2}{z+1}$	$\{0, z, 1, z^3\}$

Table 4.4: Data needed to prove that $\frac{f_1(x)}{f_2(x)} = -\frac{(x-\omega/z)(x-\omega^2/z)z^2}{(x-1)(1+x+x z)}$ obeys the relation (4.43)

h	$h(0)$	$h(\infty)$	Simplex representing $\{h(\infty)\}$ in Fig. 4.12f)
$f_1\left(\frac{1-f_2}{1-f_1}\right) = \frac{(x+\frac{1}{z+1})(z+1)}{x(z-\omega^2)}$	∞	$\frac{1}{1+\frac{\omega}{z+1}}$	$\{\infty, z, y, z^3\}$
$f_2\left(\frac{1-f_2}{1-f_1}\right) = \frac{\omega-x}{x(\omega z-1)}$	∞	$\frac{1}{1-\omega z}$	$\{\infty, y, 1, z\}$
$f_1\left(\frac{1-f_2}{1-f_1}\right)/f_2\left(\frac{1-f_2}{1-f_1}\right) = -\frac{\omega(x+\frac{1}{z+1})(z+1)}{x-\omega}$	1	$-\omega(z+1)$	$\{1, z, y, z^3\}$
$\frac{1-f_2\left(\frac{1-f_2}{1-f_1}\right)}{1-f_1\left(\frac{1-f_2}{1-f_1}\right)} = \frac{x z - 1}{\omega x - 1}$	1	$\omega^2 z$	$\{\infty, 1, y, z^3\}$
$\frac{f_1\left(\frac{f_1}{f_2}\right)(1-f_2\left(\frac{f_1}{f_2}\right))}{f_2\left(\frac{f_1}{f_2}\right)(1-f_1\left(\frac{f_1}{f_2}\right))} = -\frac{(x+1/(z+1))(x-1/z)z(z+1)}{(x-\omega)(x-\omega^2)}$	1	$-z(z+1)$	$\{\infty, 1, z, z^3\}$

Table 4.5: Data needed to prove that $\frac{1-f_2(x)}{1-f_1(x)} = -\frac{(x+1/(z+1))(x-1/z)z(z+1)}{(x-\omega)(x-\omega^2)}$ obeys the relation (4.43)

Summarizing the information contained in equations (4.89), (4.102), (4.105), (4.107) and the third columns in Tables 4.4 and 4.5 we get

$$\begin{aligned}
\{z^3\} = & -\left\{-\frac{\omega z}{z+1}\right\} + \left\{\frac{-\omega^2}{z+1}\right\} + \{\omega^2 z\} + \{-\omega\} - \{1-z\} - \left\{\frac{z}{z-1}\right\} + \{\omega z\} \\
& - \{-\omega^2(z+1)\} - \left\{-\frac{\omega^2 z}{z+1}\right\} - \{-\omega\} + \left\{\frac{1}{1-z}\right\} - \left\{\frac{1}{1+(z+1)/\omega z}\right\} \\
& + \left\{\frac{1}{1-\omega^2 z}\right\} + \{\omega z\} + \left\{\frac{-\omega^2 z}{z+1}\right\} - \left\{\frac{1}{1+\frac{\omega}{z+1}}\right\} + \left\{\frac{1}{1-\omega z}\right\} \\
& + \{-\omega(z+1)\} + \{\omega^2 z\}. \quad (4.109)
\end{aligned}$$

The simplicial complex version of (4.109) is obtained from (4.90), (4.103), (4.106), (4.108):

$$\begin{aligned}
\{\infty, 1, 0, z^3\} = & -\{0, z^3, z, x\} + \{z, z^2, z^3, x\} + \{0, z^3, z^2, x\} + \{0, z^2, z^2, x\} \\
& - \{\infty, z, 0, z^2\} - \{\infty, z^2, 0, z^3\} + \{\infty, y, z^2, z^3\} - \{\infty, y, z, z^3\} - \{y, z^2, z, z^3\} \\
& - \{\infty, y, z, z^2\} + \{\infty, 1, 0, z\} - \{0, z, z^3, x\} + \{0, z, 1, x\} + \{0, x, 1, z^3\} \\
& + \{1, z, z^3, x\} - \{\infty, z, y, z^3\} + \{\infty, y, 1, z\} + \{1, z, y, z^3\} + \{\infty, 1, y, z^3\}. \quad (4.110)
\end{aligned}$$

An easy calculation shows that the boundary of both sides of (4.110) is equal. Thus (4.110) is a homological proof of the generalized $n = 3$ Kubert identity. One can also see from equations (4.109) and (4.110) that the terms corresponding to the simplices $\{-\frac{\omega z}{z+1}\} = \{0, z^3, z, x\}$ and $\{-\omega^2(z+1)\} = \{\infty, y, z, z^3\}$ cancel each other even without going to the boundary equation. This is due to the way the right hand side of (4.110) is constructed, and is not an obvious consequence of Dupont and Sah's proof.

4.4.5 “Geometrization” of Dupont and Sah’s proof of the Kubert identity $n=4$

As expected, producing the geometric version of Dupont and Sah’s proof in the case $n = 4$ is considerably more involved than in the case $n = 3$. For one thing,

one now needs to use the roots of the polynomial

$$p(x) = 1 + x(1 + z) + x^2(1 + z + z^2). \quad (4.111)$$

In general, to follow through Dupont and Sah's proof for n , one needs to solve the polynomial equations

$$1 + x(1 + z) + \cdots + x^{n-2}(1 + z + \cdots + z^{n-2}) = 0 \quad (4.112)$$

for x . When $n = 3$, (4.112) is just the linear equation

$$1 + x(1 + z) = 0,$$

which occurred, in, for example, the denominator of (4.84).

The solutions of (4.111) are

$$\frac{-1 - z \pm s}{2(1 + z + z^2)},$$

where

$$s = \sqrt{-3 - 2z - 3z^2}. \quad (4.113)$$

The notation in (4.111) and (4.113) will be used for the rest of this subsection, and ω will denote $\sqrt{-1}$. The final diagram is shown in Figure 4.13. In order to avoid making this diagram too cluttered, all the vertices but not all the edges have been shown. Note that when rotated, the diagram in Figure 4.13 in the case $|z| = 1$ contains the diagram in Figure 4.7. The coordinates of the vertices in Figure 4.13

h	$h(\infty)$	Simplex representing $\{h(\infty)\}$ in Fig. 4.13
$f_1 = \frac{(x-\omega/z)(x-\omega^2/z)(x-\omega^3/z)z^3}{x(z-1)p(x)}$	$\frac{z^3}{z^3-1}$	$\{\infty, 0, z, z^4\}$
$f_2 = \frac{x-1}{x(1-z)}$	$\frac{1}{1-z}$	$\{\infty, 0, z^3, z^4\}$
$\frac{f_1}{f_2} = -\frac{(x-\omega/z)(x-\omega^2/z)(x-\omega^3/z)z^3}{(x-1)p(x)}$	$-\frac{z^3}{1+z+z^2}$	$\{\infty, z, 1, z^4\}$
$\frac{1-f_2}{1-f_1} = -\frac{z(x-1/z)p(x)}{(x-\omega)(x-\omega^2)(x-\omega^3)}$	$-z(1+z+z^2)$	$\{\infty, 1, z, z^4\}$
$\frac{f_1(1-f_2)}{f_2(1-f_1)} = \frac{x^4z^4-1}{x^4-1}$	z^4	$\{\infty, 1, 0, z^4\}$

Table 4.6: Expanding $\{z^4\}$ by the cocycle relation; $a = 1/z$, $b = 1$, $d = 0$.

are as follows:

$$\begin{aligned}
r &= z + \omega^3(z^2 - z) \\
t &= z(\omega + z - \omega z^2) \\
b_1 &= \frac{1}{2}z(2 + \omega - \omega z^2 - \omega(z-1)s) \\
b_2 &= \frac{z(1 + 3z + z^2 + z^3 + (z^2 - 1)s)}{2(1 + z + z^2)} \\
b_3 &= \frac{z(1 - \omega + (2 - \omega)z + z^2 + 2z^3 + (1 - \omega + z)s)}{2 + z(1 - \omega + z)(1 + z + s)} \\
g_1 &= \frac{z(1 + z - \omega z^3)}{1 - \omega + z} \\
g_2 &= \frac{\omega z^3}{z^2 + z\omega - 1} \\
g_3 &= \omega(1 - z^3) + z
\end{aligned} \tag{4.114}$$

where $s = \sqrt{-3 - 2z - 3z^2}$.

Rather than go through all the steps needed to generate the diagram in Figure 4.13 the way we did in §4.4.4, we have summarized the necessary data in Tables 4.6- 4.20. As in the case $n = 3$, replacing $R(f) = \{f(0)\} - \{f(\infty)\}$ with $\tilde{R}(f) = \{f(\infty)\}$ does not change (4.88), so there is no need to consider $\{f(0)\}$ for any of the polynomials f listed below. The choices of factors a , b , and d (see (4.54) and (4.59)) have been indicated in the captions of all the tables.

We prove that $f_1(\frac{1-f_2(f_1)}{1-f_1(f_1)}) = \frac{2\omega(x+1/z)z(1+z)}{(x-\omega^3)(1-2\omega+z+s)}$ in Table 4.10 satisfies the relation

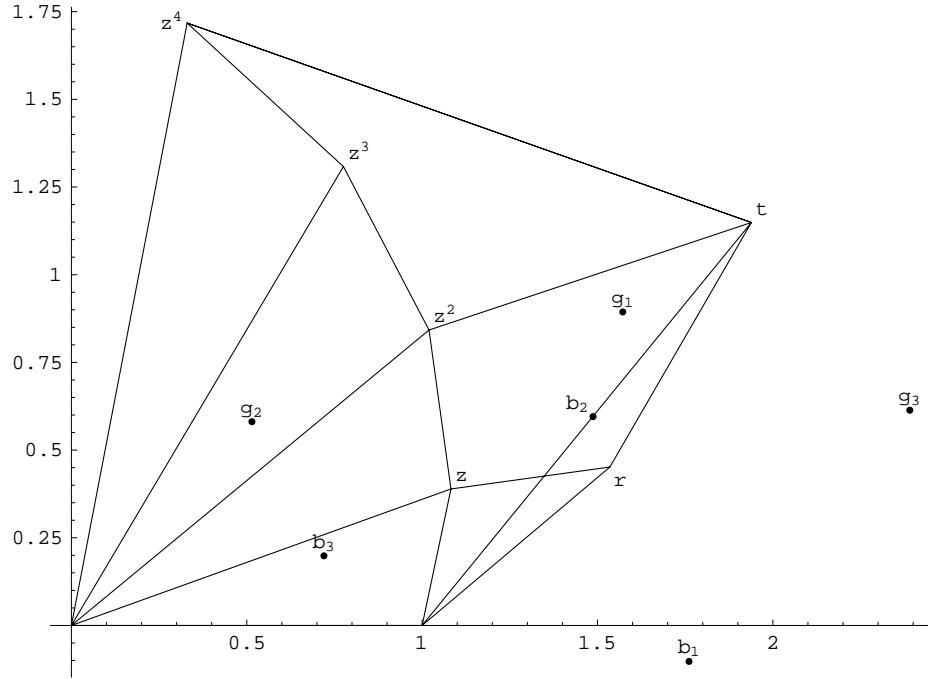


Figure 4.13: Partial sketch of the geometric proof of the generalized Kubert identity $\{z^4\} = \sum_{j=0}^4 4\{\omega^j z\}$, where $\omega = i$ and the coordinates of the vertices r , t , b_i , and g_i are given in (4.114)

h	$h(\infty)$	Simplex representing $\{h(\infty)\}$ in Fig. 4.13
$f_1(f_1) = -\frac{(x-\omega/z)(x-\omega^3/z)z^2}{x(1+x)(1+z)}$	$-\frac{z^2}{1+z}$	$\{0, z^2, z, z^4\}$
$f_2(f_1) = \frac{x(1-z)}{x+1}$	$1-z$	$\{\infty, 0, z, z^2\}$
$\frac{f_1(f_1)}{f_2(f_1)} = \frac{(x-\omega/z)(x-\omega^3/z)z^2}{x^2(z^2-1)}$	$\frac{z^2}{z^2-1}$	$\{\infty, 0, z^2, z^4\}$
$\frac{1-f_2(f_1)}{1-f_1(f_1)} = \frac{x(1+z)(1+xz)}{p(x)}$	$\frac{z(1+z)}{1+z+z^2}$	$\{\infty, z^2, z, z^4\}$
$\frac{f_1(f_1)(1-f_2(f_1))}{f_2(f_1)(1-f_1(f_1))} = \frac{(x-\omega/z)(x-\omega^2/z)(x-\omega^3/z)z^3}{x(z-1)p(x)}$	$\frac{z^3}{z^3-1}$	$\{\infty, 0, z, z^4\}$

Table 4.7: Expanding $\{z^3/(z^3 - 1)\}$ by the cocycle relation; $a = -1/z$, $b = 0$, $d = -1$.

h	$h(\infty)$	Simplex representing $\{h(\infty)\}$ in Fig. 4.13
$f_1\left(\frac{f_1(f_1)}{f_2(f_1)}\right) = -\frac{(x-\omega/z)z}{x+\omega}$	$-z$	$\{\infty, z^2, z^3, z^4\}$
$f_2\left(\frac{f_1(f_1)}{f_2(f_1)}\right) = \frac{x(1-z)}{x+\omega}$	$1-z$	$\{\infty, 0, z^2, z^3\}$
$\frac{f_1\left(\frac{f_1(f_1)}{f_2(f_1)}\right)}{f_2\left(\frac{f_1(f_1)}{f_2(f_1)}\right)} = -\frac{(x-\omega/z)z}{x(1-z)}$	$\frac{z}{z-1}$	$\{\infty, 0, z^3, z^4\}$
$\frac{1-f_2\left(\frac{f_1(f_1)}{f_2(f_1)}\right)}{1-f_1\left(\frac{f_1(f_1)}{f_2(f_1)}\right)} = \frac{(x-\omega^3/z)z}{x(z+1)}$	$\frac{z}{z+1}$	$\{0, z^2, z^3, z^4\}$
$\frac{f_1\left(\frac{f_1(f_1)}{f_2(f_1)}\right)(1-f_2\left(\frac{f_1(f_1)}{f_2(f_1)}\right))}{f_2\left(\frac{f_1(f_1)}{f_2(f_1)}\right)(1-f_1\left(\frac{f_1(f_1)}{f_2(f_1)}\right))} = \frac{(x-\omega/z)(x-\omega^3/z)z^2}{x^2(z^2-1)}$	$\frac{z^2}{z^2-1}$	$\{\infty, 0, z^2, z^4\}$

Table 4.8: Expanding $\{z^2/(z^2 - 1)\}$ by the cocycle relation; $a = \omega^3/z$, $b = 0$, $d = \omega^3$.

h	$h(\infty)$	Simplex representing $\{h(\infty)\}$ in Fig. 4.13
$f_1\left(\frac{1-f_2(f_1)}{1-f_1(f_1)}\right) = \frac{2\omega(x+1/z)z(1+z)}{(x-\omega^3)(1-2\omega+z+s)}$	$\frac{2\omega z(1+z)}{1-2\omega+z+s}$	$\{\infty, z^2, z^4, b_1\}$
$f_2\left(\frac{1-f_2(f_1)}{1-f_1(f_1)}\right) = \frac{\omega(2(1+z+z^2)x+1+z+s)}{(\omega+x)(1+z+s)}$	$\frac{2\omega(1+z+z^2)}{1+z+s}$	$\{\infty, z, z^4, b_1\}$
$\frac{f_1\left(\frac{1-f_2(f_1)}{1-f_1(f_1)}\right)}{f_2\left(\frac{1-f_2(f_1)}{1-f_1(f_1)}\right)} = \frac{(x+1/z)z(1+z)(1+z+s)}{(1+z+z^2)(1-2\omega+z+s)(x+\frac{1+z+s}{2(1+z+z^2)})}$	$\frac{z(1+z)(1+z+s)}{(1+z+z^2)(1-2\omega+z+s)}$	$\{b_1, z^2, z, z^4\}$
$\frac{1-f_2\left(\frac{1-f_2(f_1)}{1-f_1(f_1)}\right)}{1-f_1\left(\frac{1-f_2(f_1)}{1-f_1(f_1)}\right)} = \frac{x((1-2\omega)(1+z)-2\omega z^2+s)}{(1+z+s)(\omega+x-\frac{2\omega(1+z)(1+xz)}{1-2\omega+z+s})}$	$\frac{1-2\omega+z+s}{1+z+s}$	$\{\infty, z, b_1, z^2\}$
$\frac{f_1\left(\frac{1-f_2(f_1)}{1-f_1(f_1)}\right)(1-f_2\left(\frac{1-f_2(f_1)}{1-f_1(f_1)}\right))}{f_2\left(\frac{1-f_2(f_1)}{1-f_1(f_1)}\right)(1-f_1\left(\frac{1-f_2(f_1)}{1-f_1(f_1)}\right))} = \frac{x(1+z)(1+xz)}{p(x)}$	$\frac{z(1+z)}{1+z+z^2}$	$\{\infty, z^2, z, z^4\}$

Table 4.9: Expanding $\{z^3/(z^3 - 1)\}$ by the cocycle relation; $a = 0$, $b = -(1+z+s)/2/(1+z+z^2)$, $d = \omega^3$. $b_1 = z(2+\omega-\omega z^2-\omega(z-1)s)/2$

(4.43) by using (4.104). $\{f_1(\frac{1-f_2(f_1)}{1-f_1(f_1)})(\infty)\} = \frac{2\omega z(1+z)}{1-2\omega+z+s}$ corresponds to the left hand side of (4.104). The terms on the right hand side of (4.104) have been denoted as

$$\begin{aligned} \text{Term 1: } & \left\{ \frac{(d-b)a}{(c-a)b} \right\} \\ \text{Term 2: } & \left\{ \frac{(d-b)c}{(c-a)d} \right\} \\ \text{Term 3: } & \left\{ \frac{da}{bc} \right\} \\ \text{Term 4: } & \left\{ \frac{b}{d} \right\}. \end{aligned}$$

As (4.104) indicates,

$$\left\{ f_1\left(\frac{1-f_2(f_1)}{1-f_1(f_1)}\right)(\infty) \right\} = -\{\text{Term 1}\} + \{\text{Term 2}\} + \{\text{Term 3}\} + \{\text{Term 4}\}.$$

Based on Tables 4.6- 4.20 we get the following identity.

$$\begin{aligned} \{z^4\} = & \left\{ -\frac{z^2}{z+1} \right\} - \{1-z\} + \{-z\} - \{1-z\} - \left\{ \frac{z}{z-1} \right\} - \left\{ \frac{z}{z+1} \right\} \\ & - \left\{ \frac{z(1+z-s)}{2(1+z+z^2)} \right\} + \left\{ -\frac{2\omega}{1+z+s} \right\} + \{\omega z\} + \left\{ \frac{2(1+z)}{1-2\omega+z+s} \right\} \\ & - \left\{ \frac{2\omega(1+z+z^2)}{1+z+s} \right\} + \{\omega^3 z\} - \left\{ -\frac{2\omega(1+z+z^2)}{1+z+s} \right\} - \left\{ \frac{z(1+z+s)}{2(1+z+z^2)} \right\} \\ & - \left\{ \frac{2(1+z)}{1-2\omega+z+s} \right\} - \left\{ \frac{1-2\omega+z+s}{1+z+s} \right\} + \left\{ \frac{1}{1-z} \right\} - \left\{ -\frac{z^2}{z+1} \right\} + \left\{ \frac{1}{z+1} \right\} \\ & - \left\{ \frac{z}{z-\omega} \right\} + \left\{ \frac{-\omega}{z-\omega} \right\} + 2\{\omega z\} - \left\{ \frac{2z}{-1+z-s} \right\} + \left\{ \frac{2(1+z+z^2)}{1+z+2z^2-s} \right\} \\ & + \left\{ \frac{z(1+z+s)}{2(1+z+z^2)} \right\} + \left\{ \frac{2}{1+z+s} \right\} - \left\{ \frac{2(1+z+z^2)}{(1-\omega+z)(1+z+s)} \right\} \\ & + \left\{ \frac{1}{1-\omega+z} \right\} + \left\{ \frac{1+z-s}{2} \right\} + \left\{ \frac{1-2\omega+z-s}{2(1+z)} \right\} - \left\{ \frac{1}{2}(1-z-s) \right\} \\ & - \left\{ \frac{2+\omega+z(2+\omega+2z)-\omega s}{2(\omega+z)(1+z)} \right\} + \left\{ \frac{1}{2}\omega(1+z+s) \right\} - \{1+\omega+\omega z\} \\ & - \left\{ \frac{2(1+z+z^2)}{(1-\omega+z)(1+z-s)} \right\} - \left\{ \frac{1+2\omega+z-s}{2(\omega+z)} \right\} + \left\{ \frac{\omega}{z+\omega} \right\} \\ & - \left\{ \frac{2(1+z+z^2)}{1+\omega+\omega z+z^2+(1-\omega+z)s} \right\} + \left\{ \frac{2\omega}{-1+2\omega-z+s} \right\} + \left\{ -\frac{\omega}{2}(1+z+s) \right\} \\ & + \left\{ \frac{2(1+z+z^2)}{(1-\omega+z)(1+z+s)} \right\} - \left\{ \frac{z}{z-\omega} \right\} + \left\{ \frac{1}{\omega-z} \right\} + \{-z\} + \{1+\omega+\omega z\} \end{aligned} \tag{4.115}$$

Term number in (4.104)	Term value	Simplex representing Term i in Fig. 4.13
1	$\frac{z(1+z-s)}{2(1+z+z^2)}$	$\{b_1, t, z^2, z^4\}$
2	$-\frac{2\omega}{1+z+s}$	$\{\infty, z^4, b_1, t\}$
3	ωz	$\{\infty, z^4, t, z^2\}$
4	$\frac{2(1+z)}{1-2\omega+z+s}$	$\{\infty, b_1, z^2, t\}$
Left hand side of (4.104)	$\frac{2\omega z(1+z)}{1-2\omega+z+s}$	$\{\infty, z^2, z^4, b_1\}$

Table 4.10: The cocycle relation used to prove that the linear fractional transformation $f_1(\frac{1-f_2(f_1)}{1-f_1(f_1)}) = \frac{2\omega(x+1/z)z(1+z)}{(x-\omega^3)(1-2\omega+z+s)}$ obeys (4.43). $t = z(\omega + z - \omega z^2)$.

Term number in (4.104)	Term value	Simplex representing Term i in Fig. 4.13
1	$\omega^3 z$	$\{g_1, z^2, z^4, z\}$
2	$-\frac{2\omega(1+z+z^2)}{1+z+s}$	$\{b_1, g_1, z^2, z\}$
3	$\frac{z(1+z+s)}{2(1+z+z^2)}$	$\{g_1, b_1, z^2, z^4\}$
4	$\frac{2(1+z)}{1-2\omega+z+s}$	$\{b_1, g_1, z, z^4\}$
Left hand side of (4.104)	$\frac{z(1+z)(1+z+s)}{(1+z+z^2)(1-2\omega+z+s)}$	$\{b_1, z^2, z, z^4\}$

Table 4.11: The cocycle relation used to prove that the linear fractional transformation $f_1(\frac{1-f_2(f_1)}{1-f_1(f_1)})/f_2(\frac{1-f_2(f_1)}{1-f_1(f_1)}) = (x+1/z)z(1+z)(1+z+s)/((1+z+z^2)(1-2\omega+z+s)(x+\frac{1+z+s}{2(1+z+z^2)}))$ obeys (4.43). $g_1 = \frac{z(1+z-\omega z^3)}{1-\omega+z}$.

h	$h(\infty)$	Simplex representing $\{h(\infty)\}$ in Fig. 4.13
$f_1(\frac{f_1}{f_2}) = -\frac{(x-\omega/z)(x-\omega^3/z)z^2}{x(1+x)(z+1)}$	$-\frac{z^2}{z+1}$	$\{0, z, z^4, z^2\}$
$f_2(\frac{f_1}{f_2}) = \frac{x-1}{x(z+1)}$	$\frac{1}{z+1}$	$\{0, z, 1, z^2\}$
$\frac{f_1(\frac{f_1}{f_2})}{f_2(\frac{f_1}{f_2})} = -\frac{(x-\omega/z)(x-\omega^3/z)z^2}{(x^2-1)}$	$-z^2$	$\{0, 1, z^4, z^2\}$
$\frac{1-f_2(\frac{f_1}{f_2})}{1-f_1(\frac{f_1}{f_2})} = \frac{(1+x)(x+1/z)z}{p(x)}$	$\frac{z}{1+z+z^2}$	$\{1, z, z^4, z^2\}$
$\frac{f_1(\frac{f_1}{f_2})(1-f_2(\frac{f_1}{f_2}))}{f_2(\frac{f_1}{f_2})(1-f_1(\frac{f_1}{f_2}))} = -\frac{(x-\omega/z)(x-\omega^2/z)(x-\omega^3/z)z^3}{(x-1)p(x)}$	$-\frac{z^3}{1+z+z^2}$	$\{0, 1, z^4, z\}$

Table 4.12: Expanding $\{-z^3/(1+z+z^2)\}$ by the cocycle relation; $a = -1/z$, $b = 1$, $d = 0$.

h	$h(\infty)$	Simplex representing $\{h(\infty)\}$ in Fig. 4.13
$f_1\left(\frac{f_1(\frac{f_1}{f_2})}{f_2(\frac{f_1}{f_2})}\right) = -\frac{(x-\omega/z)z}{x(z-\omega)}$	$\frac{z}{z-\omega}$	$\{g_2, 0, 1, z^4\}$
$f_2\left(\frac{f_1(\frac{f_1}{f_2})}{f_2(\frac{f_1}{f_2})}\right) = -\frac{\omega(1+x)}{x(z-\omega)}$	$-\frac{\omega}{z-\omega}$	$\{g_2, z^2, 1, z^4\}$
$\frac{f_1\left(\frac{f_1(\frac{f_1}{f_2})}{f_2(\frac{f_1}{f_2})}\right)}{f_2\left(\frac{f_1(\frac{f_1}{f_2})}{f_2(\frac{f_1}{f_2})}\right)} = \frac{\omega(x-\omega/z)}{x+1}$	ωz	$\{g_2, 0, z^2, z^4\}$
$\frac{1-f_2\left(\frac{f_1(\frac{f_1}{f_2})}{f_2(\frac{f_1}{f_2})}\right)}{1-f_1\left(\frac{f_1(\frac{f_1}{f_2})}{f_2(\frac{f_1}{f_2})}\right)} = \frac{\omega(x-\omega^3/z)z}{x-1}$	ωz	$\{g_2, 1, z^2, 0\}$
$\frac{f_1\left(\frac{f_1(\frac{f_1}{f_2})}{f_2(\frac{f_1}{f_2})}\right)(1-f_2\left(\frac{f_1(\frac{f_1}{f_2})}{f_2(\frac{f_1}{f_2})}\right))}{f_2\left(\frac{f_1(\frac{f_1}{f_2})}{f_2(\frac{f_1}{f_2})}\right)(1-f_1\left(\frac{f_1(\frac{f_1}{f_2})}{f_2(\frac{f_1}{f_2})}\right))} = -\frac{(x-\omega/z)(x-\omega^3/z)z^2}{x^2-1}$	$-z^2$	$\{0, 1, z^4, z^2\}$

Table 4.13: Expanding $\{-z^2\}$ by the cocycle relation; $a = \omega^3/z$, $b = -1$, $d = 0$. $g_2 = \omega z^3/(z^2 + z\omega - 1)$.

After cancellation of terms, (4.115) becomes the generalized Kubert identity for the case $n = 4$,

$$\{z^4\} = 4[\{z\} + \{\omega z\} + \{\omega^2 z\} + \{\omega^3 z\}],$$

where $\omega = \sqrt{-1}$. Note that a total of six new points, b_i and g_i with $i = 1, 2, 3$ had to be added to the diagram in Figure 4.7. Just as in the case of the $n = 3$ generalized Kubert identity, several points, including b_1 , were used more than once. This is not obvious from Dupont and Sah's proof.

h	$h(\infty)$	Simplex representing $\{h(\infty)\}$ in Fig. 4.13
$f_1\left(\frac{1-f_2(\frac{f_1}{f_2})}{1-f_1(\frac{f_1}{f_2})}\right) = \frac{2(x+1/z)z}{x(-1+z-s)}$	$\frac{2z}{-1+z-s}$	$\{b_2, z, z^2, z^4\}$
$f_2\left(\frac{1-f_2(\frac{f_1}{f_2})}{1-f_1(\frac{f_1}{f_2})}\right) = \frac{2(1+z+z^2)x+1+z+s}{x(1+z+2z^2-s)}$	$\frac{2(1+z+z^2)}{1+z+2z^2-s}$	$\{b_2, z^2, 1, z\}$
$\frac{f_1\left(\frac{1-f_2(\frac{f_1}{f_2})}{1-f_1(\frac{f_1}{f_2})}\right)}{f_2\left(\frac{1-f_2(\frac{f_1}{f_2})}{1-f_1(\frac{f_1}{f_2})}\right)} = \frac{2(1+xz)}{2+x(1+z-s)}$	$\frac{z(1+z+s)}{2(1+z+z^2)}$	$\{b_2, 1, z^2, z^4\}$
$\frac{1-f_2\left(\frac{1-f_2(\frac{f_1}{f_2})}{1-f_1(\frac{f_1}{f_2})}\right)}{1-f_1\left(\frac{1-f_2(\frac{f_1}{f_2})}{1-f_1(\frac{f_1}{f_2})}\right)} = \frac{2(1+x)}{2+x(1+z+s)}$	$\frac{2}{1+z+s}$	$\{b_2, z, 1, z^4\}$
$\frac{f_1\left(\frac{1-f_2(\frac{f_1}{f_2})}{1-f_1(\frac{f_1}{f_2})}\right)(1-f_2\left(\frac{1-f_2(\frac{f_1}{f_2})}{1-f_1(\frac{f_1}{f_2})}\right))}{f_2\left(\frac{1-f_2(\frac{f_1}{f_2})}{1-f_1(\frac{f_1}{f_2})}\right)(1-f_1\left(\frac{1-f_2(\frac{f_1}{f_2})}{1-f_1(\frac{f_1}{f_2})}\right))} = \frac{(1+x)(x+1/z)z}{p(x)}$	$\frac{z}{1+z+z^2}$	$\{1, z, z^4, z^2\}$

Table 4.14: Expanding $\{z/(1+z+z^2)\}$ by the cocycle relation; $a = -1$, $b = -(1+z+s)/2/(1+z+z^2)$, $d = 0$. $b_2 = z(1+3z+z^2+z^3+(z^2-1)s)/2/(1+z+z^2)$

h	$h(\infty)$	Simplex representing $\{h(\infty)\}$ in Fig. 4.13
$f_1\left(\frac{1-f_2}{1-f_1}\right) = \frac{p(x)}{x(\omega+z)(1+x(1-\omega+z))}$	$\frac{1+z+z^2}{1+\omega+z+z^2}$	$\{\infty, z, r, z^4\}$
$f_2\left(\frac{1-f_2}{1-f_1}\right) = \frac{\omega(x-\omega)}{x(\omega+z)}$	$\frac{\omega}{\omega+z}$	$\{\infty, z, r, 1\}$
$\frac{f_1\left(\frac{1-f_2}{1-f_1}\right)}{f_2\left(\frac{1-f_2}{1-f_1}\right)} = -\frac{\omega p(x)}{(x-\omega)(1+x(1-\omega+z))}$	$-\frac{\omega(1+z+z^2)}{1-\omega+z}$	$\{1, r, z^4, z\}$
$\frac{1-f_2\left(\frac{1-f_2}{1-f_1}\right)}{1-f_1\left(\frac{1-f_2}{1-f_1}\right)} = -\frac{\omega z(x-1/z)(1+x(1-\omega+z))}{\omega+(1+\omega)x+x^2}$	$-\omega z(1-\omega+z)$	$\{\infty, 1, r, z^4\}$
$\frac{f_1\left(\frac{1-f_2}{1-f_1}\right)(1-f_2\left(\frac{1-f_2}{1-f_1}\right))}{f_2\left(\frac{1-f_2}{1-f_1}\right)(1-f_1\left(\frac{1-f_2}{1-f_1}\right))} = -\frac{z(x-1/z)p(x)}{(x-\omega)(x-\omega^2)(x-\omega^3)}$	$-z(1+z+z^2)$	$\{\infty, 1, z, z^4\}$

Table 4.15: Expanding $\{-z(1+z+z^2)\}$ by the cocycle relation; $a = 1/z$, $b = \omega$, $d = 0$. $r = z + \omega^3(z^2 - z)$

h	$h(\infty)$	Simplex representing $\{h(\infty)\}$ in Fig. 4.13
$f_1(f_1(\frac{1-f_2}{1-f_1})) = \frac{(1+z+2z^2+s)(x+\frac{1+z+s}{2(1+z+z^2)})}{(1+x)(-1-2\omega-z+s)}$	$\frac{1+z+2z^2+s}{-1-2\omega-z+s}$	$\{r, b_1, z^4, z\}$
$f_2(f_1(\frac{1-f_2}{1-f_1})) = \frac{x(1+z+2z^2+s)}{(1+x)(-1-z+s)}$	$\frac{1-z-s}{2}$	$\{\infty, r, b_1, z\}$
$\frac{f_1(f_1(\frac{1-f_2}{1-f_1}))}{f_2(f_1(\frac{1-f_2}{1-f_1}))} = \frac{2+x(1+z-s)}{x(1+2\omega+z-s)}$	$\frac{2+\omega+z(2+\omega+2z)-\omega s}{2(\omega+z)(1+z)}$	$\{\infty, b_1, z^4, z\}$
$\frac{1-f_2(f_1(\frac{1-f_2}{1-f_1}))}{1-f_1(f_1(\frac{1-f_2}{1-f_1}))} = \frac{1+2\omega+(2+\omega)x(1+z)+z+2xz^2+\omega(\omega+x)s}{2(\omega+z)(1+x(1-\omega+z))}$	$\frac{2+\omega+z(2+\omega+2z)+\omega s}{2(\omega+1+z+z^2)}$	$\{\infty, b_1, r, z^4\}$
$\frac{f_1(f_1(\frac{1-f_2}{1-f_1}))(1-f_2(f_1(\frac{1-f_2}{1-f_1})))}{f_2(f_1(\frac{1-f_2}{1-f_1}))(1-f_1(f_1(\frac{1-f_2}{1-f_1})))} = \frac{p(x)}{x(\omega+z)(1+x(1-\omega+z))}$	$\frac{1+z+z^2}{1+\omega+z+z^2}$	$\{\infty, z, r, z^4\}$

Table 4.16: Expanding $\{(1+z+z^2)/(1+\omega+z+z^2)\}$ by the cocycle relation; $a = (-1-z+s)/2/(1+z+z^2)$, $b = 0$, $d = -1$. $r = z + \omega^3(z^2 - z)$, $b_1 = z(2 + \omega - \omega z^2 - \omega(z-1)s)/2$

Term number in (4.104)	Term value	Simplex representing Term i in Fig. 4.13
1	$\frac{2(1+z+z^2)}{(1-\omega+z)(1+z+s)}$	$\{z^4, g_3, b_1, r\}$
2	$\frac{1}{1-\omega+z}$	$\{g_3, z, z^4, r\}$
3	$\frac{1+z-s}{2}$	$\{g_3, b_1, z, r\}$
4	$\frac{1-2\omega+z-s}{2(1+z)}$	$\{g_3, z, b_1, z^4\}$
Left hand side of (4.104)	$\frac{1+z+2z^2+s}{-1-2\omega-z+s}$	$\{r, b_1, z^4, z\}$

Table 4.17: The cocycle relation used to prove that the linear fractional transformation $f_1(f_1(\frac{1-f_2}{1-f_1}))$ obeys (4.43). $r = z + \omega^3(z^2 - z)$, $b_1 = z(2 + \omega - \omega z^2 - \omega(z-1)s)/2$, $g_3 = \omega(1 - z^3) + z$.

Term number in (4.104)	Term value	Simplex representing Term i in Fig. 4.13
1	$\frac{\omega(1+z+s)}{2}$	$\{\infty, z^4, t, b_1\}$
2	$1 + \omega + \omega z$	$\{\infty, z^4, t, r\}$
3	$\frac{2(1+z+z^2)}{(1-\omega+z)(1+z-s)}$	$\{b_1, r, t, z^4\}$
4	$\frac{1+2\omega+z-s}{2(z+\omega)}$	$\{\infty, r, b_1, t\}$
Left hand side of (4.104)	$\frac{2+\omega+z(2+\omega+2z)+\omega s}{2(\omega+1+z+z^2)}$	$\{\infty, b_1, r, z^4\}$

Table 4.18: The cocycle relation used to prove that the linear fractional transformation $(1 - f_2(f_1(\frac{1-f_2}{1-f_1}))) / (1 - f_1(f_1(\frac{1-f_2}{1-f_1})))$ obeys (4.43). $r = z + \omega^3(z^2 - z)$, $b_1 = z(2 + \omega - \omega z^2 - \omega(z - 1)s) / 2$.

h	$h(\infty)$	Simplex representing $\{h(\infty)\}$ in Fig. 4.13
$f_1\left(\frac{f_1\left(\frac{1-f_2}{1-f_1}\right)}{f_2\left(\frac{1-f_2}{1-f_1}\right)}\right) = -\frac{\omega(2(1+z+z^2)x+1+z-s)}{x(1-\omega+z-\omega z^2-\omega(1-\omega+z)s)}$	$\frac{2(1+z+z^2)}{1+\omega+\omega z+z^2+(1-\omega+z)s}$	$\{b_3, r, 1, z\}$
$f_2\left(\frac{f_1\left(\frac{1-f_2}{1-f_1}\right)}{f_2\left(\frac{1-f_2}{1-f_1}\right)}\right) = \frac{(x-\omega)(1+z+s)}{(x(1+2\omega+(1+2\omega+2\omega z)z+s))}$	$\frac{2\omega}{-1+2\omega-z+s}$	$\{b_3, z, r, z^4\}$
$\frac{f_1\left(\frac{f_1\left(\frac{1-f_2}{1-f_1}\right)}{f_2\left(\frac{1-f_2}{1-f_1}\right)}\right)}{f_2\left(\frac{f_1\left(\frac{1-f_2}{1-f_1}\right)}{f_2\left(\frac{1-f_2}{1-f_1}\right)}\right)} = -\frac{\omega(2+x(1+z+s))}{2(x-\omega)}$	$-\frac{\omega}{2}(1+z+s)$	$\{b_3, z^4, r, 1\}$
$\frac{1-f_2\left(\frac{f_1\left(\frac{1-f_2}{1-f_1}\right)}{f_2\left(\frac{1-f_2}{1-f_1}\right)}\right)}{1-f_1\left(\frac{f_1\left(\frac{1-f_2}{1-f_1}\right)}{f_2\left(\frac{1-f_2}{1-f_1}\right)}\right)} = \frac{2+x(1+z-s)}{2+2x(1-\omega+z)}$	$\frac{1+z-s}{2(1-\omega+z)}$	$\{b_3, 1, z, z^4\}$
$\frac{f_1\left(\frac{f_1\left(\frac{1-f_2}{1-f_1}\right)}{f_2\left(\frac{1-f_2}{1-f_1}\right)}\right)(1-f_2\left(\frac{f_1\left(\frac{1-f_2}{1-f_1}\right)}{f_2\left(\frac{1-f_2}{1-f_1}\right)}\right))}{f_2\left(\frac{f_1\left(\frac{1-f_2}{1-f_1}\right)}{f_2\left(\frac{1-f_2}{1-f_1}\right)}\right)(1-f_1\left(\frac{f_1\left(\frac{1-f_2}{1-f_1}\right)}{f_2\left(\frac{1-f_2}{1-f_1}\right)}\right))} = -\frac{\omega(1+z+z^2)}{1-\omega+z}$	$-\frac{\omega(1+z+z^2)}{1-\omega+z}$	$\{1, r, z^4, z\}$
$-\frac{\omega p(x)}{(x-\omega)(1+x(1-\omega+z))}$		

Table 4.19: Expanding $\{-\omega(1+z+z^2)/(1-\omega+z)\}$ by the cocycle relation; $a = -(1+z+s)/2/(1+z+z^2)$, $b = \omega$, $d = 0$. $r = z + \omega^3(z^2 - z)$, $b_3 = z(1 - \omega + (2 - \omega)z + z^2 + 2z^3 + (1 - \omega + z)s) / (2 + z(1 - \omega + z)(1 + z + s))$

h	$h(\infty)$	Simplex representing $\{h(\infty)\}$ in Fig. 4.13
$f_1\left(\frac{1-f_2\left(\frac{1-f_2}{1-f_1}\right)}{1-f_1\left(\frac{1-f_2}{1-f_1}\right)}\right) = \frac{z(x-1/z)}{x(z-\omega)}$	$\frac{z}{z-\omega}$	$\{\infty, t, 1, z^4\}$
$f_2\left(\frac{1-f_2\left(\frac{1-f_2}{1-f_1}\right)}{1-f_1\left(\frac{1-f_2}{1-f_1}\right)}\right) = \frac{x+1}{x(\omega-z)}$	$\frac{1}{\omega-z}$	$\{1, z^4, r, t\}$
$\frac{f_1\left(\frac{1-f_2\left(\frac{1-f_2}{1-f_1}\right)}{1-f_1\left(\frac{1-f_2}{1-f_1}\right)}\right)}{f_2\left(\frac{1-f_2\left(\frac{1-f_2}{1-f_1}\right)}{1-f_1\left(\frac{1-f_2}{1-f_1}\right)}\right)} = -\frac{z(x-1/z)}{x+1}$	$-z$	$\{\infty, 1, r, t\}$
$\frac{1-f_2\left(\frac{1-f_2\left(\frac{1-f_2}{1-f_1}\right)}{1-f_1\left(\frac{1-f_2}{1-f_1}\right)}\right)}{1-f_1\left(\frac{1-f_2\left(\frac{1-f_2}{1-f_1}\right)}{1-f_1\left(\frac{1-f_2}{1-f_1}\right)}\right)} = \frac{\omega(1+x(1-\omega+z))}{x+\omega}$	$1 + \omega + \omega z$	$\{\infty, t, r, z^4\}$
$\frac{f_1\left(\frac{1-f_2\left(\frac{1-f_2}{1-f_1}\right)}{1-f_1\left(\frac{1-f_2}{1-f_1}\right)}\right)(1-f_2\left(\frac{1-f_2\left(\frac{1-f_2}{1-f_1}\right)}{1-f_1\left(\frac{1-f_2}{1-f_1}\right)}\right))}{f_2\left(\frac{1-f_2\left(\frac{1-f_2}{1-f_1}\right)}{1-f_1\left(\frac{1-f_2}{1-f_1}\right)}\right)(1-f_1\left(\frac{1-f_2\left(\frac{1-f_2}{1-f_1}\right)}{1-f_1\left(\frac{1-f_2}{1-f_1}\right)}\right))} = \frac{-\omega z(x-1/z)(1+x(1-\omega+z))}{\omega+(1+\omega)x+x^2}$	$-\omega z(1 - \omega + z)$	$\{\infty, 1, r, z^4\}$

Table 4.20: Expanding $\{-\omega z(1 - \omega + z)\}$ by the cocycle relation; $a = 1/(\omega - 1 - z)$, $b = -1$, $d = 0$. $r = z + \omega^3(z^2 - z)$

Chapter 5

Conclusion

This dissertation started with a discussion of volume formulas for hyperbolic polyhedra and their connection to scissors congruence problems. At this point in time, there is no dearth of volume formulas in terms of the Lobachevsky function, but the reasons for their equivalence to each other are frequently far from obvious. The equivalence of two volume formulas for a hyperbolic polyhedron can be viewed as a scissors congruence and also as an identity on the Lobachevsky function.

As far as scissors congruence in hyperbolic space, a great deal is still unknown. The conjecture that the volume and Dehn invariant form a complete system of invariants for scissors congruence in hyperbolic space is still open. In this work we have shown several examples of scissors congruences in \mathbb{H}^3 which support this conjecture. However, a proof of the conjecture, as well as an algorithm for proving scissors congruence in Euclidean space, where the conjecture was shown to be true by Sydler, are still unknown. In particular, there still exists no constructive proof that the family of Regge symmetric tetrahedra in Euclidean space are scissors congruent. Their Dehn invariants and volumes agree, as shown by Roberts in [13], so by Sydler's theorem they are scissors congruent. It would be a natural extension of this work to specialize the proof presented in Chapter 3 to this problem.

As for the identities of the Lobachevsky function, there is a great deal to explore in this area as well. For example, the following conjecture of Milnor ([10]) has not

yet been solved:

Conjecture. If we consider only angles θ which are rational multiples of π , then every \mathbb{Q} -linear relation

$$q_1\mathfrak{J}(\theta_1) + \cdots + q_n\mathfrak{J}(\theta_n) = 0$$

is a consequence of the relations

$$\mathfrak{J}(\pi + \theta) = \mathfrak{J}(\theta), \quad \mathfrak{J}(-\theta) = \mathfrak{J}(\theta), \quad \mathfrak{J}(n\theta) = \sum_{k \pmod n} \mathfrak{J}(\theta + k\pi/n).$$

Milnor's conjecture hints at the key role of the Kubert identities in this field. In [5] Dupont and Sah have shown that the Kubert identities are a scissors congruence, and in Chapter 4 we have produced an actual simplicial complex illustrating their proof. While one could write an algorithm to produce these complexes for any n by following Dupont and Sah's proof, the complexes in Chapter 4 were constructed so that they use fewer vertices than the hypothetical "computer-generated" ones. This raises the question of the existence of the most efficient geometric proof of the Kubert identities. Specifically, it is doubtful that following through the steps of the inductive proof of Dupont and Sah provides the most efficient algorithm for the geometric proof of the Kubert identities. For example, the proofs in §4.3.3 used a proper subset of the vertices which arose from geometrizing Dupont and Sah's proof. From an algebraic point of view, using the key relation (4.43) led to a very elegant proof of the generalized Kubert identities. Whether there exists a proof of (4.43) different from that of Dupont, Sah and Poulsen remains to be seen.

Bibliography

- [1] S. J. Bloch. *Higher Regulators, Algebraic K-Theory, and Zeta Functions of Elliptic Curves*. American Mathematical Society, 2000.
- [2] Y. Cho and H. Kim. On the volume formula for hyperbolic tetrahedra. *Discrete and Computational Geometry*, 22:347–366, 1999.
- [3] J. L. Dupont. *Scissors congruences, group homology and characteristic classes*. World Scientific Publishing Company, 2001.
- [4] J. L. Dupont and E. T. Poulsen. Generation of $\mathbb{C}(x)$ by a restricted set of operations. *Journal of Pure and Applied Algebra*, 25:155–157, 1982.
- [5] J. L. Dupont and C.-H. Sah. Scissors congruences, II. *Journal of Pure and Applied Algebra*, 25:159–195, 1982.
- [6] W. Fenchel. *Elementary Geometry in Hyperbolic Space*. Walter de Gruyter, 1989.
- [7] H. Flanders. *Differential forms with applications to the physical sciences*. Dover Publications, Inc., 1989.
- [8] W. Hsiang. On infinitesimal symmetrization and volume formula for spherical or hyperbolic tetrahedrons. *Quarterly Journal of Mathematics Oxford*, 39:463–468, 1988.
- [9] G. Leibon. personal communication.
- [10] J. Milnor. Hyperbolic geometry: the first 150 years. *Bulletin of the American Mathematical Society*, 6(1):9–24, 1982.
- [11] J. Milnor. On polylogarithms, Hurwitz zeta functions, and the Kubert identities. *L'Enseignement Mathématique*, 29:281–322, 1983.

- [12] J. Murakami and M. Yano. On the volume of a hyperbolic and spherical tetrahedron. *Pre-print.*, 2002.
- [13] J. Roberts. Classical $6j$ -symbols and the tetrahedron. *Geometry and Topology*, 3:21–66, 1999.
- [14] C.-H. Sah. Scissors congruences, I, Gauss-Bonnet map. *Mathematica Scandinavica*, 49:181–210, 1982.
- [15] W. P. Thurston. *Three-Dimensional Geometry and Topology*. Princeton University Press, 1997.
- [16] E. B. Vinberg. Volumes of non-Euclidean polyhedra. *Russian Mathematical Surveys*, 48(2):15–45, 1993.